

MARKET ACCEPTANCE OF RENEWABLE ENERGY TECHNOLOGIES FOR
POWER GENERATION

A Dissertation

Submitted to the Faculty

of

Purdue University

by

Liz Wachs

In Partial Fulfillment of the

Requirements for the Degree

of

Doctor of Philosophy

August 2020

Purdue University

West Lafayette, Indiana

THE PURDUE UNIVERSITY GRADUATE SCHOOL
STATEMENT OF DISSERTATION APPROVAL

Dr. Bernard Engel, Chair

Department of Agricultural and Biological Engineering

Dr. R.P. Kingsly Ambrose

Department of Agricultural and Biological Engineering

Dr. Michael Ladisch

Department of Agricultural and Biological Engineering

Dr. Juan Pablo Sesmero

Department of Agricultural Economics

Approved by:

Dr. Nathan Mosier

Head of School

This is dedicated to my husband, Juan Pablo, and my children Norah, Agustin and Martin. You make this worthwhile.

ACKNOWLEDGMENTS

I acknowledge my professional mentors, former bosses and role models. Thanks to Bernard Engel who welcomed me into his research group and advised me as I entered new territory for both of us. Thanks to Mark Plotkin and Liliana Madrigal, who employed me at Amazon Conservation Team and first taught me about the applied work of conservation and how to get work done while remaining true to your principles. Thanks to Alon Tal, my supervisor in my master's degree who first taught me the academics of public policy and sustainability and whose career is an inspiration. Thanks to Robin Venuti for being a true mentor.

My husband Juan Pablo was my constant companion, read countless drafts of different ideas and emails, and always encouraged me to keep going when I was discouraged. My children, Norah, Agustin and Martin, you are my joy and inspiration. Thank you to my family, my parents and siblings, aunts, uncles and cousins. Thanks to my friends for being supportive and providing an escape from the office.

Thanks to my committee for your time and patience with me, as well as for the helpful comments on the work. Also thanks to the research groups of Dr. Engel and Dr. Singh, especially Nehika Mathur and Shuyuan Wang, for friendship and feedback. Sushant Mehan's friendship and advice was invaluable during my PhD process. Colleen Gabauer also helped me immeasurably. Project work from Prof. Mario Ventresca's course on Nature-Based Computing provided the seed for much of this work.

I also thank all the organizations that helped me by providing support and opportunities over the past few years: my department, the College of Agriculture, the College of Engineering, the Women's Initiatives Committee of AIChE, GTAP, and USAEE.

TABLE OF CONTENTS

	Page
LIST OF TABLES	x
LIST OF FIGURES	xiv
ABSTRACT	xix
1 Introduction	1
1.1 Research Questions	4
1.1.1 Research Question 1	4
1.1.2 Research Question 2	4
1.1.3 Research Question 3	4
1.1.4 Research Question 4	5
1.2 Organization of the Dissertation	5
1.3 Forecasting world energy use and supply: Energy Systems Models	6
1.4 Market Acceptance	8
1.4.1 Consumers	9
1.4.2 Firms	11
1.4.3 Investors	12
2 Projecting the Urban Energy Demand for Indiana, USA in 2050 and 2080 . .	16
2.1 Introduction	16
2.2 Background: Modeling Urban Energy Consumption	18
2.3 Methodology for Energy Demand Change at Urban Scale	21
2.3.1 Heating, Electricity and Transportation Projections	21
2.3.2 Cooling	24
2.3.3 Data Collection	26
2.4 Results and Discussion	31
2.4.1 Limitations and Model Robustness	34

	Page
2.5 Conclusions	35
3 Reliability versus Renewables: Modeling Costs and Revenue in CAISO and PJM	42
3.1 Introduction	42
3.2 Background and Literature Review	43
3.3 Methods	44
3.3.1 Testbed	44
3.3.2 Modeling Framework	44
3.3.3 Optimization Description	45
3.3.4 Net Present Value	47
3.3.5 Data	51
3.3.6 Verification	55
3.4 Results	55
3.5 Discussion	58
3.5.1 Overview	58
3.5.2 Differences between CAISO and PJM	61
3.5.3 Capacity Markets as a Barrier for Renewables	63
3.5.4 MOPR Expansion	64
3.5.5 Limitations	65
3.6 Conclusions	68
4 Quantifying Barriers to Market Acceptance of Renewables: A Portfolio Optimization Approach	70
4.1 Introduction and Background: Social Acceptance of Renewables and the Use of Portfolio Optimization	70
4.2 Methods	73
4.2.1 Data	73
4.2.2 Portfolio optimization in energy planning literature	74
4.2.3 Return	75
4.2.4 Quantifying Technology Cost Risk	75

	Page
4.2.5 Correlation between Cost Categories and Technologies	77
4.2.6 Deriving Single Values for Correlation	78
4.2.7 Optimization Problem and Approach	80
4.2.8 Solution Methods	81
4.2.9 Sustainability	81
4.2.10 Sustainability Optimization	82
4.3 Results	83
4.4 Discussion	85
4.4.1 Best Solutions Based on Returns	85
4.4.2 Sustainability	90
4.4.3 Sustainability versus Market	91
4.4.4 Limitations	96
4.5 Conclusions	97
5 Land Use for United States Power Generation: A Critical Review of Existing Metrics with Suggestions for Going Forward	99
5.1 Abstract	99
5.2 Introduction	101
5.2.1 Four conundrums	101
5.2.2 Power Generation Units	103
5.2.3 Looking forward and backward	103
5.3 Existing Methods	104
5.3.1 Summary of Three Indicators	105
5.3.2 Converting Between Power Density and Land Use Intensity . .	109
5.4 Analysis of Major Power Generation Technologies	110
5.4.1 Solar	110
5.4.2 Wind	111
5.4.3 Coal	113
5.4.4 Natural Gas	120

	Page
5.4.5 Biomass	121
5.4.6 Hydropower	122
5.4.7 Geothermal	123
5.4.8 Nuclear	124
5.4.9 Storage	126
5.5 Results	127
5.6 Discussion	129
5.6.1 Temporal Scale	129
5.6.2 System Boundaries	131
5.6.3 Secondary effects, land degradation and end of life	133
5.6.4 Incomparabilities	134
5.7 Conclusions	134
6 Conclusions and Implications for Future Work	137
6.1 Overview	137
6.2 Limitations	139
6.3 Impact on Field of Power Generation	141
6.4 Impact for other fields	141
REFERENCES	143
A Market Penetration	159
B Supplementary Material for Chapter Two	160
B.1 New data set for electricity modeling	161
B.2 Detailed Results for Fig. 1 in Main Text	163
B.3 Hidden extrapolation test results	163
B.3.1 MATLAB Code to check for hidden extrapolation in one result dataset	164
C Supplement to Chapter Three on Reliability and Renewables	173
C.1 Repository for models and data files	173
C.2 Annual Cost of Energy in PJM and CAISO	173

	Page
C.3 Data used with sources	173
C.4 Verification	180
C.5 Energy Return on Investment (EROI)	180
D Appendix for Chapter Five on Quantifying Market Barriers to Renewables	184
D.1 Supporting Data for Correlation and Risk Calculations	184
D.2 Sustainability Indicators	191
D.3 Life Cycle Water Use	192
E Appendix to Chapter Five on Land Use for Power Generation	194
E.1 Literature Estimates for Land Use	194
E.2 Coal Production Today	194
E.2.1 Measurements and Bounds from the Literature	197
VITA	200

LIST OF TABLES

Table	Page
1.1 Estimates of 2015 power generation mixture by IEA in 2009 [29] versus actual generation mixture in 2016 (2015 data not available) [30]. The estimates that varied by over 20% from the actual values are in bold . . .	3
1.2 Models considered by Pfenninger et al. [37] by type and focus	7
2.1 Singh Kennedy (S-K) Model for Urban Energy Estimation. For heating demand, only the heating degree days is a significant variable. For electricity, both heating degree days and inverse population density are significant. For transportation only inverse population density is significant. Inverse population density refers to urban area per capita.	22
2.2 Kennedy Megacities (K-M) Model for Urban Energy Estimation. Full details can be found in [32]).	23
2.3 Cities studied with population figures as used for 2015, 2050 and 2080. Indianapolis, the largest city, is forecast to increase significantly in population over this period.	28
2.4 Temperature changes in °C from 2015 to 2080 under the two scenarios considered for all cities studied. Average increases in high (h) and low (l) temperatures for each 3-month period are shown. The northernmost cities are shaded. Temperature increases higher than 4°C are shown in bold. . .	30
3.1 Parameters used for optimization. Link to full code in Appendix C	46
3.2 Minimum offers for affected technologies in the RPM	52
3.3 Parameters required for discount rate calculations from literature and as used in model, shown on the right. PJM literature values from [114,115]. .	53
4.1 Potential technical resources for renewable technologies in regions. These are conservative estimates since they cover the entire states: NV and CA in CAISO, and DE, IL, IN, KY, MD, MI, NJ, NC, OH, PA, TN, VA, WV and DC for PJM. The solar PV figures are an underestimate since they are based on technical potential from 2012.	74
4.2 Sustainability scores closer to 1 are on a blue scale, darker blue meaning more sustainable. Lower scores are on a red scale, with lower scores shown in darker red.	84

Table	Page
5.1 Data on Mining land use found in the two principal source papers. Smil's numbers, which were given in W/m^2 , have been multiplied by an efficiency factor of 0.35 to convert to representative Watt of electricity (W_e)/ m^2 . .	116
5.2 Land use intensities for land for coal power plants assuming different capacity factors. We use the average from Fthenakis and Kim updated with a capacity factor of 0.5 as the representative value for coal power plant land use intensity.	117
5.3 Our assessed land use intensities for the systems considered as well as a representative case. Mountaintop mining based systems have the highest land-use intensity, whereas the other systems are similar to each other, with the representative case doing slightly better.	119
B.1 Data used for the electricity regression model referred to in the text as S-K161	
B.2 Data used for heating regression. Based on the published S-K model. Industrial heating shares were assumed for each city and the modified totals were used for the regression.	162
B.3 Heating demand by city for each time period. Demand is measured in GJ/capita and the cumulative percent increase or decrease from the 2015 figure is included.	163
B.4 Electricity demand by city for each time period. Demand is measured in MWh/capita and the cumulative percent increase or decrease from the 2015 figure is included.	164
B.5 Cooling in kWh per capita. Efficiency gains are assumed for air conditioning systems. The cumulative percent increase or decrease from the 2015 figure is included.	165
B.6 Cooling in kWh per capita. No efficiency gains are assumed for air conditioning systems. The cumulative percent increase or decrease from the 2015 figure is included.	166
B.7 H values for Heating Model	168
B.8 H values for Electricity Model	169
B.9 Heating Test values for Hidden Extrapolation	170
B.10 Electricity Test Values for Hidden Extrapolation. Shaded values indicate extrapolation.	170
B.11 In the work published in [63] the efficiency figure of 3.81 was used for 2015. This table gives the city by city cooling results with no efficiency change (so 3.81 is used for all years), that correspond to that report.	171

Table	Page
B.12 In the work published in [63] the efficiency figure of 3.81 was used for 2015. This table gives the city by city cooling results with efficiency changes that correspond to that report.	172
C.1 Cost of energy in PJM from 2014-2018 with breakdown according to cost type (2018 data from table 1-8 in [104], prior years' data from [205]) . . .	174
C.2 Cost of energy in CAISO from 2013-2017 broken down by cost type [122].	174
C.3 Data sources for the NPV calculations	175
C.4 Energy sources with parameters used for modeling. Abbreviations used in headings are average capacity (AC), capacity factor (CF), LCOE Midpoint (L-M), LCOE overnight (L-O), and useful capacity (UC). All units are per MWh. Greenhouse gases are in carbon dioxide equivalents.	176
C.5 Parameters used for NPV calculations in both regions	177
C.6 Region specific parameters used in the NPV calculations	178
C.7 Parameters used for NPV calculations independent of technology.	179
C.8 Counties whose planned generation was included for PJM Verification calculations.	181
D.1 The relative weighting of each cost category by technology and region. CO ₂ costs for PJM are based on Regional Greenhouse Gas Initiative (RGGI) prices. CO ₂ costs are higher in CAISO, so the proportion of CO ₂ costs tends to be higher in CAISO. Insurance and Ad Valorem costs also differ between the two regions, leading to different proportions of OCC and O&M costs. Fuel costs between the two regions are similar, so their proportion is also similar in the two regions.	184
D.2 Volatility (sigma) values for each technology and cost category. CAISO and PJM have different values for CO ₂ pricing. Biomass doesn't have a long enough time series to estimate its volatility, so the value for coal is used.	185
D.3 The correlation coefficients between cost categories shown as a heat map. Note that natural gas and PJM energy prices are almost perfectly correlated since natural gas is the marginal energy supplier. Cap here refers to capacity.	186

Table	Page
D.4 Risk factors for each technology type in PJM and CAISO. The largest are for combined cycle technologies, which have a high relative proportion of fuel costs from natural gas, whose prices experience high variability. Off-shore wind's construction costs are relatively high and variable. Coal also has high fuel costs, but coal prices have been less variable than natural gas prices in US markets. Since lack of data prevented calculating a variability for biomass costs, coal's value was used.	187
D.5 Correlation coefficients used for O&M costs between technologies. Assumptions are detailed in the text. Shading is used to make the scale of correlation clear; dark blue is very close correlation (~ 1) and dark red is a strong negative correlation (~ -1). Abbreviations for technologies are used including natural gas combined cycle (NGCC), natural gas combustion turbine (NG CT), coal integrated gasification combined cycle (IGCC). . .	188
D.6 Correlation matrix obtained for CAISO using the determinant method. Row names are omitted for fit, but are identical to column names. . . .	189
D.7 Correlation table for PJM obtained using the determinant method. Column and row names are identical but row names are omitted for fit. . . .	189
D.8 CAISO correlation matrix obtained using scaled matrix method. Row names are omitted for fit but are identical to column names.	190
D.9 Correlation table for PJM using the scaled matrix method. The row names are the same as the column names but are omitted for fit.	190
D.10 Sustainability indicators used in this analysis. The future category (F) represents risks with current (C) as a separate category. Quantitative factors (Q) have defined functions. Categorical indicators (C) are step functions.	191
E.1 Values for land use intensity from three sources with any necessary unit conversions made by the author. Note that while Trainor et al. pioneer the idea of landscape level versus direct footprint, they do not differentiate here in the case of coal. Values from Fthenakis and Kim come from visual inspection of Fig. 6. Values for Smil come from pages 135-136.	198

LIST OF FIGURES

Figure	Page
1.1 Global consumption of primary energy from 1965-2017, according to figures from BP [13]	2
1.2 Visualizing the market with consumers, firms and investors as actors. Consumers act on the demand side, while firms act on the supply side. Finance links investors to firms, and thereby influences the supply of goods.	8
1.3 CAISO's supply curve at 6 pm, March 2016 according to data analysis in [46]. Supply is highly inelastic both at very low quantities and at high quantities, and highly elastic in between.	10
1.4 PJM's supply curves in 2014, 2016 and 2017 from [47], shown along with loads in 2016 and 2017. The supply curve is highly elastic, as predicted, until threshold values are reached when it becomes vertical.	10

Figure	Page
2.1 Per capita urban residential and commercial heating and electricity projections using the revised S-K model for each city are shown in a and b for the RCP 8.5 scenario. The distinction between north and south is with respect to 40 degrees latitude. Heating demand falls steadily in all cities whereas electricity demand rises. Urban residential per capita cooling estimates are shown in c and d with and without efficiency gains. Most cooling demand changes occur by 2050 with smaller changes through 2080. When efficiency gains are included in some cases, particularly in the southern cities, cooling demand falls from 2015-2080. Full data for figures as well as for the RCP 4.5 scenario is available in Appendix B, Tables 3-6.	38
2.2 Total electricity and heating demand are shown as modeled by the two techniques. Electricity shows consistent growth in both models, while heating demand falls in the RCP 8.5 scenario, even accounting for population growth. Note that in the K-M model there is no difference between the electricity projections based on temperature, so RCP 8.5 and 4.5 give the same results. Growth for electricity demand is also very similar between the two scenarios in the S-K model.	39
2.3 Projections for total cooling demand (GWh) by city are shown for the RCP 4.5 scenario, including the efficiency improvement assumption (so the most conservative estimate) are shown on the left, to contrast with the most aggressive estimate given by RCP 8.5 with no efficiency gains, shown at right. The sequence and shading denote the years in the study. When population is taken into account, most increases are still primarily seen from 2015-2050, with flatter increases from 2050-2080, and absolute decreases for Evansville, Kokomo and Terre Haute in the conservative scenario. Indianapolis dominates the total demand here due to its large population.	40
2.4 Changing energy use categories over time forecast using the S-K model. Forecasts are for residential and commercial energy demand. Electricity should include cooling, but the projections for cooling are from a different methodology so are not indicated here. Also, since cooling projections are only for residential, they will represent a small portion of the total electricity demand shown here.	41

Figure	Page
3.1 Histogram showing the total amount of available capacity installed over 20 runs of optimization model from unique solutions in the Pareto set based on national figures. On the left, results are not constrained by Eq. 3. On the right, the total contribution from solar PV (including commercial and residential) and onshore wind is constrained to no more than 30%, 50%, or 70% of the total.	56
3.2 CAISO profitability with 20, 30 and 40 year lifetimes is shown on the left. PJM profitability is on the right, including the baseline scenario, the MOPR with a low threshold for entry into the RPM, with RECs (states with RPS).	57
3.3 Response to a 10% perturbation in variable value, shown in CAISO and PJM, variables ordered by the \$ amount change in PJM. The percentage refers to either the total revenue or total costs, depending on the variable. Revenue is affected by: Discount Rate – R, Capacity Price, Price, Capacity Factor – R, and Inflation – R. Costs are affected by: Installed Costs, Discount Rate – C, Fuel Cost, O&M, Interest Rate, Capacity Factor – C, Ad Valorem, Inflation – C, Insurance, State Tax and GHG emissions. For taxes, which do not appear on either revenue or costs, the NPV is used.	59
3.4 New capacity additions planned in PJM territory and California as of 2017, according to EIA Form 860 (does not include pre-existing generation assets).	60
3.5 Increases in the NPV for each technology due to the expanded MOPR in states with no RPS, with no assumption made as to the ability of the asset to receive a winning bid. The color code refers to the lifetime of the asset, with more gains to the technology on a cumulative basis.	66
3.6 Two scenarios for the extension of the MOPR in states subject to RPS. On the left, only NGCC, NG CT, and solar PV plants win bids in the RPM auction, so their NPV is bolstered. On the right, supercritical coal and nuclear plants also win capacity income.	67
4.1 Summary of approach to quantifying barriers to market acceptance of renewables and identifying desirable portfolios from market and sustainability perspectives taken in this paper.	72
4.2 PJM portfolios with each constraint level for VREs differentiated by color and symbol: no constraint on VRE is shown with purple asterisks; a 70% constraint on VREs is shown with turquoise diamonds; a 50% constraint is shown with green circles; and a 30% constraint on VREs is shown with red exes.	86

Figure	Page
4.3 Pareto fronts for CAISO with each constraint level for VREs differentiated by color and symbol: no constraint on VRE is shown with purple asterisks; a 70% constraint on VREs is shown with turquoise diamonds; a 50% constraint is shown with green circles; and a 30% constraint on VREs is shown with red exes.	87
4.4 Sustainable portfolios for CAISO and PJM. The colors and symbols represent the percentage of VREs allowed in the scenario: no constraint on VRE is shown with purple asterisks; a 70% constraint on VREs is shown with turquoise diamonds; a 50% constraint is shown with green circles; and a 30% constraint on VREs is shown with red exes.	88
4.5 A comparison of the effect of correlation method on the proportion of each technology chosen in average portfolios. Results are for CAISO using levelized costs.	89
4.6 Differences between average sustainable portfolio values and average values from cost scenarios below the median value. Color coding shows scenario and region.	92
4.7 Differences between average sustainable portfolio values and average values from risk scenarios below the median value. Color coding shows scenario and region.	93
5.1 Schematic of major life cycle phases for power production from coal. Three major methods of extraction are used: mountaintop removal, underground mines, and surface mines. For underground mines, the indirect land use from wooden supports can be significant. Mined coal is typically transported by rail to power plants where it is burned for power generation. The major land use phase is mining, but rail transport makes up 6-53% of the land use according to Fthenakis and Kim [165]. The power generation phase is a very small part of the total land use.	114
5.2 Nuclear energy process diagram	124
5.3 Land use intensities for technologies considered, shown in m ² /GWh. While natural gas is least land-intensive in both metrics, wind is much more attractive if only the direct footprint is considered.	127
5.4 Power densities in W _e /m ² for technologies considered. Note that the density is higher when only the direct footprint is considered.	128
6.1 Illustration of a product with respect to hypothetical Pareto front according to sustainability criteria	142

Figure	Page
E.1 Land use intensity estimates from literature review. Fthenakis and Kim estimates taken from visual inspection of results figure 3 [165]. Smil estimates taken from visual inspection of Fig. 7.3 [35]. Hand et al. [166] estimates available only for renewables. Capacity factors from our work were used on their values from table A-10 [166]. Gagnon's biomass estimate for wood wastes was used [34].	195
E.2 Power density estimates from literature. Fthenakis and Kim estimates taken from visual inspection of results figure 3 [165]. Smil estimates taken from visual inspection of Fig. 7.3 [35]. Hand et al. [166] estimates available only for renewables. Capacity factors from our work were used on their values from table A-10 [166]. Gagnon's biomass estimate for wood wastes was used [34].	196

ABSTRACT

Wachs, Liz Ph.D., Purdue University, August 2020. Market Acceptance of Renewable Energy Technologies for Power Generation. Major Professor: Bernard Engel.

The perception of climate change as an emergency has provided the primary impetus to a transition from conventional fossil-based energy sources to renewables. The use of renewable energy sources is essential to sustainable development, since it is the only way that quality of life can remain high while greenhouse gas emissions are cut. Still, at the time of writing, renewables contribute a small part of the total primary energy use worldwide. Much research has gone into understanding barriers to the full-scale adoption of renewable energy sources. Still, many of the tools used have focused primarily on optimal paths, which are useful in the long-term but problematic in non-equilibrium markets. In the shorter term, behavior is thought to be more governed by existing institutions and commitments until those frameworks can be changed. This means that understanding people's attitudes towards renewables is key towards understanding how adoption will take place and how best to incentivize such action. Particularly, decisions are made by investors, who serve as intermediaries between what customers/public want and the existing institutions (what is possible). Understanding their responses to the current state of affairs as well as perturbations in the form of policy changes is important in order to effect change or make sure that policies will work as intended.

First, the shifting demand landscape is considered, specifically in Indiana cities. Heating is shrinking as a driver of primary energy use over time due to climate change, while transport increases relatively. Electricity demand continues to increase, and the potential for electrification of transport can add to this potential. This led to a focus on the electricity sector for further work. Noticing that adoption lags public support

led to a comparison of levelized cost of electricity and net present value metrics for 18 dominant technologies in two power markets in the US. Capacity markets and solar renewable energy credits lead to differences between cost and net present value in PJM, making natural gas the most attractive technology there. Noting the difference in electricity price between the two markets also provides a caution regarding the employment of carbon pricing in PJM, since that is an additional cost to the consumer who is already paying twice to fossil based generation in that region, once for energy provision and once for reliability.

Individual technologies represent only part of the question, however, since generation capacity is added to bolster existing supplies. In order to study the portfolio, historical risk is considered along with levelized costs to identify optimal portfolios in CAISO and PJM. Then electricity is treated as a social good, and a sustainability profile was built for each technology balancing current equity and risks to future generations. This allowed quantification and identification of barriers to market acceptance of renewables, but it also led to a recognition of where useful metrics are still lacking. For example the use of land provides an important barrier to the adoption of renewables, and is a potent potential barrier for future acceptance. It is not well understood, however, which led to a critical review of existing technologies.

The work in this dissertation provides one of the first mixed methods attempts to assess energy demand for cities including the end use of cooling. It provides a simple model that demonstrates the importance of capacity markets in determining the profitability of different energy technologies. It provides a guide to the emerging issue of land use by energy systems, a key consideration for the study of the food-energy-water nexus. It is the first use of portfolio optimization for sustainability studies. This is an important methodological tool since it allows a comprehensive sustainability analysis while providing a sense of the difference between immediate and future risks. The tool also allows users to diagnose which technologies are incentivized and which are deterred by market factors, as well as the strength of the deterrence. This is helpful for policy makers in understanding how incentives should be structured.

1. INTRODUCTION

Risks of climate change and associated global warming have led to a clean energy transition, which depends on the substitution of renewable energy sources for fossil fuels to allow quality of life to remain high while greenhouse gas emissions are cut [1]. Suboptimal choices due to poor information availability at the time critical decisions are made can lead to a “lock-in” that is costly to exit [2]. The “techno-institutional complex,” involving expertise, network externalities, and both public and private institutions surrounding the energy sector [1,3] can then dampen the speed of change. Thus, short-term decisions are especially important to ensure that the adoption over the long-term follows the best path.

The importance of making correct decisions on technology adoption is heightened because primary energy consumption has been increasing despite increased attention to climate change (Fig. 1.1). Large-scale investments in renewables have occurred as well [4] coupled with planning and speculation concerning a movement to energy systems powered only by renewables [5,6]. Such 100% renewables systems likely require electrification of industry, transportation and heating [7,8]. At present, however, the US electric grid is based primarily on fossil fuels, and electric transport is still in its infancy [9]. In 2018, most new generation capacity was based on natural gas [10], despite concerns about stranded assets [11]. Based on past retirements [12], the lifetimes of these plants may extend 30-60 years into the future.

Researchers have worked to understand what keeps people from adopting renewables even when they theoretically agree with their use. Wüstenhagen et al. wrote about social acceptance of renewables, identifying the major paths to implementation of as sociopolitical, community and market acceptance [14]. Wüstenhagen et al. described market acceptance as behavior from consumers, investors and firms.

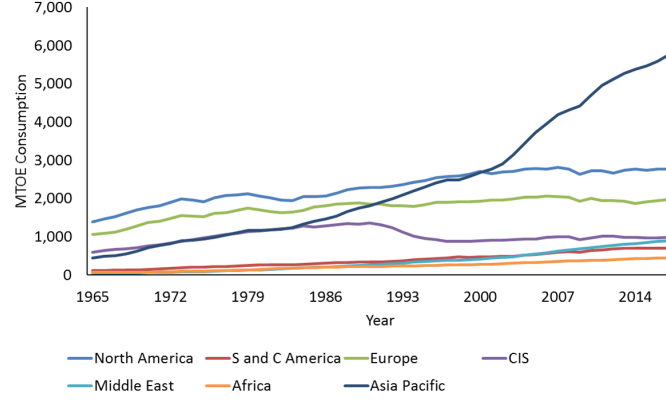


Fig. 1.1.: Global consumption of primary energy from 1965-2017, according to figures from BP [13]

Since then, work has been done to understand investors [15,16], financing [17–19] and risk [20–22].

Acceptance literature does not deal directly with a related question, which is that renewables come with their own trade-offs [23], so choosing the correct renewables is a difficult problem in itself. Some researchers have worked to choose methods and indicators that allow choosing the best technologies [24–26]. Recently LCA has been employed to perform a global assessment of power generation technologies [27].

Still, many problems remain, in part because sustainability and the optimality of portfolios are interconnected with costs [26], which are extremely dynamic for emerging technologies. LCA does not include the social and economic indicators that are important to an overall sustainability assessment [27], and does not address the issue of portfolio selection. Sustainability indicators outside of global warming potential are left out of energy models which can lead to solutions that are not in keeping with sustainable development objectives [28], and are also left out of most commercial software used by utilities for integrated resource planning, leading to criticism about other important environmental issues. Long-term energy models have typically underestimated the adoption of renewables (see table 1.1).

Table 1.1.: Estimates of 2015 power generation mixture by IEA in 2009 [29] versus actual generation mixture in 2016 (2015 data not available) [30]. The estimates that varied by over 20% from the actual values are in bold

	2015 forecast (TWh)	2016 actual (TWh)	% Above Forecast
Total	24,352	24,765	2%
Fossil fuels	16,302	16,136	-1%
Coal	10,461	9,282	-11%
Gas	4,982	5,850	17%
Oil	859	1,004	17%
Nuclear	3,107	2,611	-16%
Renewables	4,944	6,018	22%
Hydro	3,692	4,070	10%
Bioenergy	408	566	39%
Wind	678	981	45%
Solar PV	67	303	352%
Other renewables	99	98	-1%

In this thesis, the best portfolios of technologies will be identified using an innovative and transparent framework for holistic sustainability assessments. The framework will be used to provide a diagnostic tool that identifies market acceptance barriers to renewable technologies. First, the demand landscape for Indiana cities will be studied to assess how heating, electricity and transportation demand will vary with relation to each other under climate change and population growth. Then, two US regions, with high and low adoption of renewables, are studied to compare costs and revenues for different technologies. This analysis provides the groundwork for a cost and risk analysis that can be contrasted with the sustainability analysis to identify market barriers in CAISO and PJM. While developing the sustainability assessment

framework, a critical review of land use metrics for power generation is performed, in order to include this crucial indicator in the analysis.

1.1 Research Questions

1.1.1 Research Question 1

How will a warmer climate affect urban energy use in terms of electricity, heating and transportation and what is the time frame for the changes?

The backdrop for the energy transition is the climate change expected over the next century [31]. Most energy use can be divided into electricity, heating and transportation. The relative proportions of these uses may change in the future, and in the case of transportation and electricity, may coalesce. Will most changes happen soon, or later? Where might the largest changes occur in Indiana's cities? How much certainty is there about these estimates, and what is needed to improve on this? Existing models will be used to assess these questions in Indiana's cities [32, 33].

1.1.2 Research Question 2

Do capacity markets represent barriers to renewables? Reliability is a key feature of energy systems. In many deregulated markets, load serving entities are remunerated for their commitments to make generation capacity available. This thrust looks at whether renewables are compatible with this understanding of resource adequacy, or whether these markets present a barrier to renewables. Pricing is examined, and cost and profit metrics are compared for their correspondence with generation capacity installed.

1.1.3 Research Question 3

How should land use by power generation technologies be measured? Since at least 2000, researchers have warned about the need for large amounts of land for

some renewable technologies [23,34,35]. Land use is a frequently mentioned indicator and is linked to biodiversity as well as other important impacts. How should it be assessed temporally, physically, and in terms of impacts? Literature will be surveyed to compare existing methods and analyze land use by power generation technologies typically employed.

1.1.4 Research Question 4

How can market barriers to technologies be quantified? A diagnostic tool that measures market barriers to individual technologies is created. This requires identifying optimal portfolios from a market perspective and contrasting them with optimal portfolios from a sustainability perspective. The tool is applied to CAISO and PJM markets.

1.2 Organization of the Dissertation

The dissertation is divided into six chapters. Chapter two has been published in *Climatic Change* [36], and resolves the first research question. In the third chapter, prices, costs and profitability are calculated for 18 commonly considered technologies in PJM and CAISO. These are used to understand which metrics are most correlated with planned generation installations. The PJM capacity market and the recent obligatory expansion of its minimum offer price rule are explored to understand its role as a potential market barrier (research question 2). Chapter four documents the application of mean variance portfolio optimization to find optimal portfolios based on market and sustainability criteria, and finds market barriers and boosts for 18 technologies in CAISO and PJM (research question 4). Chapter five provides a critical review of land use metrics for power generation (research question 3). Conclusions and directions for future work are summarized in chapter 6. The rest of the introduction provides background on energy systems models, market acceptance, and financing in the sector.

1.3 Forecasting world energy use and supply: Energy Systems Models

The importance of forecasting energy use has been noted since the 1970's [37]. Energy systems include the resources exploited for energy, conversion technologies and distribution, as well as use for provision of services [38]. Energy systems are complex, involving multiple scales, industries, interactions and actors. While this dissertation does not use the energy models surveyed here, this brief literature review provides some guiding principles used in the construction of models for this work.

Widely used models for energy supply estimation include MARKAL (according to [37] MARKAL is probably the most widely used energy systems model) and TIMES, from the IEA, MESSAGE (IIASA) and TIMER. MARKAL is specifically geared towards energy supply, whereas TIMES and TIMER are part of integrated assessment models (IAM). The ETSAP-TIAM (Integrated MARKAL-EFOM System) is the implementation of TIMES as an IAM [39]. TIMES is a partial equilibrium model, so supply and demand are balanced based on the elasticity of demand specified by the user. [39].

Pfenninger et al. reviewed energy systems models [37], with regard to temporal and spatial resolution, handling uncertainty and showing assumptions, simplifications/complexity accurately modeled, and treatment of human behavior and risk. The models considered were divided into four classes, shown in table 1.2. Trutnevyte showed that half of the energy forecasts developed by the integrated assessment models for the 5th meeting of the Intergovernmental Panel on Climate Change were prepared via cost optimization, and 80% of those models relied on the perfect foresight¹ assumption as well [40].

Systems models contain both aleatory and epistemic uncertainty [37, 41], particularly when they model future states. Aleatory uncertainty is random error [41], which cannot be modeled but it can be minimized by using approaches such as Monte Carlo or stochastic programming (sometimes integrated with MARKAL or MES-

¹Perfect foresight is necessary for equilibrium conditions to be met according to economic theory, allowing the assumption of marginal pricing to be justified.

Table 1.2.: Models considered by Pfenninger et al. [37] by type and focus

Type	Models	Focus
Optimization	MARKAL, MESSAGE, TIMES, OSe-MOSYS	Normative
Simulation	NEMS, PRIMES, LEAP	Forecasting
Power/electricity	WASP, PLEXOS, ELMOD, EMCAS	Planning & Ops
Hybrid/qualitative	UK Dept for Energy and Climate Change 2050 Pathways, Mackay’s Scenarios, Climate Stabilization Wedges	Scenarios

SAGE). Epistemic uncertainty refers to strength of data collection [37]. DeCarolis distinguishes instead between structural and parametric uncertainty [42]. Parameter uncertainty is addressed by scenario analysis which can be effective as long as the scenarios themselves are designed to be exhaustive. Parameter uncertainty can also be addressed by using Monte Carlo simulation or a stochastic optimization approach [42]. Even if parameter uncertainty were zero, the uncertainty in long-range energy models would still be high, due to complexity and random effects [42]. Structural uncertainty refers to how models are built, which parameters and processes are included versus which are ignored. This type of uncertainty is difficult to handle, and frequently managed by building more complicated models that include more processes, but these additional elements may not contribute to better validation [42]. Assumptions made by modelers also have a large effect on results, so they need to be transparent [37]. When used as a method for generating predictions for the future, Pfenninger et al. point to a commentary from Klosterman [43] which claims that simpler models tend to perform as well as complex models. Pfenninger et al. also allude to the importance of human factors in the contribution to uncertainty, as individual behavior related to preferences and culture is not usually captured by energy systems models. Trutnevyte conducted an ex-post analysis of the UK electricity sector’s

shifts from 1990-2014 in order to study whether cost-optimization can approximate real energy transitions [40]. The study showed that for shorter range forecasts the cost optimization worked well, but for longer-term forecasts it was necessary to use a range of near-optimal scenarios to include the true transition values.

1.4 Market Acceptance

Market acceptance encompasses behavior both on the demand and supply side. Consumers primarily influence demand. Investors influence future supply and firms influence supply (and future supply). Supply and demand are related, and economic models are based on the assumption that at equilibrium conditions, supply and demand are equal. In Fig. 1.2, the structure of flows between three groups: consumers, firms and investors, is visualized.

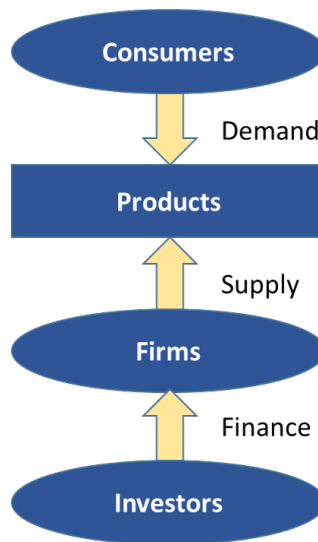


Fig. 1.2.: Visualizing the market with consumers, firms and investors as actors. Consumers act on the demand side, while firms act on the supply side. Finance links investors to firms, and thereby influences the supply of goods.

The supply curve has a positive slope, where the quantity produced increases with increasing prices. The demand curve is typically negatively sloped, with the

amount demanded increasing as price decreases. The slope of the curves reflects the elasticity of the good. If a good is elastic, the demand or supply changes quite a bit when price fluctuates. When goods are inelastic, price changes do not correspond to much movement on the demand or supply curves. Goods with an inelastic demand function tend to be those whose consumption is necessary at a certain level. A high price cannot cause people to reduce their consumption, and a low price won't cause much of an increase since they don't need more. On the supply side, inelastic goods are those whose supply is hard to change.

Since energy is a necessity for people, energy demand should be fairly inelastic. This inelasticity is augmented by the usually unvarying rates that consumers can be charged. This may not be as true for its income elasticity, since people without access to electricity who can gain access with an increase in means will increase its use. The supply side for energy is different. While generation capacity is capital intensive, there is typically an oversupply of capacity in developed countries, so it is not very difficult to increase generation at any point in time. Still, when the maximum is reached, higher demand can cause power outages, as has been seen in the past. Thus, supply is inelastic after a certain point. This can be seen in Figs. 1.3, 1.4. This phenomenon presents a challenge for electricity markets. Demand peaks that hit the vertical areas on the supply curve are sudden and somewhat unpredictable, so may not effectively stimulate firms to provide services in the case of such high prices. There is a robust literature on the missing money that cannot be quantified in the case of a blackout, and this has led to the theoretical basis for capacity markets that have been instituted in PJM and most other ISO/RTOs in the US, with corresponding price caps in the energy market [44, 45].

1.4.1 Consumers

Consumers directly influence demand by deciding how much of a product to purchase. Firms, on the other hand, decide how much to provision, which means that

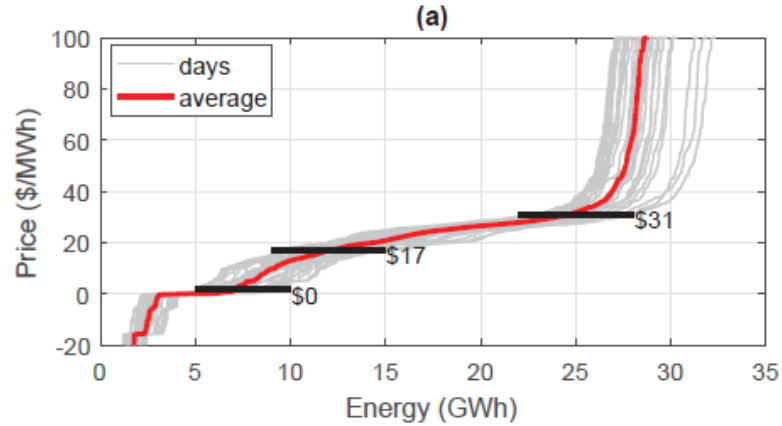


Fig. 1.3.: CAISO's supply curve at 6 pm, March 2016 according to data analysis in [46]. Supply is highly inelastic both at very low quantities and at high quantities, and highly elastic in between.

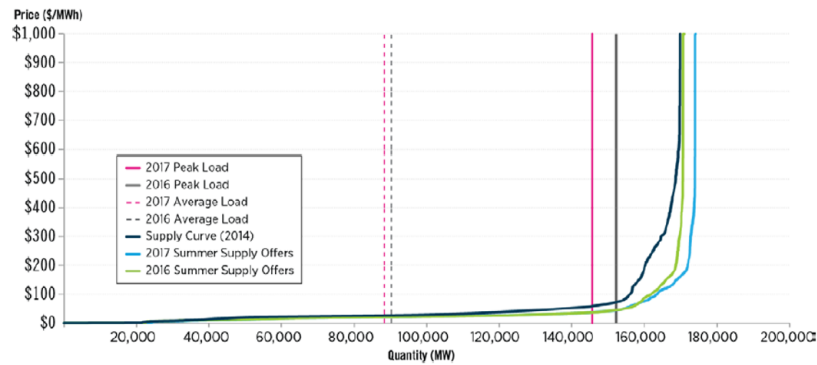


Fig. 1.4.: PJM's supply curves in 2014, 2016 and 2017 from [47], shown along with loads in 2016 and 2017. The supply curve is highly elastic, as predicted, until threshold values are reached when it becomes vertical.

consumers have an indirect feedback on supply since firms wish to know how much consumers want. Firms have a direct link to supply. Investors have a more indirect role, since they decide how much financing to provide to firms. In some situations, the consumers have a lot of power. In the case of regulated electricity markets, however, households have power, since they have no choice over the mixture of power generation technologies used. Still, commercial enterprises in particular as well as localities

have made well-publicized commitments to reduce impacts on climate change, whose potential effects are explored in [48].

1.4.2 Firms

Profit Motive

Just as there is both a supply and demand side in the marketplace, decisions about operations and investments are made both by attempting to minimize costs and maximizing revenues. The difference between the revenues and costs is the profit. There is a time dimension to profit, since an operation may be profitable over time, but not immediately. Both the cumulative sense, or the integral, and the immediate sense are important, since cash flow is determined at a point in time. Income is closely linked to demand, since it is tied to the actions of people buying the products. Since electricity prices to consumers can be constrained, profit opportunities are more limited than in some sectors, while utilities enjoy a low-risk revenue stream.

Adoption Strategies and Payoffs

Firms must decide whether to continue using older technologies or to adopt newer technologies. Market penetration is described mathematically in appendix A. In a study of energy technologies, Schilling and Esmundo studied S-curves of technology improvements versus cost of investment, finding that the return on investment in research and development for fossil fuel-based power generation was much lower and declining versus the returns for investment in renewables [49]. This analysis was inspired in part by previous work on the S-shaped curve for technology by Christensen [50, 51] and Ayres [52]. Christensen found that incumbent firms maintained strategic advantage while pursuing a “jump” in the S-curve for a new technology in components because implementation of new technologies can be more challenging than originally anticipated [50]. On the other hand, for architectural shifts, new entrants had an

advantage, and there was an advantage to early adoption [51]. The advantage was seen because the architectural shifts made the product lag in acceptance by traditional markets, as it would underperform according to the existing metrics, forcing the product into emerging markets, where it could develop and then quickly take over the former standard once the technical barriers were overcome [51].

1.4.3 Investors

Investment is the exchange of money for the proceeds of a given asset [15]. The asset can be real, in which case it has a physical realization like a turbine or generation plant, or financial, in which case it is a contract [15]. The investment can be in the form of equity, in which case the investor is buying a portion of the asset, or debt [15]. Assets are grouped into classes according to their characteristics of risk and returns: equities (stocks), commodities, cash and cryptocurrencies, derivatives, real estate, and fixed income (bonds).

In deregulated electricity markets, projects need the blessing not of central planners but rather of investors, who need to assess a monetary advantage to the project. Private investors can be grouped into the following categories: a) corporations, b) retail investors (private individuals), c) partnerships such as hedge funds or firms, d) financial intermediaries (such as banks, pension funds or insurance firms), and e) endowments (typically held by universities or foundations) [15]. They can be broken down into two classes: strategic and financial investors [15]. Strategic investors involved in the industrial sector already, for example existing energy firms or utilities that invest in renewables for strategic reasons (mainly from group a). Financial investors are mainly groups b - e, and they are more focused on financial gains. While strategic investors are involved in renewable projects as part of their core business, financial investors are prone to exit the sector if risks increase [15].

When new projects are proposed, their profitability is assessed by potential investors. The simplest metric is the return on investment, shown in equation 1.1:

$$ROI = \frac{P - C}{C} \quad (1.1)$$

Where P is profits and C is costs. Estimating the ROI is not as simple as equation 1.1 suggests, however, since in most cases, neither the profits nor costs can be known with certainty ahead of time. This means that investors must factor in risk. The decision problem for investors is whether the price they must pay to enter the market will allow them to profit. The return they are interested in must be adjusted for risk. Donovan describes asset pricing as the method of understanding this risk, defining the asset price according to equation 1.2 [15].

$$A_t = E(d_{t+1}, \Pi_{t+1}) \quad (1.2)$$

The asset price at time t (A_t) is here a function of the discount factor d at time t+1 and the payoff (Π) at time t+1. The basic form of the asset pricing model is given in equation 1.3 [53].

$$A_t = E_t\left(\beta \frac{u'(c_{t+1})}{u'(c_t)} \Pi_{t+1}\right) \quad (1.3)$$

Here β is the discount factor, which is specified as the subjective discount factor. Marginal utility of consumption is $u'(c)$. Note that the product of the asset price with the marginal utility of consumption at time t is equivalent to the expected value of the product of the marginal utility of consumption at time t+1 with the expected payoff and the subjective discount factor [53]. Thus the discount factor d_{t+1} can be defined as:

$$d_{t+1} = \beta \frac{u'(c_{t+1})}{u'(c_t)} \quad (1.4)$$

Substituting into equation 1.3 gives the expression in equation 1.2.

Time Cost of Money and Metrics

The value of money is not constant over time, due to inflation, interest, opportunity cost and uncertainty. Many metrics are used to evaluate potential investments.

In these investments, costs and cash flow occur in multiple time periods. Hence, investments must be considered in terms of their net present value (NPV), or discounted profitability, described more fully in chapter 3, section 3.3.4. The discount rate can be evaluated and understood in a variety of ways, but it is a measure of the time value of money [54] as well as risk in some cases [15]. NPV, while a powerful tool, does not allow for a full accounting of risks and opportunities over the project timeline. For example, tying up the capital in a project today may make it impossible to invest in an even better project a few years down the line. Or if a worst-case type scenario occurs in one of the risks that affects the project, it is invisible in an NPV calculation. For example, in power generation plants, particularly biomass, commodity prices can be volatile. NPV will not take that into account. If either the costs of the raw materials or the price of the final product makes the technology infeasible, the project may be abandoned before being finished.

Since most discount rates cannot be known ahead of time, they are a source of uncertainty and multiple discount rates may be used to give estimates (see section 1.4.3 for more thorough discussion of risk and uncertainty). The government publishes recommended discount rates for public projects. For private investment, the cost of capital is generally used, ideally the marginal cost of capital [54]. Firms can compute the weighted average cost of capital (WACC), described in detail in chapter 3, section 3.3.5.

NPV is a powerful analytical tool, but it does not allow for a full accounting of risks and opportunities over the project timeline [55]. In other words, while a positive NPV represents a good investment, it is not always the best investment. Also, while these metrics are simple in that they give a single value that is easy to interpret, that can be misleading since the anticipated costs really represent probability distributions, and thus are frequently calculated using Monte Carlo, and looking at the results as a distribution can give a different sense than the single number [54].

Risk and Uncertainty for Investors

Two assumptions implicit in the use of NPV have led to the development of different methods to assessing desirability and risk: reversibility of investment (no sunk costs) and inability to postpone investments (ignoring opportunity costs). Both assumptions show that NPV underestimates the price of investing, leading to a lower barrier for investment than firms actually use.

Reversibility is the idea that once an investment has begun, it can be easily reversed. In many cases, however, risk affects all customers the same way. Therefore, if an asset loses its value to its initial purchaser, it may have lost value for all potential purchasers. This is the case when a purchase is firm-specific or industry-specific, and is also termed a “sunk cost.”

The temporal element is likened to the asset market. An option to invest at a given time can be purchased without being exercised. There is an opportunity cost to investing, represented by the option cost, which is forfeited when the investment is made. Firms face a similar dilemma when choosing to invest in new technological options, knowing that an innovation might become available which will enable them to make a better product more efficiently. For this reason, there are times when the purchaser will find it advantageous to wait. This type of risk is frequently modeled using real options theory [56, 57].

2. PROJECTING THE URBAN ENERGY DEMAND FOR INDIANA, USA IN 2050 AND 2080¹

2.1 Introduction

Cities are home to a majority of the world’s population but make up less than 3% of terrestrial land [58], and possibly as little as 0.51% [59]. Accordingly, the International Energy Agency posited that 64% of global primary energy use took place in cities in 2013 [60]. This trend has also been found in the US [61], which is important both for forecasting future energy use and targeting policies. While this work is focused on the consequences of climate change in terms of energy use, energy use is also one of the largest contributors to greenhouse gas emissions, representing a feedback loop. Particularly after the exit of the US from the Paris Accords, increasing attention has been placed on the potential for more distributed action by the more than 300 “climate mayors,” who have affirmed their commitment to meet international goals for climate change mitigation [62].

As part of the Indiana Climate Change Impacts Assessment (IN CCIA), high resolution forecasts were made available for Indiana for the time period up to 2100 for two climate change scenarios: representative concentration pathway (RCP) 4.5 and RCP 8.5. The numbers in the scenario names refer to the amount of radiative forcing present in the atmosphere in 2100 in W/m^2 . The principal tasks of the energy working group for the IN CCIA were to project the effects of climate change on state-wide energy consumption, and estimate the effects of policies on the supply mixture [63]. An understanding of the energy demand changes spatially across the state, specifically centered in urban areas, was desirable in order to develop an actionable plan to

¹Reprinted by permission from: Springer *Climatic Change* “Projecting the urban energy demand for Indiana, USA, in 2050 and 2080” by Liz Wachs and Shweta Singh, COPYRIGHT 2019

meet the changing energy demand in response to climate change. According to the US Census Bureau’s classification of urban areas, Indiana is home to 15 cities or parts of cities [64], which contain 77% of the state’s population according to 2010 census numbers (5,036,573 of 6,483,802 inhabitants) [64]. Hence, in this work we focused more narrowly on Indiana’s urban areas and their energy demand, specifically considering how residential and commercial urban energy consumption is likely to shift due to climate change.

The RCP 4.5 scenario assumes the adoption of carbon pricing and other mitigation policies, with emissions peaking near 2040 and stabilizing near 525 ppm CO_2 and 650 ppm CO_2 equivalents [65]. RCP 8.5 is sometimes referred to as a “business as usual” or “baseline” scenario. It assumes that no global greenhouse gas emission mitigation strategy is adopted. Instead, the world population continues growing, reaching 12 billion by 2100, with low levels of economic growth and technological innovation. Thus, fossil fuels present a more economical choice than renewables, leading to a high level of use for coal (cleaner coal technologies like gasification are employed over time) and nontraditional petroleum products [66]. Some criticism of RCP 8.5 as a reference case has emerged since estimates of coal’s availability may prevent its use as a “backstop” fuel in such a scenario [67]. Still, the RCP 8.5 scenario reads as familiar, since it assumes the use primarily of fossil fuels for energy provision while in the policy sphere a higher priority is placed on air pollution than climate change mitigation. Recently in the US there has been much talk of reviving interest in “clean coal.” Indiana, the site of our study, has high levels of coal production (8th among states in the US as of 2015 [68]), and receives the majority (>70% as of Nov 2017 [68]) of electricity from coal power generation plants—Indiana is currently the third largest consumer state of coal in the US, and recently opened a clean coal electricity generation plant (in Edwardsport), so RCP 8.5 indeed presents a relevant storyline here.

In order to estimate urban energy demand, it is necessary to understand the driving reasons behind its changes. Energy demand change is a complex phenomenon

with several driving variables that may change simultaneously, including increased urbanization, population growth, population density change and income increases. The specific questions driving our work were: how a warmer climate would affect urban energy use? What is the time frame for the changes i.e. will most changes happen soon, or later? Where might the largest changes occur in Indiana’s cities? How much certainty is there about these estimates, and what is needed to improve on this?

To address these research questions, two time periods: 2050 and 2080, were examined and compared with 2015 estimates. Energy demand for heating, electricity and transportation in Indiana’s urban areas was estimated by two methodologies, one developed in [33] and the other from [32]. Residential cooling was estimated by a method developed in [69] and refined in [70]. These estimates provide a greater spatial and temporal resolution to the energy demand forecasts published in [63], thus making results more relevant for individuals and stakeholders. While the methods we used here were not developed specifically for this project, the combination of methods we have used allows for projections below national scale, which is poorly represented in the literature. This is one of the only studies that provides projections of energy demand at the city scale including end-uses.

2.2 Background: Modeling Urban Energy Consumption

A robust literature seeks to predict and model energy consumption, including in urban areas. On a national scale in the US, the Energy Information Administration (EIA) makes detailed forecasts according to multiple scenarios on a national level. MARKAL [71] is frequently used at national scale to model supply, and an Indiana-specific version of MARKAL was used in [63]. The long range energy alternatives planning (LEAP) system [72] is also frequently used at national scale. Still, models applicable to a range of places at a higher spatial resolution (subnational, below state level) are lacking. In the US two national studies have focused on urban energy

demand estimation. The Vulcan model [73] was used for a study of US urban areas by Parshall et al. [61]. Vulcan has not been updated after 2002, however, and the work in [61] could not be disaggregated to focus on individual cities.

Brown and Logan [74] purchased proprietary data for use in their study of residential electricity, transportation and fuel consumption in the 100 largest US cities by population. They also performed statistical analysis to find significant predictors for residential carbon footprints. The most recent data source was 2005. Interestingly, Indianapolis had the 3rd highest per capita carbon footprint for residential electricity and fuel use in 2000 and 4th highest in 2005. When electricity alone was considered, Indianapolis was 7th in 2000 and 5th in 2005 [74].

At global scale, Singh and Kennedy sought to model urban energy demand change in response to climate change based on predictive variables [33], with a statistical methodology that is adaptable to any group of cities. The model was developed based on empirical data on energy consumption at city scale along with the estimates of predictor variables calculated at same city scale. The modeling focused on urban energy demand in three major categories: transportation, electricity and heating. Both electricity and heating were found to be dependent on temperature accounted by the variable of Heating Degree Days (HDD), thus directly effected by changing climate. In this work, the cooling energy demand was accounted for in electricity consumption. This model was applied globally for 3436 cities after testing for extrapolations using statistical approach of leverage to caution for any projection errors.

Kennedy et al. [32] classified material flows more broadly in “megacities,” along with including predictive characteristics of variables for energy demand in urban areas, similar to Singh and Kennedy [33]. This work also looked at electricity, heating and transportation, but only heating was tied to temperature, perhaps due to the nature of “megacities” where electricity was mostly driven by urban form and GDP, which were highly correlated. However, both works independently confirmed temperature to be a major driver of heating energy consumption in urban areas.

Cooling Energy Modeling: The contemporaneous trends of development and climate change have led to interest in projecting changes in global adoption of space cooling technologies. In many of the hottest places, people have historically had little access to air conditioning, but this may change in the coming years. Whether, where and how quickly this might change has been the focus of several studies [69,70,75,76]. Cooling is particularly important because in many areas it has a large impact on the peak load despite its relatively small proportion of overall energy use.

Cooling degree days (CDD) has been used as predictor variable for cooling energy estimation since it captures the effective number of days when cooling is required with respect to a baseline temperature that represents thermal comfort for people. Hence, CDD is a good proxy variable for quantifying cooling energy demand as in the model by Isaac and van Vuuren [70]. Sivak [75] found that many of the fastest growing cities had very high CDD, indicating a high potential for future cooling demand in cities in the developing world. Likewise McNeil and Letschert [69] looked at the emerging adoption of air conditioning in the residential sector of developing countries. Isaac and van Vuuren [70] expanded their approach to a global scale for inclusion in the TIMER model. Air conditioners are much more energy intensive (i.e. to achieve the goal of space cooling, air conditioners use a large amount of energy) and expensive than other cooling technologies (e.g. fans). Their energy intensity makes their usage a good proxy for space cooling energy use. McNeil and Letschert noted that ownership of air conditioners is strongly correlated with income, following an S-shaped diffusion curve [69], so that once a certain threshold income level is reached (in [70] it is around \$10,000 per capita), ownership rises rapidly. This income threshold has been met in the US, usually considered one of the areas with the highest adoption of air conditioners. In the US, 87% of homes have air conditioning as of 2015, and 65% of homes have central air [77].

Saturation of air conditioners in a given area is also highly dependent on climate [69] [78] and the interaction of climate and income is even more important [76]. Sailor and Pavlova show a logarithmic type curve for the climate effect, since in

cooler climates people are unlikely to purchase air conditioners, but in hot climates the saturation is near unity [78]. Once air conditioners are available in a household, their usage is highly correlated with climate, with strong increases shown when it is very hot. Davis and Gertler showed in their study of Mexican households that each day with temperatures over 90°F (32.2°C) increased monthly electricity usage by 3.2% [76]. This certainly implies that as climate change results in higher temperatures in certain regions, it will have a direct impact on higher energy demand.

We could not find a model for cooling energy estimation in the commercial sector that could be used at urban scale for the needed projections. Recently in the US, work by Lokhandwala and Nateghi [79] analyzed data from the Commercial Buildings Energy Consumption Survey (CBECS) to determine the variables with predictive capability for commercial cooling load. They note the wide agreement that building area is a determining variable, and look at energy use intensity [kWh/m²], showing that while in the past (2003) [79] and prior [80] CDD was the most predictive variable, principal building activity now surpasses CDD as a predictor. They also note that the predictive capability of CDD has decreased with respect to energy use intensity, most likely due to improvements in efficiency. Still they note that with those improvements, cooling energy use intensity has not decreased.

As part of the IN CCIA project, Nateghi and Mukherjee [81] developed a framework for including climate change effects in energy demand estimates. They estimated an increase in commercial demand for space cooling in Indiana in the same study period, but a decrease in residential demand for space cooling. Their work, however, does not address the spatial variability below the state level.

2.3 Methodology for Energy Demand Change at Urban Scale

2.3.1 Heating, Electricity and Transportation Projections

As mentioned above, Singh and Kennedy [33] (S-K) and Kennedy et al. [32] (K-M) both published regression models that can be used for estimation of transportation,

Table 2.1.: Singh Kennedy (S-K) Model for Urban Energy Estimation. For heating demand, only the heating degree days is a significant variable. For electricity, both heating degree days and inverse population density are significant. For transportation only inverse population density is significant. Inverse population density refers to urban area per capita.

	Heating Degree Days	Inverse Pop Density (ha/cap)
Heating* (GJ/cap)	0.014725	-
Electricity* (MWh/cap)	0.000994	144.7
Transportation (GJ/cap)	-	1374.9

*Adjusted from published model as described in section 2.3.1

electricity and heating energy demand. The models were developed using a regression based approach that tested the relationship of explanatory variables such as gross domestic product (GDP), CDD, HDD, population density and inverse population density with empirical data on energy consumption in a group of world cities. Tables 1 and 2 show the variables proven to be significant predictors along with parameters and regression coefficients for energy estimation in each category for each model. Although these models were developed independently using two different datasets, they showed similar significant predictor variables for each category of energy providing confidence in using this methodology for the forecast of energy demand in urban areas.

Full methodologies as well as data sets for deriving the two regressions are discussed in the source papers. The S-K dataset included cities from all over the world with varying population sizes, densities and stages of development [33]. The K-M model set had 27 cities with a wider geographic range but included only “megacities,” the largest cities in terms of population size in the world [32]. For this reason, the K-M model is used here to provide a benchmark for the total projections for heating, electricity and transport.

Table 2.2.: Kennedy Megacities (K-M) Model for Urban Energy Estimation. Full details can be found in [32]).

	Heating Degree Days	Inverse Pop Density (km^2/cap)
Heating (GJ/cap)	0.02	57 722
Electricity (MWh/cap)	-	21 614
Transportation (GJ/cap)	-	92 858

The S-K model was slightly modified in this work. Since our focus is on the commercial and residential sectors, we excluded a proportion of the heating energy from the dataset based on assumptions of the relative contribution of industry in heating energy demand in those cities. The coefficients included here in Table 2.1 reflect the adjustments for the exclusion of industrial heating. For the electricity modeling, we combined the datasets from the original work in [33] and [32], using the S-K data in the case of duplicate cities. We also added electricity usage from Indianapolis, in order to have a more robust dataset with a higher variability in urban form. The source data for the modified regressions in the S-K model used are available in Tables 1 and 2 of the SI (Appendix B).

To use these models, data for density were required. HDD and CDD were required for all cities, which were calculated based on temperature data from the climate group and GIS based methodology proposed in Singh and Kennedy [33]. Further, population data was necessary in order to calculate total energy consumption in each category for all cities. The data collection and calculations for HDD & CDD are discussed in section 2.3.3.

2.3.2 Cooling

Residential Cooling Estimation A separate estimation for per capita cooling energy consumption was made based on models developed by McNeil and Letschert [69] and Isaac and van Vuuren [70]. Cooling consumption cannot be directly calculated from the regression models described above, mainly because the data used for development of regression models aggregated space cooling energy requirements as simply part of electricity consumption. Cooling makes up a relatively small component of energy use (mainly electricity). Nevertheless, the question of whether increased cooling energy use will outpace declines in heating demand has generated much study (see for example [82, 83]).

The model used here is based on statistical analysis examining both extensive and intensive behavior related to the use of space cooling equipment. The decision to purchase air conditioning units is a long term or extensive type choice. People run the air conditioners more or less in a given year (intensive) based on current weather conditions. Hence, the total energy consumption in this model is a function of both total amount of equipment present and the usage of the cooling equipment.

The total per capita urban cooling energy demand in this model is calculated by equation 2.1, which is from [70] but in a per capita format:

$$T = \frac{P}{h} \times \frac{UEC}{EE} \quad (2.1)$$

In Equation 2.1, T is the total per capita cooling energy use [kWh/capita], h is the household size [people/household], P is penetration [%](the extensive variable—taking into account the proportion of households that own air conditioners), UEC is the unit energy consumption [kWh/household/year] (usage—the intensive variable indicating how often people use their air conditioners) and EE is the efficiency factor [%]. Since, UEC depends on CDD (Cooling Degree Days) and GDP per household i.e., income (I) (See Equation 2.2), the per capita energy consumption depends on both on climate and income change. The UEC model (equation 2.2) was developed by Isaac and van Vuuren, who ran a linear regression on 37 data points to estimate the usage variable, UEC against the explanatory variables of Income (I) and CDD [70]. The maximum value allowed is 3500 kwh/year following [84].

$$UEC = CDD \times (0.865 \times \ln(I) - 6.0) \quad (2.2)$$

In equation 2.2, I is income, approximated by GDP per household. Next, we assume that penetration in the US depends only on climate (CDD) (equation 2.3) as in the original model. Logically, this is true since investment in cooling equipment is driven by the general weather of region, hence households in warm weather (with higher CDD) are more likely to purchase cooling equipments as captured by Equation 2.3 from [69].

$$P = 1 - 0.949 \times e^{-0.00187 \times CDD} \quad (2.3)$$

We present results assuming no efficiency gains as well as results based on a forecast of cooling technology improvement (seasonally averaged COP values—variable EE in Equation 2.1). For 2015 we use a COP value of 3.35, a weighted average of the efficiency values based on cooling stock in US residences from table 22 of the 2017 Annual Energy Outlook [85]. This has been revised from the higher value of 3.81 (given as a 2020 value in Iyer et al. [86]) used in Gotham et al. [63] since we were able to calculate this more accurate value for 2015. We estimate expected efficiency gains in cooling technology by interpolating from predicted efficiency increases in the cooling sector through 2100 given by equation 2.4, where y is the year:

$$EE = -0.0003y^2 + 1.05y - 1092.6 \quad (2.4)$$

This equation was found by plotting the values of 2.4 for 2000, 3.2 for 2020 and 4.39 for 2100 which follow a polynomial improvement given by the Pacific Northwest National Laboratory [87]. These efficiency values for 2050 and 2080 of 4.02 (the Annual Energy Outlook [88] gives a weighted average value of 4.026 for 2050) and 4.39 respectively are included in equation 2.1 following the approach used by Isaac and van Vuuren [70].

Since no city-level data or estimates of energy use are available, the models were run to create baseline estimates for 2015 to be used as reference year. We used the projected changes in CDD for 15 Indiana cities over time, relying on the estimates by the climate group in this issue [89], as the basis for our projections. We also made assumptions about income as described below in section 2.3.3.

2.3.3 Data Collection

Geographical Coverage: The largest city in Indiana is Indianapolis, the capital, whose population was estimated at 2,000,400 in 2015. Indiana is located in the Midwest region of the US, and for the EIA it is in the East North Central region of the Midwest. It can be split into a southern portion that falls in the “mixed-humid” region (according to the Building America Climate Regions), and the northern part of

the state which lies in the “cold” region. The northwest corner of the state includes Gary, which is part of the Chicago metropolitan area. Indiana is bordered to the north by Lake Michigan and Michigan. To the west it borders Illinois, to the south Kentucky, and to the East, Ohio. The cities included in this work range in latitude from Michigan City-La Porte, the northernmost city with latitude 41.7, to Evansville, with latitude 38.0. The list of Indiana’s 15 cities is provided in Table 2.3.

Population: For these urban areas, population projections in five year increments extending to 2050 were available in [90]. Since no population projections were available for 2080, we extended the population numbers to 2080 for each city based on its growth rate from 2045-2050, assuming the annual growth rate for the period of 30 years. The population estimates for each city at each point in the study time period are shown in Table 2.3.

Area and Inverse Population Density: Population density was calculated separately. Where the urban agglomeration’s population resided principally outside of Indiana’s borders (Cincinnati-Middletown, Louisville-Jefferson and Gary Division), density data from [91] were used. For other cities the land area for the named components of each city (i.e. Indianapolis and Carmel cities proper) from county and township level census data [92] was summed to perform the calculations for 2010. The population density was projected forward assuming a 1% yearly decline attributed to the phenomenon of urban sprawling.

Temperatures: As part of the IN CCIA project, temperature projections were made based on 31 global climate models, from which 10 were selected to best capture the range of results. The values were statistically downscaled to 1/16 degree resolution, approximately 5 by 7 km, for the RCP 4.5 and 8.5 scenarios based on the Coupled Model Intercomparison Project, Phase 5 (CMIP5) [89]. High and low daily temperatures from three time periods were modeled: 2011-2040, 2041-2070 and 2071-2100. For this work we took an average for each time period to represent the

Table 2.3.: Cities studied with population figures as used for 2015, 2050 and 2080. Indianapolis, the largest city, is forecast to increase significantly in population over this period.

City	2015	2050	2080
Bloomington	166,210	198,766	224,365
Cincinnati*	42,063	47,352	45,471
Columbus	79,194	88,112	93,421
Elkhart-Goshen	204,959	248,764	286,441
Evansville*	272,443	292,128	297,881
Fort Wayne	429,967	497,948	544,459
Gary	723,879	778,362	801,495
Indianapolis	2,000,400	2,584,097	3,018,845
Kokomo	82,029	70,080	59,267
Lafayette	211,029	251,032	278,182
Louisville*	287,666	330,988	353,713
Michigan City-LaPorte	112,111	106,949	99,697
Muncie	117,220	109,859	103,194
South Bend-Mishawaka*	268,533	274,940	276,554
Terre Haute	173,132	166,141	157,087

* refers to the Indiana portion of larger metropolitan area

three years of 2015, 2050 and 2080. Note that since these forecasts were not developed specifically for use at urban scale, the urban heat island effect may not be fully shown. Using latitude and longitude, the distance from cities was calculated using the great circle distance method (see description in [33]), and temperatures recorded in any spot less than 10 miles from the city's latitude and longitude were averaged to compute maximum temperature (t_{max}) and minimum temperature (t_{min}) values for the city. Table 2.4 shows the temperature increases by 2080 for the cities studied under both scenarios. Highlighted cities as well as Fort Wayne all sit above 41 degrees latitude, so represent the northernmost cities.

For RCP 8.5, by 2050 minimum temperatures are projected to rise by 1.21 (Apr and Nov) to 2.08 degrees C on average in the cities studied. Maximum temperatures increase on average 2 degrees or higher for Jul-October, with the highest increases seen in August, where some cities see an increase of more than 3 degrees (Bloomington and Cincinnati are at 3 even, Columbus and Kokomo are over 3 degrees). The 4 northernmost cities see above average minimum temperature rise in the winter (Dec-Feb), but not during the rest of the year.

By 2080 average minimum temperatures are projected to rise by between 2.87-4.7 degrees in the cities studied. In all time periods and scenarios except Dec-Jan-Feb in RCP 4.5, the maximum temperatures increase more than the minimum temperatures. In winter the northernmost cities see the highest increase in minimum temperature. The increase in maximum temperatures is more pronounced, with average increases ranging from 3.23 degrees in April to 5.92 degrees in August.

The largest temperature increase forecast in this model was for the Jun-Jul-Aug period in RCP 8.5, which shows more than a 5 degree increase for the cities. Cities with projected maximum temperature increases above 6 degrees (all > 6 °C increases were seen in the month of August) are Cincinnati, Columbus, Fort Wayne, Indianapolis, Kokomo, and Muncie. In both scenarios pronouncedly larger increases in temperature are seen in summer months by 2080, as compared to winter and transition seasons.

RCP 4.5 temperature increases forecast for the cities were less than 2 °C except in the Jun-Aug time period. RCP 8.5, on the other hand, shows temperature increases over 3 °C in all the time periods. August heat increases are more pronounced in the more southern or central parts of the state (highest in Indianapolis), but for other months the 4 northernmost cities generally see the highest temperature increases, with increases at or above the median and average in all months except April, where Gary is just below these markers.

Table 2.4.: Temperature changes in °C from 2015 to 2080 under the two scenarios considered for all cities studied. Average increases in high (h) and low (l) temperatures for each 3-month period are shown. The northernmost cities are shaded. Temperature increases higher than 4°C are shown in bold.

City	Temperature Increase in °C 2015-2080															
	Dec-Jan-Feb				Mar-Apr-May				Jun-Jul-Aug				Sep-Oct-Nov			
	RCP 4.5		RCP 8.5		RCP 4.5		RCP 8.5		RCP 4.5		RCP 8.5		RCP 4.5		RCP 8.5	
	h	l	h	l	h	l	h	l	h	l	h	l	h	l	h	l
Bloomington	1.63	1.61	3.27	3.07	1.40	1.32	3.30	3.05	2.21	1.72	5.24	4.26	1.75	1.44	4.55	4.07
Cincinnati	1.61	1.60	3.22	3.07	1.40	1.32	3.31	3.05	2.19	1.74	5.33	4.31	1.77	1.43	4.59	4.12
Columbus	1.61	1.63	3.25	3.06	1.41	1.33	3.30	3.06	2.21	1.73	5.24	4.24	1.73	1.44	4.56	4.05
Elkhart-Goshen	1.71	1.82	3.56	3.65	1.51	1.35	3.45	3.07	2.24	1.71	5.13	4.27	1.85	1.37	4.62	3.89
Evansville	1.61	1.55	3.16	3.05	1.41	1.26	3.25	2.98	2.08	1.65	4.97	4.19	1.74	1.38	4.44	4.03
Fort Wayne	1.69	1.73	3.48	3.43	1.50	1.35	3.42	3.07	2.25	1.72	5.24	4.31	1.83	1.38	4.65	3.98
Gary	1.77	1.83	3.63	3.68	1.50	1.32	3.45	3.03	2.14	1.73	4.91	4.15	1.87	1.42	4.54	3.97
Indianapolis	1.66	1.65	3.35	3.17	1.43	1.33	3.33	3.04	2.23	1.73	5.27	4.26	1.78	1.42	4.59	3.99
Kokomo	1.72	1.67	3.49	3.35	1.42	1.34	3.36	3.04	2.31	1.78	5.24	4.31	1.87	1.41	4.69	4.05
Lafayette	1.72	1.74	3.53	3.42	1.44	1.31	3.35	3.02	2.25	1.73	5.12	4.22	1.89	1.40	4.63	3.95
Louisville	1.61	1.65	3.21	3.12	1.41	1.32	3.29	3.03	2.18	1.70	5.12	4.23	1.75	1.42	4.51	3.96
Mich. Cty-L. P.	1.73	1.84	3.60	3.68	1.51	1.33	3.44	3.07	2.22	1.72	5.06	4.20	1.89	1.39	4.61	3.91
Muncie	1.67	1.68	3.43	3.27	1.42	1.34	3.35	3.08	2.25	1.72	5.30	4.27	1.81	1.40	4.67	4.01
South Bend-Mish.	1.71	1.82	3.56	3.65	1.52	1.35	3.46	3.07	2.24	1.71	5.14	4.26	1.86	1.37	4.60	3.88
Terre Haute	1.69	1.61	3.37	3.09	1.43	1.28	3.30	2.94	2.12	1.69	5.03	4.20	1.80	1.37	4.54	3.93
Average	1.68	1.70	3.41	3.32	1.45	1.32	3.36	3.04	2.21	1.72	5.16	4.25	1.81	1.40	4.59	3.99

For the modeling work, temperature data was needed to calculate HDD and CDD. We first calculated the average monthly temperatures (t_{avg}) from t_{max} and t_{min} . Then HDD was calculated using Equation 2.5 around a base temperature of 18°C.

$$HDD = \sum_{n=1}^{12} (18 - T_{avg}) D_n \quad (2.5)$$

Where D_n is the number of days in the month, n. When the average temperature is higher than 18 for a given month, HDD = 0. The CDD calculation was done with the same equation, but the argument in the summation has the reverse signs.

Household Size: For cooling energy estimation, average household sizes were obtained for each city from the United States Census Bureau’s QuickFacts database [93]. Since the rate of change in household size has been very small and includes fluctuations, it was assumed constant for 2050 and 2080.

Gross Domestic Product : The US Census Bureau provides estimates of GDP per capita on a city level. They were assumed to rise 1% per year. Since GDP by household was needed, the GDP per capita values were multiplied by household size.

2.4 Results and Discussion

Per Capita Energy Demand Projections: Fig. 2.1 shows per capita heating and electricity projections for the cities studied using the S-K method as well as cooling per capita both with and without efficiency gains in cooling equipments. Per capita heating demand is expected to fall in Indiana’s cities by 7.8-13.3% by 2050 and 12.9-27.4% by 2080 (bounds correspond to the RCP 4.5 and 8.5 scenarios respectively). The spatial variation among cities for per capita heating demand declines over time as both scenarios project a more similar climate among IN cities over time. Modeled electricity demand is much less dependent on climatic shifts as the primary driver of electricity use as predicted by our model is decreasing inverse density due to urban sprawl. Per capita electricity usage is projected to increase over time by quite a

bit—29.8-30.98% average increases are expected by 2050 and 64.38-67.56% increases are expected by 2080. Still the tight bounds on these estimates are due to the low impact of climate. The higher electricity costs for RCP 4.5, which has cooler temperatures than RCP 8.5, are due to electric heating’s inclusion in the S-K model dataset that is, all electricity end uses are accounted for and in the cities modeled electric heating will be larger than air conditioning. In part to overcome that limitation, we looked more closely at the end use of space cooling.

In the case of cooling, we evaluated two cases. In one case we held the efficiency of cooling equipment constant for future scenarios, whereas in the second case we assumed improvements in efficiency. In Evansville, the urban area that currently has the highest projected per capita cooling energy use, as well as Bloomington, Cincinnati, Columbus, Indianapolis and Louisville the per capita use falls in both time periods in the high efficiency (HE) case. Other cities show an increase, most notably in the northern half of the state. Michigan City-La Porte shows the most dramatic increases, between 25-54% higher in 2050 and 51-63% higher in 2080 in the HE cases. With no efficiency improvements both Michigan City and South Bend would see over 100% increases in per capita cooling by 2080 in both the RCP 8.5 scenario.

Most striking is the falling standard deviation in cooling energy use, from 29-61% lower across all scenarios in 2050, and 54-69% lower by 2080, showing that the overall profile for Indiana would be more homogeneous in terms of cooling needs under climate change. Accordingly, the penetration of air conditioners averaged 74.2% in our modeled estimates for 2015, but rises to over 90% in all cities by 2080 in the RCP 8.5 scenario. This is supported by [89], who predict an increase in the number of “hot days,” days with a high temperature of over 35°C, across all Indiana urban areas included in their analysis, from historical numbers of 2.5-10.5 to a range of 58.6-98.2 days in the RCP 8.5 scenario. Full results by city are shown in Tables 5 and 6 in the supplementary information. The results indicate changing spatial patterns of energy

demand in the state which will have implications on the grid load and also cost of energy specifically for cooling demand.

If the urban residential cooling demand competes with industrial demand (in some parts of Indiana, manufacturing industries such as corn-ethanol manufacturers are the major consumers of electricity in cooling towers) a major economic pricing issue may emerge, forming both a social and economic challenge. Hence, it is necessary to have better and accurate understanding of spatial changes in the energy demand due to climate change.

Total Energy Demand Projections: If population growth is included we forecast an increase of energy use for space cooling in the residential sector for urban areas of Indiana. Heating demand, however, would increase in RCP 4.5 over time and in RCP 8.5 would actually decline as the climate effect overwhelms the effects of population growth, as shown in Fig. 2.2. Our population predictions are more uncertain for 2080, however. For overall electricity demand, which increases in both scenarios, inverse density and population growth dominate the climate effects.

Cooling demand increases vary spatially, as shown in Fig. 2.3. Here it is also clear that most of the increased cooling demand in both scenarios comes by 2050.

Indianapolis is already a key driver of urban energy demand in Indiana currently accounting for 41% of Indiana’s urban electricity use, 38% of urban heating, and 42% of urban transportation energy demand, according to our model. The population and growth trends anticipated over the course of the studied timespan are expected to intensify this, with Indianapolis driving 48% of Indiana’s urban energy demand by 2080. Indianapolis’ portion of total cooling can also be clearly seen in Fig. 2.3, where it dominates the contributions. Indianapolis’s increased cooling demand represents between 44-56% of the total increases in the higher efficiency scenario and 43-50% of the increases in the same efficiency scenario.

As the heating needs shrink and urban density declines, transportation is expected to represent an increasing share of the total energy use. Fig. 2.4 shows this change

over the time periods studied from the S-K model results. The K-M model shows the same trend, with transport rising from 38% of modeled energy use in 2015 to 46-47% in 2080.

2.4.1 Limitations and Model Robustness

One of the major limitation of urban energy demand projections is the lack of data at this level of fine resolution. While most data on energy consumption are aggregated at state or national scale, energy consumption is centered in urban areas. Hence, a better energy demand projection responsive to changing factors such as climate change, economic prosperity, demographics etc, will need to be made at finer scale such as urban scale. The existing S-K and K-M models were made possible by projects that supported data collection at such a fine scale and both these studies have cautioned about the use of these models for non-representative cities. Most statistical models run into the issue of extrapolation if the models are used for projections beyond the underlying modeling data. The models used here were based on a global set of cities with a generally higher population density. To address this limitation and ensure the applicability of the S-K model to Indiana cities a hidden extrapolation test was run as used by Singh and Kennedy [33] and also described in [94]. This test defines the minimal convex area containing all regressor data points and determines whether the model results fall inside the area, since if they are outside extrapolation takes place. In the future, fine scale data on urban energy demand would help improve the applicability of the S-K model, since regressions could be run with regional specificity. Still, according to the extrapolation test, for 2050 over 90% of the cities modeled are within the reasonable bounds of the S-K model. As time goes on our uncertainty about the parameters increases as does the amount of extrapolation present in our model. All extrapolation test results are provided in Appendix B, section 3, Tables 7-10.

HDD and CDD are calculated from average monthly temperatures providing an underestimation if calculated using daily temperatures, since some of the variation is lost. This means that peaks in temperature are lost, as are any effects from build-up of temperature. Results from [33] show that this still represents the trends adequately, although finer time scale resolution will improve accuracy. The urban heat island is also not fully represented by the temperature forecasts, so may lead to underestimates of cooling and overestimates of heating demand in urban areas.

Cooling energy use is strongly affected by the efficiency of space cooling equipment. In the calculations initially done as reported in [63] our baseline data for 2015 was calculated using an efficiency value of 3.81, hence the trend lines shown here differ in terms of magnitude in the no efficiency improvement scenario, and in terms of relative increase in the high efficiency scenario. For 2050 and 2080 projections we relied on estimates of technological improvements from [87], but this may be conservative. The high efficiency scenario from GCAM [86] includes an efficiency factor of 7.03 for 2050, much higher than the factor of 4.02 used in our model. Using this factor for 2050 and 2080 would show decreased cooling demand in all years and scenarios, ranging from a 14% average decrease in 2080 for RCP 8.5 to a decrease of 32% in 2050 for RCP 4.5. Again there is spatial variability, with the highest increase (26%) shown in Elkhart-Goshen, one of the northernmost cities with a very moderate climate currently, with a corresponding decrease of 49% in Kokomo, which for 2015 shows a higher penetration of air conditioning than more northern cities (RCP 8.5 scenario, 2080).

2.5 Conclusions

Urbanization drives energy demand patterns throughout the world, hence most countries are now focusing on future strategies based on urban demand changes. Climate change impacts will differ in urban areas within the same region, however, due to their specific climatic conditions. Hence, coupling the results from downscaled climate change models with urban energy demand models is necessary to provide

reliable information about impact of climate change at fine scale. This will improve the strategies for addressing climate change impacts.

This work is an initial attempt to understand the spatial changes in energy demand in Indiana’s urban regions and to quantify the demand changes in response to long-term projections related to climate change. The underlying temperature changes show higher maximum and minimum temperatures, with the summer maxima outpacing other increases. Warmer winters will be seen, with more of the change in winter happening in the northernmost parts of the state. Indiana’s winter climate loses some of its spatial variability in cities as the state as a whole becomes much warmer, see also table S1 in [89]. As described in section 2.4.1, the projected heating or cooling demand may be lower than seen elsewhere since the CDD and HDD estimated are reduced when an average monthly temperature is used rather than calculated with higher temporal resolution. Yet in previous work HDD estimated this way has been shown to adequately demonstrate the trend. In the case of cooling, we still show all cities using the maximum cooling energy per capita by the end of the study period.

In terms of energy demand, this means a lower heating but a higher cooling bill. While we do expect an overall decline in energy costs due to climate change for the residential sector, a general projection for the commercial sector was not done. If we consider data from the most recent CBECS report [95] together with our classification of cities in terms of HDD and CDD by proxy using 2014 real temperatures, Indiana’s cities move from the category of 11% of electricity in the commercial sector devoted to cooling to the category of 20-27% of electricity devoted to cooling. Nateghi and Mukherjee [81] estimated an increase in cooling energy demand for the commercial sector of 5.1-5.4% during the same model period. So while we were not able to model the urban portion of the commercial cooling, it is likely to increase.

A recent study that performed a detailed simulation of energy use by buildings in the eastern region of the US found similar results in terms of overall energy use—lower heating loads and increased cooling energy use in buildings [82]. They also found, however, that the additional cooling load would result in additional generation ca-

capacity needs, particularly in Minnesota, where a projected 23% increase in cooling would result in more than 100% of increased electricity capacity generation. We have not studied this issue since we modeled energy demand totals, but spatial trends here may indicate the need for closer study. By the end of the study period we forecast a per capita cooling load in northern Indiana cities comparable to current cooling loads in southern Indiana cities except in the highest efficiency scenario, which may have ramifications for generation capacity in these areas. In fact, most of the increase happens by 2050, so within the planning horizon.

The S-K model results show that based on current usage trends, transportation takes up an increasing portion of the energy usage over time. But this has to be put in context in terms of other large scale changes that may occur, such as electrification of transport. Currently electric vehicles make up a small portion of the fleet, but signs point to a potentially precipitous increase. A recent study [96] looks at the potential for electric vehicles and the autonomous technology to change the business model for transportation, causing a rapid shift from the car ownership model to a transportation services model. Such a shift would allow electric vehicles to act as storage capacity for renewables.

This study shows that much of Indiana’s energy needs will come in urban centers, particularly Indianapolis. Transportation will become increasingly important as heating needs diminish and cooling needs are expected to increase. Improvements in efficiency may modulate demand increases from cooling.

More data on urban energy demand and usage would be helpful in order to develop modeling tools with higher spatial resolution. Further, improving the demand change model to include urban heat island effects would further improve the accuracy of demand projections. Commercial cooling models are limited as well.

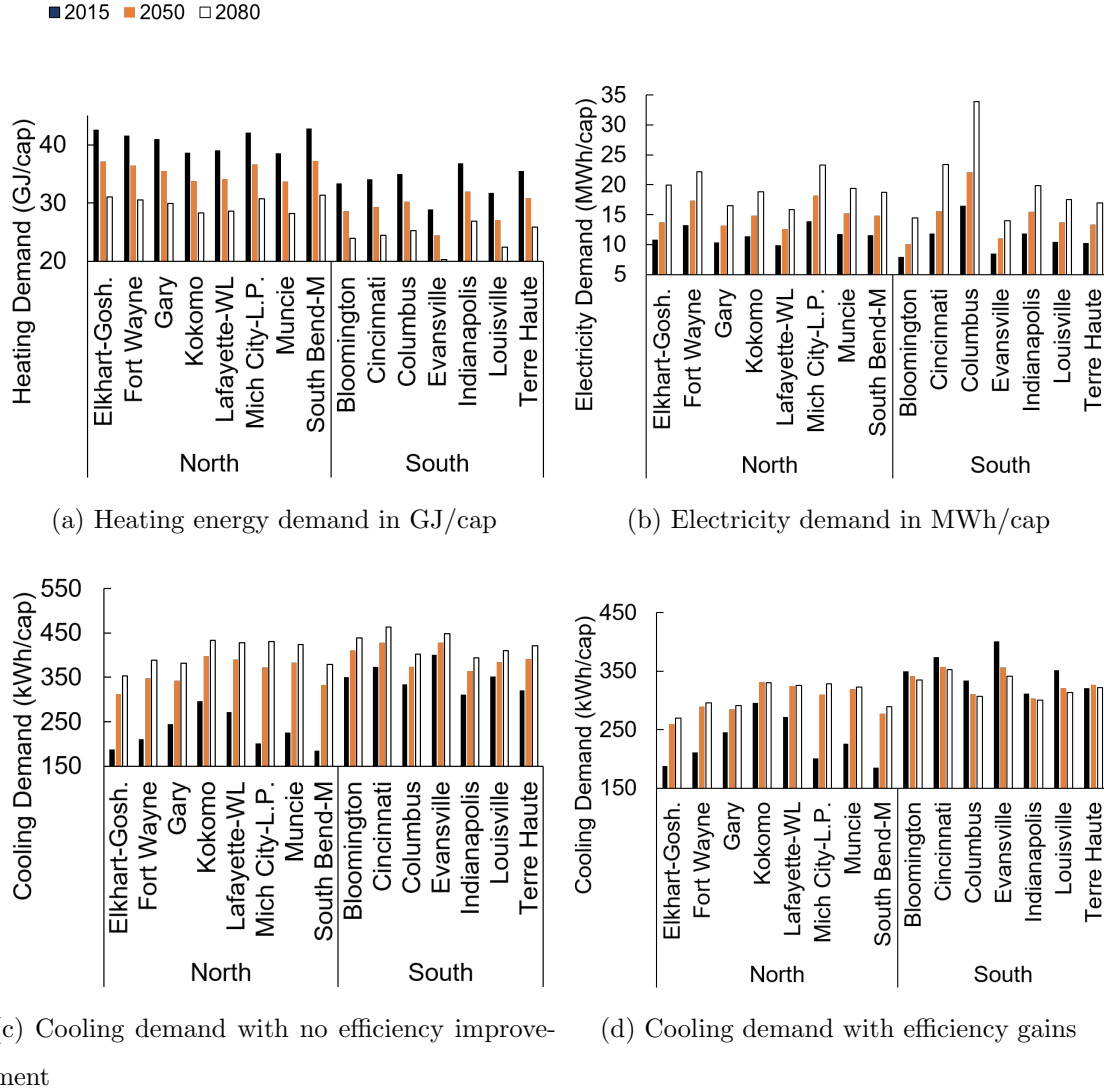


Fig. 2.1.: Per capita urban residential and commercial heating and electricity projections using the revised S-K model for each city are shown in a and b for the RCP 8.5 scenario. The distinction between north and south is with respect to 40 degrees latitude. Heating demand falls steadily in all cities whereas electricity demand rises. Urban residential per capita cooling estimates are shown in c and d with and without efficiency gains. Most cooling demand changes occur by 2050 with smaller changes through 2080. When efficiency gains are included in some cases, particularly in the southern cities, cooling demand falls from 2015-2080. Full data for figures as well as for the RCP 4.5 scenario is available in Appendix B, Tables 3-6.

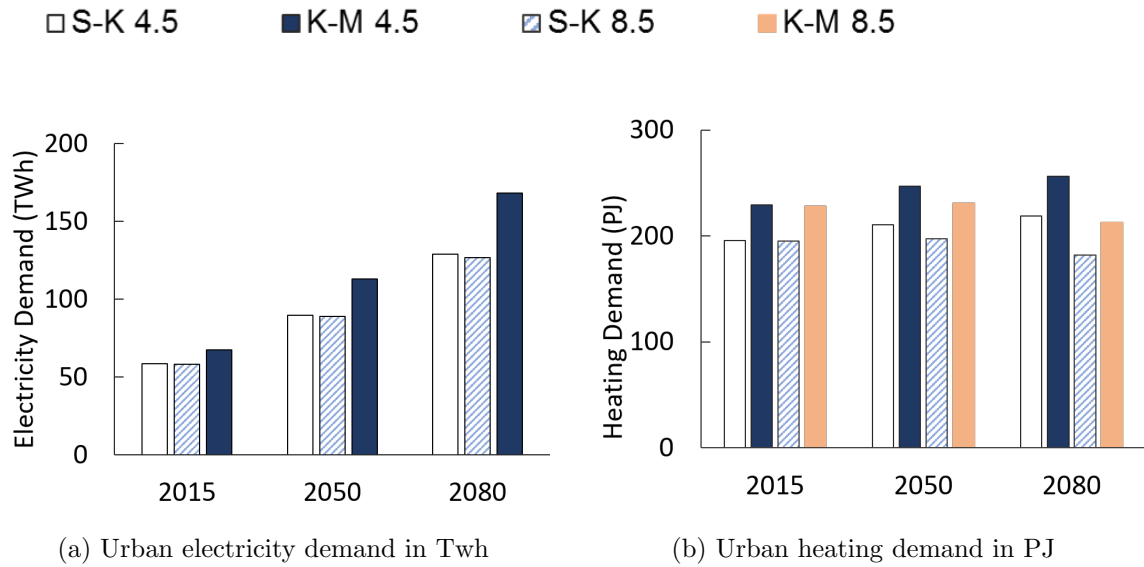


Fig. 2.2.: Total electricity and heating demand are shown as modeled by the two techniques. Electricity shows consistent growth in both models, while heating demand falls in the RCP 8.5 scenario, even accounting for population growth. Note that in the K-M model there is no difference between the electricity projections based on temperature, so RCP 8.5 and 4.5 give the same results. Growth for electricity demand is also very similar between the two scenarios in the S-K model.

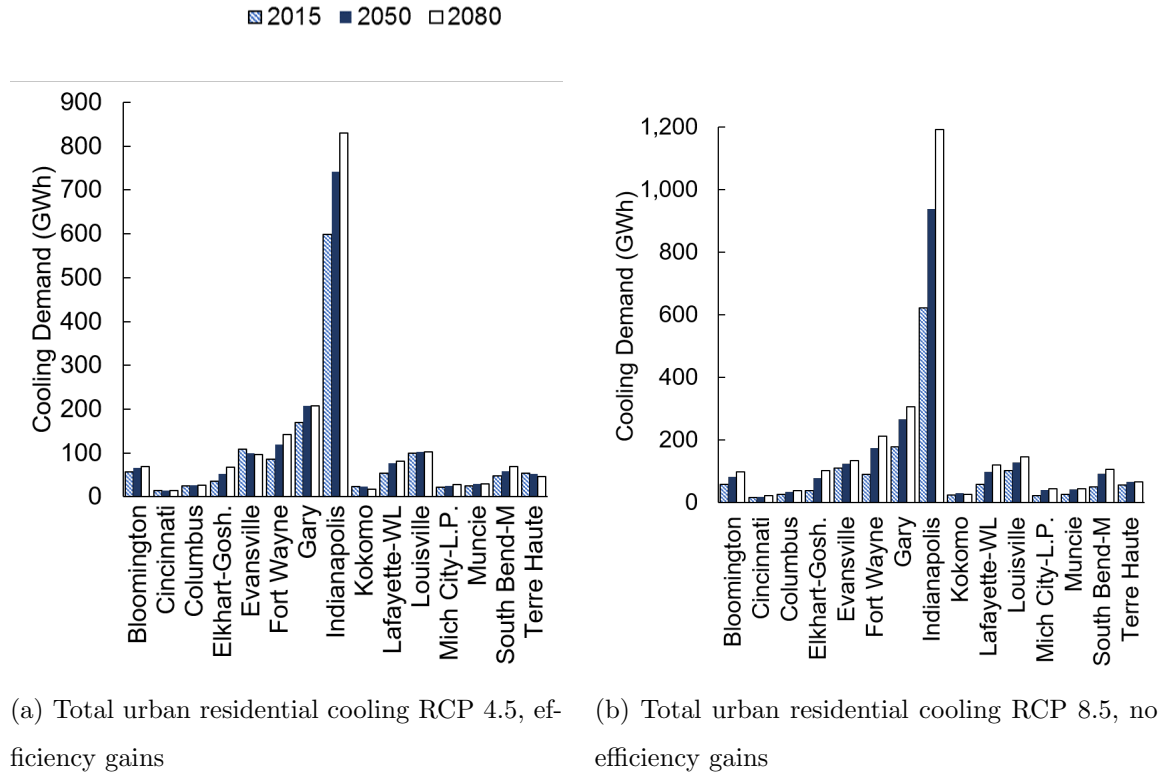


Fig. 2.3.: Projections for total cooling demand (GWh) by city are shown for the RCP 4.5 scenario, including the efficiency improvement assumption (so the most conservative estimate) are shown on the left, to contrast with the most aggressive estimate given by RCP 8.5 with no efficiency gains, shown at right. The sequence and shading denote the years in the study. When population is taken into account, most increases are still primarily seen from 2015-2050, with flatter increases from 2050-2080, and absolute decreases for Evansville, Kokomo and Terre Haute in the conservative scenario. Indianapolis dominates the total demand here due to its large population.

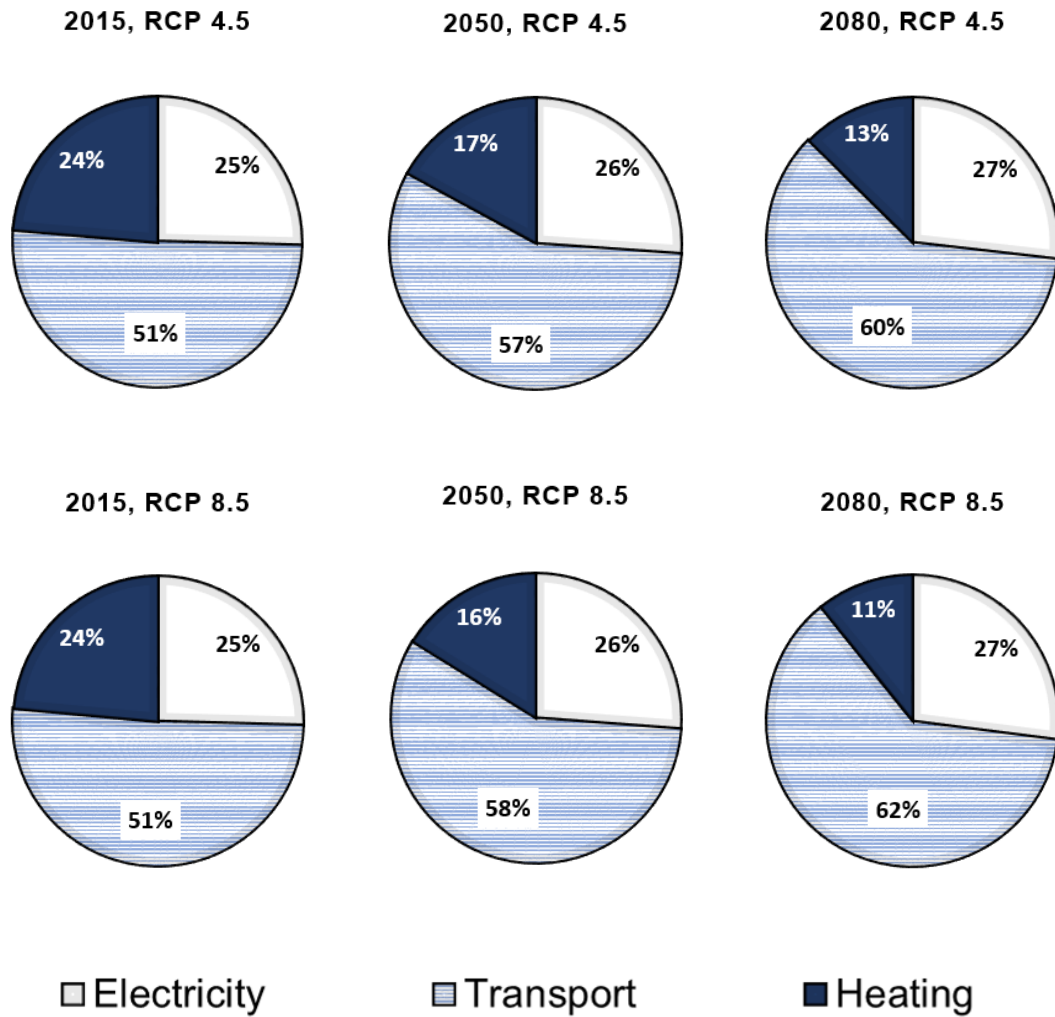


Fig. 2.4.: Changing energy use categories over time forecast using the S-K model. Forecasts are for residential and commercial energy demand. Electricity should include cooling, but the projections for cooling are from a different methodology so are not indicated here. Also, since cooling projections are only for residential, they will represent a small portion of the total electricity demand shown here.

3. RELIABILITY VERSUS RENEWABLES: MODELING COSTS AND REVENUE IN CAISO AND PJM

3.1 Introduction

As climate change concerns have intensified, electrification of industry, transportation and heating have been explored as possible means to reduce or eliminate greenhouse gas emissions from these sectors (see [7, 8] among others). US electric grids, however, are still based primarily on fossil power production, and renewables accounted for just over 12% of primary energy production in 2018 [9]. As recently as 2018, the majority of new generation added to the grid was natural gas-based [10], with technology lifetimes that likely extend 30-60 years into the future¹.

In their seminal paper, Wüstenhagen et al. posited three critical hurdles for the adoption of renewable energy technologies: social, community and market acceptance [14]. Assuming that market acceptance is the limiting factor to the adoption of renewables, this study compares costs and profitability of generating technologies in two US markets. The paper is organized as follows: section 3.2 presents background for the study with literature review. Methods, introducing a framework for the study and placing it into the testbed regions of the California Independent System Operator (CAISO) and PJM, are explained in section 3.3. Results are presented in section 3.4, and discussed and interpreted in Section 3.5. Findings are summarized in section 3.6.

¹This is an assumption based on ages of recently retired plants. See [12] for discussion of recent power plant retirements and probable causes and drivers. Their analysis showed that ages of recently retired natural gas steam turbines mostly ranged from 40-60 years old, combustion turbines were 40-50 years old, and combined cycle plants were 30-40 years old.

3.2 Background and Literature Review

Due to the importance of energy for development and meeting basic needs, as well as to the dynamic nature of the energy system, many models have been developed, notably MARKAL, TIMES, MESSAGE and TIMER [37]. Cost optimization is generally the central mechanism of energy systems models, underlying half of the energy forecasts developed for the 5th meeting of the Intergovernmental Panel on Climate Change [97]. Real solutions implemented in UK electricity markets deviated substantially from the cost-optimal solutions projected, however [97].

Joskow noted that while many energy models used levelized cost of electricity (LCOE) as a comparative metric, metrics such as net present value (NPV) were needed to account for dispatchability of different technologies [45]. Reichelstein and Sahoo applied correction factors to the LCOE to account for price differences for generated electricity [98].

The treatment of individual technologies by cost, environmental and revenue metrics is compared. Including the revenue side allows tracking of the hurdles for renewable development and the likely paths for the deployment of the renewables transition. NPV calculations are scarce in the literature. The California Energy Commission [99] model is specific to California and assumed a different price for each technology according to its break-even costs. The National Energy Modeling System is difficult to adapt to state level analysis and uses proprietary data. The ReEDS model [100] results are used in the National Renewable Laboratory's Annual Technology Baseline (ATB), which does not include NPV estimates and has very limited regionalization. For the purposes of this study, therefore, a model is developed that integrates the suggestions of Joskow [45] and Reichelstein and Sahoo [98], but can easily be used to understand the current situation in PJM and CAISO vis-à-vis commonly considered generation technologies.

Many US markets have implemented capacity remuneration mechanisms. The consideration of these mechanisms in the scientific literature tends to focus on theo-

retical design, with a shortage of empirical data² Electricity is treated as “perfectly substitutable” in these works, so welfare considerations assume that no additional costs are borne by the marketplace regardless of the additional carbon footprint of the technologies. PJM’s Reliability Pricing Model (RPM) is included, making one of the only examinations based on empirical data.

3.3 Methods

3.3.1 Testbed

Two US regions with very different profiles are studied. The California Independent System Operator (CAISO), powers California and a small area of Nevada. Solar already provides a large portion of California’s electricity, and coal provides less than 1%. Geothermal and solar thermal technologies are viable here. Capacity is guaranteed by obligating load-serving entities to ensure that they have access to the capacity required by their customers [102]. PJM is the regional transmission organization covering the Mid-Atlantic extending inward to the Midwest and down to the Southeast. PJM’s solar PV resource is less favorable than in CAISO, and wind speeds generally lower than 5.5 m/s [103] leave most of its territory outside traditional hubs for on-shore wind. Coal mining and hydraulic fracturing are prevalent, with the Marcellus Shale providing the largest portion of the US natural gas resource. PJM’s generation mixture has been shifting from roughly 1/3 nuclear, 1/3 coal and 1/3 natural gas toward natural gas. PJM’s RPM is a capacity auction operating 3 years ahead of time and with balancing auctions 20, 10 and 3 months before deployment [104].

3.3.2 Modeling Framework

Two methods of are employed to compare generating technologies: LCOE and environmental cost minimization, and NPV calculations. The optimization is performed

²Empirical data is included in the analysis of [101].

with no cap on solar PV and onshore wind and then constraining their combined total at 30%, 50% and 70% of the total to simulate a perceived technical reliability need³. Various scenarios for NPV calculations are explored: generating lifetimes of 20, 30 and 40 years in both regions, inclusion/exclusion of renewable energy credits (RECs) in PJM and a consideration of the effects of the minimum offer price rule (MOPR) extension.

3.3.3 Optimization Description

The optimization is modeled as a discrete problem using a minimization version of the bounded knapsack problem. Costs include the LCOE, human health scores, and greenhouse gas emissions⁴. Genetic algorithms were used to provide a variety of solutions, thus reflecting the multitude of decision-making processes and the lack of certainty for costs. The problem is formulated:

$$\begin{aligned}
 \min \quad & C(x) = \sum_{j=1}^n \sum_{i=1}^m c_i x_{ij} \\
 \text{s.t.} \quad & \sum_{j=1}^n a_j x_j \geq D \\
 & S_j - x_j \geq 0 \\
 & x_j \geq 0
 \end{aligned} \tag{3.1}$$

Where c represents costs, subscript i represents the type of cost (human health, greenhouse gas emissions, or LCOE), x is number of plants, for technology j . Available capacity (nameplate capacity discounted by capacity factor), is denoted by a , and total demand is D . The supply of a given technology (S_k) must not exceed its limits. A need of 10,000 MW was selected so that large nuclear plants could still appear.

³The midpoint of 50% was chosen based on the assertion by [105] that a grid with more than 50% VRE in any instant becomes inverter-dominated.

⁴Energy return on investment was examined as well as a constraint, but was ultimately excluded since it turned out not to affect the outcomes (see Appendix C, section C.5 for discussion of this metric).

Plant capacities were rounded so that size would not bias adoption. The rounding mechanism used to determine capacity, p , is shown by:

$$p = \begin{cases} 1 & \text{if } cap_{name} \times cf < 5 \\ roundToMultiple(cap_{name} \times cf, 10) & \text{if } 5 \leq cap_{name} \times cf < 100 \\ roundToMultiple(cap_{name} \times cf, 50) & \text{otherwise} \end{cases} \quad (3.2)$$

Where cap_{name} is the representative nameplate capacity chosen to represent the given technology, and cf is the average capacity factor for the technology based on usage data. This gave distributed solar and hydro a p value of 1, whereas other technologies are multiples of 10 or 50, depending on size.

The VRE constraint is:

$$vD - a_{solar}x_{solar} - a_{wind}x_{wind} = 0 \quad (3.3)$$

Where v refers to the portion of demand met by VRE. MATLAB's multiobjective optimization toolbox was used, which uses the non-dominated sorting genetic algorithm II (NSGA II). Parameters are shown in table 3.1.

Table 3.1.: Parameters used for optimization. Link to full code in Appendix C

Parameter	Value
Number of experiments	20
Population Size	150
Maximum Generations	200
Tolerance	1e-16
Representation	Integer
Crossover	Arithmetic mean of two parents, integer
Mutation	Gaussian integer

3.3.4 Net Present Value

NPV is calculated by adding the discounted profits over the course of the project's lifetime (L) as incurred in each time period (t):

$$NPV = \sum_{t=1}^L \frac{Profit_t}{(1 + r_{disc})^t} \quad (3.4)$$

Where r_{disc} refers to the discount rate, the after tax weighted average cost of capital (ATWACC). Profit is calculated according to:

$$Profit_t = R_t - C_{var,t} - C_{fix,t} - T_t \quad (3.5)$$

Where R is revenue, C_{var} is variable costs, C_{fix} is fixed costs, and T is taxes.

Costs

Fixed Costs

Fixed costs are incurred regardless of how much the plant operates over a given year. Fixed costs are calculated by:

$$c_{fix,t} = c_{OM,t} + T_{property,t} + c_{Ins,t} \quad (3.6)$$

Where $c_{Ins,t}$ is the insurance cost, $T_{property,t}$ is the property tax, and $c_{OM,t}$ is the operations and maintenance cost (increasing with inflation), all for t, the year studied. For all generating types except nuclear, the insurance cost is the product of an assumed insurance rate with the assessed value of the asset. The assessed value is the original installed cost (approximated by the overnight cost) with the depreciation deducted. By the end of the generating lifetime (assumed at 30 years for all generation types), the asset is fully depreciated. Thus, the insurance cost decreases every year. Insurance costs for nuclear plants are governed by the Price-Anderson Act. Their costs are estimated at \$1.3 million annually per site (increasing with inflation).

A depreciation schedule for the assessed value for property tax purposes is assumed and the yearly property tax (ad valorem) is the product of the installed cost, the depreciation percentage by year, and the property tax rate assumed.

Variable Costs

Variable costs $c_{var,t}$ depend on the plant's level of operation. Here they are calculated by:

$$c_{var,t} = c_{fuel,t} + c_{ghg,t} \quad (3.7)$$

Fuel costs, $c_{fuel,t}$ are the product of the heat rate, fuel price and assumed generation of the technology in the given year. Fuel prices are assumed to rise with inflation. Greenhouse gas emissions costs $c_{ghg,t}$ are the product of generation, GHGe/MWh and the carbon price in the given area. Carbon prices are assumed to rise with inflation. Variable operations and maintenance costs are omitted in the interest of parsimony.

Investment Costs

Overnight capital costs are used to represent installation costs. These are financed by a combination of debt and equity. Investment costs are calculated using MATLAB's `payper` function to compute the periodic payment of a loan, so an assumption is made that the loan payment will be equal for each month in the lifetime of the loan:

$$I_t = \frac{r_{debt}(OCC \times Debt_{portion})}{1 - (1 + r_{debt})^{-n}} \quad (3.8)$$

Where r_{debt} is the interest rate assumed for debt, OCC is the overnight capital costs, $Debt_{portion}$ refers to the plant's capital structure, the portion of the OCC paid by debt, and n is the debt period in years.

State taxes are calculated by:

$$T_{state,t} = r_{state} \times (Income_t - (Int_t + Dep_{state,t})) \quad (3.9)$$

Where r refers to the tax rate, $Income$ is the net income, Int_t refers to the interest portion of the debt payment, and Dep refers to the depreciation loss for the given year. The depreciation lifetime for state taxes is assumed to be 20 years. The total annual debt payment, I_t , was calculated in equation 3.8. Its interest portion changes over time, and is calculated by the following algorithm:

Algorithm 1 Calculate Int_t

```

for  $t = 1:L$  do
    Interest payment =  $r_{debt} \times$  loan amount
    Principal portion =  $I_t - Int_t$ 
    Loan amount = Loan amount – Principal portion
end for

```

The maximum of 0 or the calculated state tax is used.

Federal tax is calculated by:

$$T_{fed,t} = r_{fed} \times (Income_t - (Int_t + Dep_{fed,t})) \quad (3.10)$$

The depreciation lifetime for federal taxes is assumed to be 5 years, a simplification since the recovery period ranges from 5-20 years depending on fuel source, with renewables and natural gas on the low end and nuclear and coal on the high end [106].

Revenue

Generators receive revenue from electricity sales, resource adequacy commitments, ancillary services and subsidies. Resource adequacy provisions exist since it is theoretically possible for supply to be insufficient to meet demand. California's resource adequacy provision is met by load-serving entities. In PJM it is met by the RPM (section 3.3.1). Some generation technologies are eligible for subsidies including RECS. Ancillary services are ignored here since they typically make up a small portion of the cost of energy (see tables C.2 and C.1 in appendix C).

Price

Revenue is the product of price and generation. Since electricity prices vary during the course of the day and the year, electricity prices for a sample of times were taken for each study area. For each technology, the maximum capacity was approximated by the highest generation g for the technology in the hours h sampled.

$$cap_{max} = \max_h g \quad (3.11)$$

Then, the de facto capacity factor CFD was calculated for each hour:

$$cf_h = \frac{g_h}{cap_h} \quad (3.12)$$

A price indicator coefficient PM for each time period was calculated:

$$PM_h = cf_h \times P_h \quad (3.13)$$

The weighted average price was calculated for each technology:

$$P_{avg} = \frac{\sum PM_h}{\sum cf_h} \quad (3.14)$$

A price factor for each technology is calculated by dividing its average price by the overall average price for generation in the region. While this is an approximation, for CAISO all price-taking generation types received price factors lower than 1, while opportunistic generation types received price factors greater than 1.

An average capacity price from the past 15 years was assumed, rising with inflation, for PJM's RPM. REC prices are volatile, and typically decline over time as new capacity is added (in 2018 the prices were below \$10/MWh in all PJM states [107]), so \$0 REC prices for CAISO and \$5 REC prices in PJM were assumed for states with renewable portfolio standards (RPS). Six states (Delaware, Illinois, Maryland, New Jersey, Ohio, Pennsylvania) in PJM as well as the District of Columbia issue solar renewable energy credits (SREC), with a price range of \$32-\$445/MWh [107], approximated as \$200.

Generation

Generation for energy and REC revenue is calculated by:

$$g_t = cap_{name} \times cf \times (1 - F_{degradation,t}) \quad (3.15)$$

Nameplate capacity cap_{name} and capacity factor are assumed constant over the lifetime of the asset with a degradation factor $F_{degradation}$ representing the loss of performance over time. Generating capacity is bid into the RPM according to its unforced capacity $UCAP$:

$$UCAP = ICAP \times (1 - EFOR_d) \quad (3.16)$$

Installed capacity $ICAP$ is the capacity available under peak demand conditions as determined by tests run at plant sites. $EFOR_d$ refers to the outage rate for the particular generating type. Renewables are assumed to have an $EFOR_d$ of 0, but their $ICAP$ is established by a flat discount rate on their nameplate capacity according to PJM (at time of writing 42.0% for solar, 14.7% for onshore wind and 26.0% for offshore wind [108]). In December 2019, the Federal Energy Regulatory Commission (FERC) ruled that PJM should extend the MOPR to all units eligible for state subsidies. Affected units must bid into the RPM at the administratively determined cost of new entry (see table 3.2).

3.3.5 Data

Data requirements are summarized in table C.3 (appendix C). The technologies were taken from the ATB [109]. Emissions values for air pollution were taken from [110] and multiplied by International Reference Life Cycle Data System characterization factors in [111]. Capacity factors were based on US EIA statistics [112]. A higher capacity factor for solar PV is used in CAISO [113]. For PJM, 2018 capacity factors were used (p. 298 of [104]).

Table 3.2.: Minimum offers for affected technologies in the RPM

Technology	\$/MW ICAP/Day
Combustion Turbine	\$355
Solar PV	\$387
Combined Cycle	\$438
Coal	\$1,023
Hydropower	\$1,066
Nuclear	\$1,451
Onshore wind	\$2,489
Offshore Wind	\$4,327

NPV Parameters

Discount Rate

The discount rate is key to determining profitability. The ATWACC, which measures the cost of a capital investment since firms finance investments by a combination of equity (selling ownership) and loans is calculated by:

$$ATWACC = \frac{Eq}{Eq + Debt} \times r_{eq} + \frac{Debt}{Eq + Debt} \times r_{debt} \times (1 - r_{tax}) \quad (3.17)$$

Where Eq is the amount of equity, $Debt$ is the amount of debt, r_{eq} is the rate for equity, r_{debt} is debt rate, and r_{tax} is the tax rate. Ideally, discounting should be project-specific and not company-specific ATWACC [117]. While firms have different costs of capital, many costs (fuel) are the same for everyone. Loan payment amounts are known with high certainty. Some fuel costs fluctuate in cycles with the market, and some counter to the market [117]. Still, these fluctuations are difficult to predict. The persistently volatile natural gas price is no longer as closely linked to oil prices as in the past [118], and in fact in the US is set primarily by competition with other gas supplies [119]. It is also not clear that oil prices maintain a negative covariance

Table 3.3.: Parameters required for discount rate calculations from literature and as used in model, shown on the right. PJM literature values from [114,115].

	Literature values			Model		
	PJM	PJM ^a	PJM ^b	PJM	CAISO	Source
	2013	2018	2018			
Return on Equity	13.80%	15.00%	12.80%	11.95%	11.95%	calculated
Cost of Debt	7.00%	7.50%	6.50%	6.50%	6.50%	assumed
Capital Structure						
Debt Weight	60%	55%	65%	55%	55%	assumed
Equity Weight	40%	45%	35%	45%	45%	assumed
Tax Rate	40.50%	29.25%	29.25%	29.25%	30.04%	current
Risk-free Rate	3.40%	4.00%	3.50%	4%	4%	^c
Market Risk Premium	6.50%	6.90%	6.90%	5.00%	5.00%	^d
Implied Beta	1.6	1.59	1.35	1.59	1.59	assumed
Asset Beta	0.85	0.85	0.58	0.85	0.85	calculated
WACC	9.70%	10.90%	8.70%	9.00%	9.00%	calculated
ATWACC	8.00%	9.70%	7.50%	7.90%	7.90%	calculated

^a from [114]

^b from [115]

^c 2% bond return + 2% inflation

^d from [116]

with the economy (see [120]). Firm-wide discount rates such as ATWACC are biased towards higher risk-higher return projects at the expense of lower risk-lower return projects that still have an acceptable payoff [55]. Nevertheless, many firms still use a single discount rate to avoid special treatment for preferred projects [55]. Firms do frequently apply an additional percentage to the ATWACC to account for unknown risks, leading to a higher rate [55].

The ATWACC represents the market perception of the liabilities of the firm [55]. An investor's true cost of capital cannot be directly measured [116], and therefore it is the product of subjective decisions by modelers. Still, the ATWACC will be roughly equal to the long-term return on invested capital [116], so can be checked against this trend. The ATWACC depends on four principal components: the capital structure, that is the percentage of capital to be raised by equity and the percentage that comes from debt; the cost of equity; the cost of debt; and the tax rate. Of these, the easiest to pinpoint is the tax rate, because while it varies, the rate is fixed and published. The cost of equity is usually estimated using the capital asset pricing model:

$$r_{eq} = r_f + \beta_i(E(R_m) - r_f) \quad (3.18)$$

Where r_f is the risk-free rate of return, β_i is the unlevered asset beta, or the similarity of the risk profile of the given investment to the overall market risk profile, and the difference $(E(R_m) - r_f)$ is the market risk premium, since $E(R_m)$ is the expected market return. The parameters given in table 3 are used to estimate r_{eq} . The risk-free rate is estimated using a long-term bond return of 2% [116] summed with the inflation rate of 2% used in the model. A risk premium of 5% is assumed [116]. The beta value used has been approved in other energy filings by FERC [114]. It is higher than values generally found for either utilities (0.5-0.7) or integrated oil and gas (0.7-0.8) (exhibit 13.9 in [116]), so it can be considered a smoothed beta value. The cost of debt is dynamic, but bond rates are published. Each firm has a bond rating, and an average, which may not correspond to a particular project, is used. A cost of debt of 6.5% [115] gives a WACC of 9% for both regions and an ATWACC of 7.9%. This is in keeping with historical ROIC rates for utilities, although higher, so represents a mixture of utilities and energy services companies.

Other Parameters

An inflation factor of 2% is used. Higher inflation rates make generation more profitable. Inflation rates vary over time, and no thirty-year period is seen with a constant inflation rate or one consistently between 1-3%. Electricity prices are mean-reverting [121] but volatile due to the need to balance supply and demand. Hence, electricity prices are based on the weighted average price for PJM and CAISO from their respective reporting [104,122]. The methodology for the price factor derivations has been explained above, and documentation is available in the appendix.

The average PJM capacity price over the period 2007-2022 was used, increasing with inflation. Using a stochastic capacity price did not change results for profitability significantly. Prices for greenhouse gas permits were initially set at \$17/t rising with inflation based on prices in [123].

3.3.6 Verification

Results were compared with data from the EIA form 860, which records planned generation over 1 MW in the US by state and county [124]. For CAISO, data from all planned generation in California was used. Only planned generation in the counties also covered by PJM (see table C.8 appendix C) was used for states with less than 50% coverage by PJM.

3.4 Results

Optimization results representing all unique best solutions (Pareto front) from twenty runs are shown in a histogram in Fig. 3.1. For comparison purposes, scenarios constraining VRE to 30%, 50% and 70% of the total need (using LCOE Mid) were also run. Solar PV has the highest amount of installation when no VRE constraints are used, and solar PV, nuclear and wind show up in over 70% of scenarios. The use of the mid-range LCOE versus overnight costs is most important for hydropower. Natural

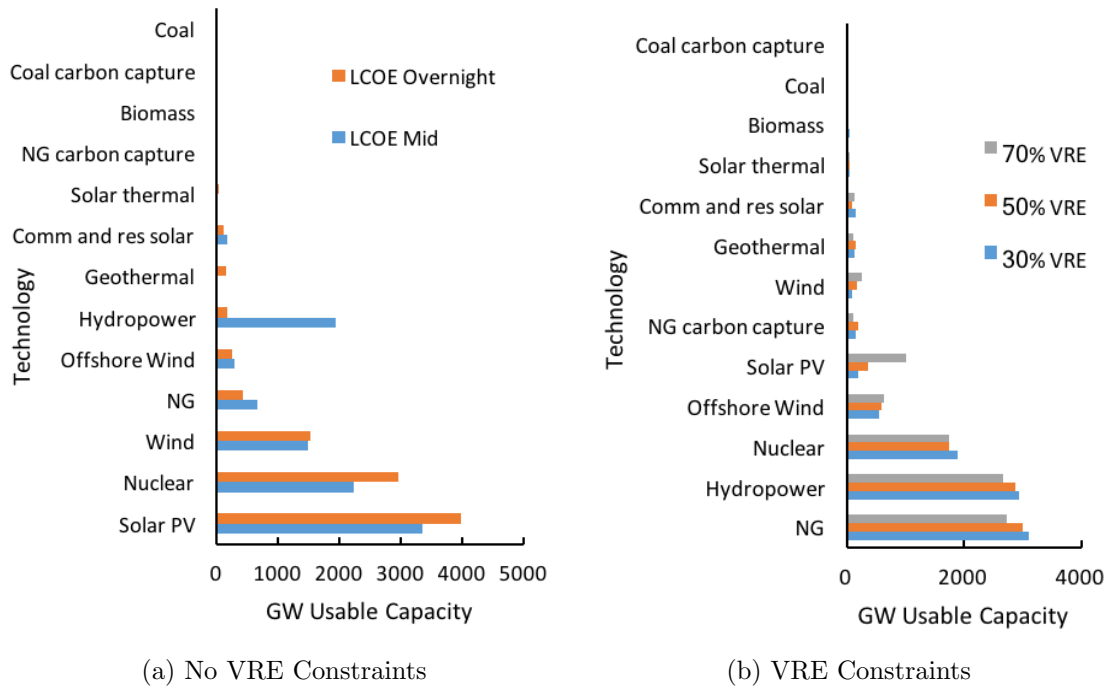


Fig. 3.1.: Histogram showing the total amount of available capacity installed over 20 runs of optimization model from unique solutions in the Pareto set based on national figures. On the left, results are not constrained by Eq. 3. On the right, the total contribution from solar PV (including commercial and residential) and onshore wind is constrained to no more than 30%, 50%, or 70% of the total.

gas is the most popular technology choice in VRE constrained scenarios. The NPV for each technology in both study areas is shown in Fig. 3.2. A range of generating lifetimes is shown in CAISO since many firms make decisions with a shorter payback period, and assets may be kept operational for longer than the standard timeline. In CAISO, solar PV, wind and natural gas combined cycle (NGCC) plants are profitable in the model. In PJM, solar PV and NGCC are profitable in all scenarios. Due to the higher capacity prices anticipated with the extension of the MOPR, NG CT becomes profitable in PJM. Biomass, coal with carbon capture, and offshore wind are the least profitable in both areas. Local sensitivity analysis results are shown in

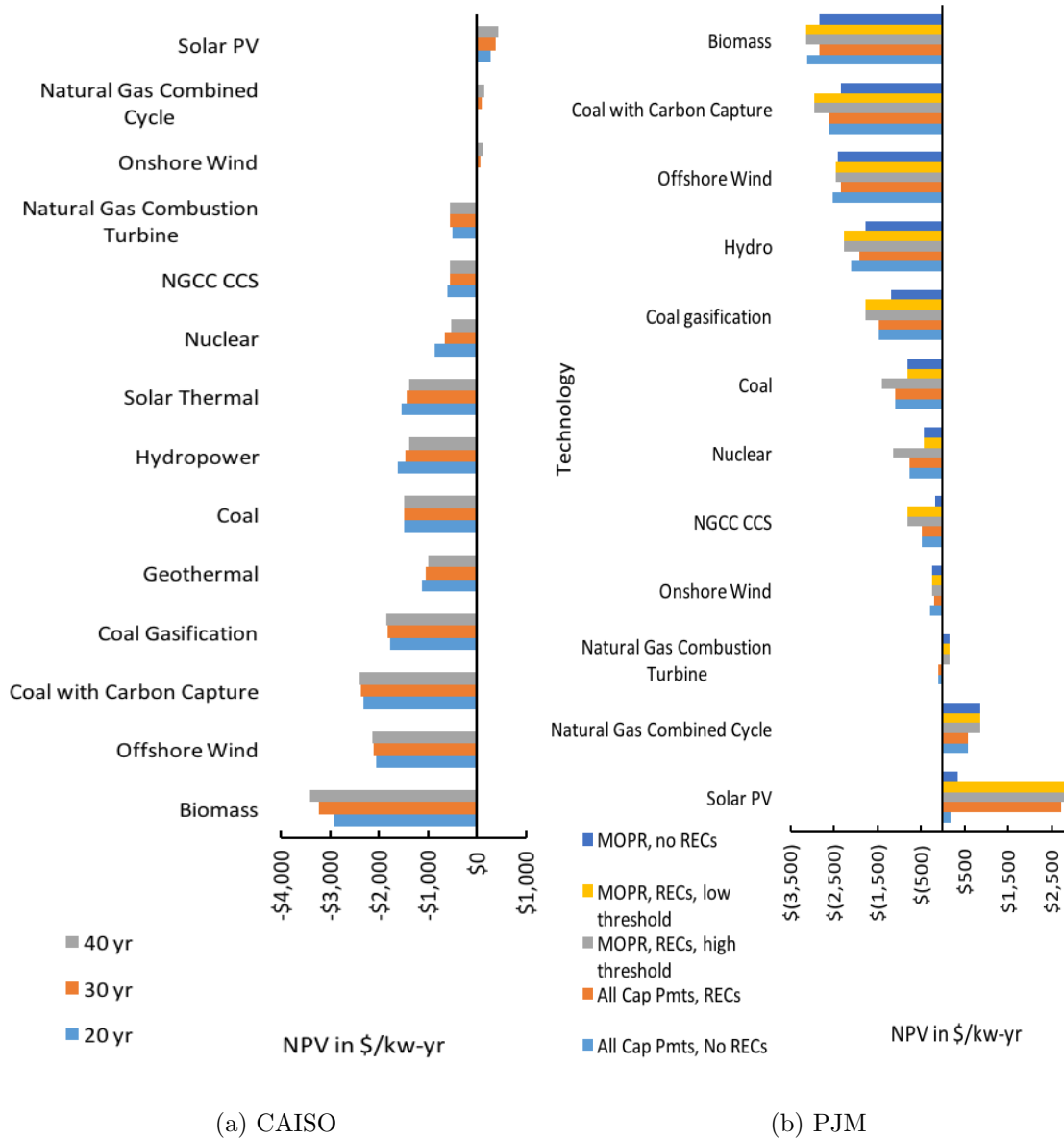


Fig. 3.2.: CAISO profitability with 20, 30 and 40 year lifetimes is shown on the left. PJM profitability is on the right, including the baseline scenario, the MOPR with a low threshold for entry into the RPM, with RECs (states with RPS).

Fig. 3.3. For PJM the analysis was run on the scenario with no expanded MOPR with capacity prices awarded to all technologies. All variables were changed by 10% and the change in costs or revenues were estimated in \$/kw-yr as well as percentage.

The dollar amount can be compared across all categories to give a sense of the relative magnitude of a change in the variable. Variables greater or equal than 10% include installed costs, discount rate, capacity factor and price. Installed costs are the most sensitive variable in both regions, both in terms of percentage and dollar amount. Capacity prices are not particularly sensitive, with a 10% change shifting revenues on average just 1.4%. This is not evenly distributed since natural gas combustion turbine (NG CT) changes the most at 4.4% and wind changes the least, less than 1%.

Verification shows that model results track closely with the planned generation for California and the PJM area as of 2017 (Fig. 3.4). In PJM, 88.7% of the planned generation and 83% of the planned generation capacity in CAISO were profitable according to the model. In PJM, NGCC, solar PV, NG CT and onshore wind accounted for 97.2% of planned generation, with over 85% NGCC. In CAISO the majority was solar PV, followed by NGCC and NG CT. The rankings were similar in the planned generation versus the model.

3.5 Discussion

3.5.1 Overview

This study examines the electricity markets in CAISO and PJM to demonstrate how technologies fare in terms of cost and profitability. It confirms that NPV performs better than LCOE as a predictor of technology adoption. It shows how revenue streams, including prices, capacity markets and RECs, which do not appear in LCOE calculations, are important to the adoption rate of renewables and conversely to the establishment of natural gas-based power plants. This study adds weight to criticisms of capacity markets as barriers to renewables, since results show that the RPM bolsters natural gas with respect to other technologies. The model provides a helpful tool for further studies as changes to the capacity market represent a complex policy topic.

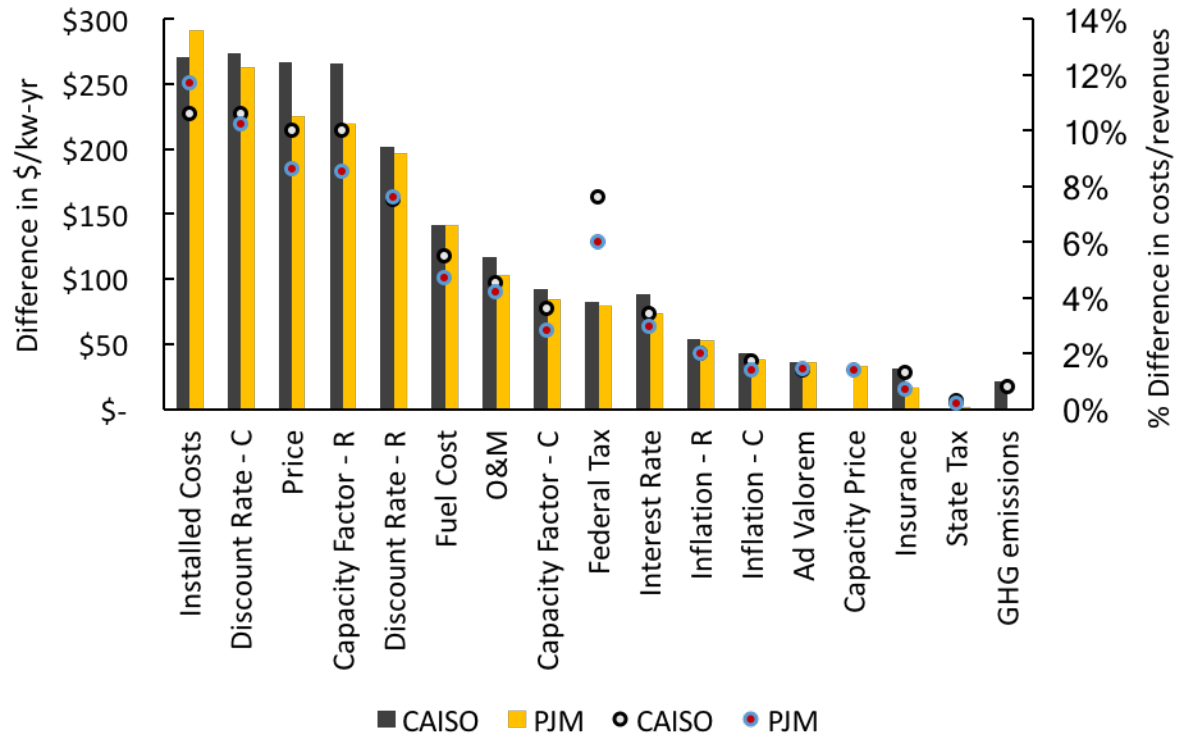


Fig. 3.3.: Response to a 10% perturbation in variable value, shown in CAISO and PJM, variables ordered by the \$ amount change in PJM. The percentage refers to either the total revenue or total costs, depending on the variable. Revenue is affected by: Discount Rate – R, Capacity Price, Price, Capacity Factor – R, and Inflation – R. Costs are affected by: Installed Costs, Discount Rate – C, Fuel Cost, O&M, Interest Rate, Capacity Factor – C, Ad Valorem, Inflation – C, Insurance, State Tax and GHG emissions. For taxes, which do not appear on either revenue or costs, the NPV is used.

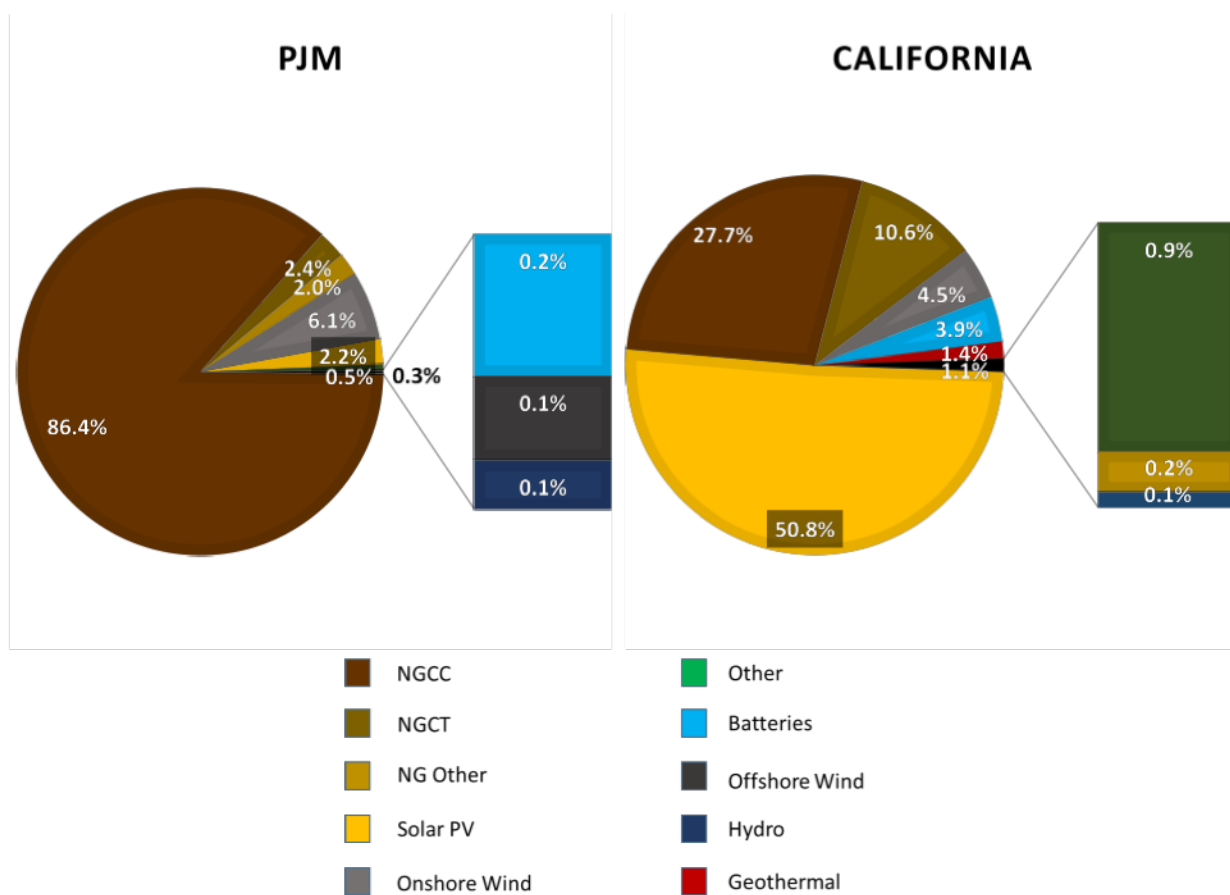


Fig. 3.4.: New capacity additions planned in PJM territory and California as of 2017, according to EIA Form 860 (does not include pre-existing generation assets).

Considering technologies on the basis of environmental costs and LCOE alone led to a wide variety of options, with solar and nuclear adopted the most. A reliability assumption modeled by hard constraints of 30%, 50% or 70% VRE made natural gas the most frequently chosen technology. The unconstrained optimization results do not bear a close resemblance to the capacity additions planned in each region since they factor in environmental costs and do not include revenue. Nuclear fared well in the cost optimization but not in the NPV calculations or planned implementation.

The NPV assessment predicted planned generation capacity expansion well. It showed that most profitable power plants rely in part on additional revenue streams such as RECs or capacity remuneration. The absences of coal-based generation and carbon capture and storage technologies from planned generation in PJM are supported since they are not profitable in the model, even when assigned higher capacity prices.

3.5.2 Differences between CAISO and PJM

NGCC and solar PV are profitable in both CAISO and PJM, yet verification data shows less installation of NGCC and more installation of solar PV in CAISO. This is due to a combination of factors, including relative profitability. Wind is profitable in CAISO and NG CT is profitable in PJM. Still, NG CT is installed at a higher proportion in CAISO. Although capacity markets are not present in CAISO and accordingly the cost of energy is lower (see table C.2), private reliability contracts are made with prices similar to those of PJM (recent prices hovered between \$2.87-\$3.25 /kW-month [125]). NG CT benefits from these contracts and retains its level of profitability with a very low assumed capacity factor (8% in CAISO and 6.9% in PJM). Thus in CAISO, where renewable mandates are increasing, NG CT is a better bet than NGCC. In PJM, there seems to be little risk of NGCC being forced out due to RPS. Also, higher profit margins due to capacity markets, even at low generating

lifetimes, make NGCC a safer investment in PJM. NGCC shows profitability above \$500/kw-yr in all scenarios.

Revenue complicates the picture for solar PV, the lowest cost technology. In both regions, the model predicts that solar PV receives lower than average prices. In CAISO this is partially due to the high adoption of solar. In PJM it is due to a price peak in January when little solar power was available, reducing its ability to take advantage of the highest prices. The lack of opportunism will continue to hamper the attractiveness of solar generation without storage.

In certain regions of PJM, the directed policy of SRECS has led to a very high upside for solar PV. Therefore, the adoption of solar PV in PJM will likely be guided mostly by the presence of RPS that provide additional incentives for solar energy. The model probably overestimates SREC revenues since they will decrease unpredictably over time as solar penetration increases. NGCC is more profitable than solar PV in PJM states with no SRECs due to the higher prices NGCC receives as well as its better position in capacity markets.

The low profitability of generation capacity (no generating technology shows profitability above \$500/kw-yr in CAISO) makes it easy to understand why California utilities are looking at getting out of generation [126]. It also demonstrates why California may seek innovative solutions to the problem of peak demand, like the Building Initiative for Low-Emissions Development (BUILD) and Technology and Equipment for Clean Heating (TECH). In PJM, carbon pricing and RPS are applied only in parts of the coverage area. Lower prices for wind, low resource availability, and low qualification for capacity revenue led to wind's lack of profitability in PJM. Higher capacity prices in PJM under the extended MOPR are expected to bolster natural gas plants, particularly as compared to wind. This focus occurs because higher costs for many technologies excludes them from receiving capacity auction bids, and because the high UCAP classification for natural gas plants qualifies them for higher payments than renewables.

3.5.3 Capacity Markets as a Barrier for Renewables

Resource adequacy is a single dimension issue of grid reliability. Markets cannot adequately compensate firms for the provision of reliability due to “missing money” in the case of blackouts [44]. Thus, capacity markets exist to correct a market failure. PJM’s capacity market should provide the shortfall between energy market revenue and the fixed costs of the least expensive dispatchable technology [127].

Much literature about the need for and proper design of capacity markets [101, 102, 128–130] considers electricity as perfectly substitutable, thereby excluding environmental and social costs. Additional context, including political climate and transmission, is also excluded. A system free from corruption, with all necessary infrastructure to ensure the availability of the basic service of power generation can also be called “resilience” [131]. In fact, most blackouts, or losses of reliability, are not due to adverse weather events, pointing more frequently to distribution level failures and aging infrastructure rather than resource inadequacy [131, 132]. Silverstein et al. suggest a framework for evaluating reliability aids, finding that capacity remuneration tends to have “low value” from the consumer side [131].

This study shows that capacity markets in PJM aid profitability of natural gas based generation more than renewables. Solar PV is only the most profitable technology when it can rely on highly priced SRECs. Hydropower and nuclear arose frequently in the optimization results, but are not profitable, and only benefit from the MOPR extension in states with no RPS, or in the case that they are more profitable already than other plants of their type. Therefore, the results and model contribute to questions regarding the efficacy of capacity markets. The high correspondence of NGCC installation (see Fig. 3.4) to the desirability in the constrained optimization scenarios (right side of Fig. 3.1) suggests that PJM incentives match the ideas represented by these constraints. Given that states and taxpayers already pay billions of dollars to support the installation of renewables in many parts of the region via RPS, any inconsistency with overall goals needs to be examined.

Solar PV is aided by the PJM capacity markets, receiving a higher capacity credit than would be expected in bilateral power purchase agreements based on capacity factor. Wind's capacity credit is lower than its straight capacity factor. Still, for renewables to offer the same level of reliability as fossil plants, a storage block must be added to form a hybrid system. In PJM, while the UCAP of 10 hours of storage can be added to the UCAP of the solar resource in hybrid systems [133]; the total UCAP will still fall below a typical value for a fossil-based system.

The cost of energy in PJM is higher than in CAISO. PJM estimates that the cost is primarily from energy prices, with reliability capacity making up roughly 20% of energy costs between 2014-2018 (calculations from data in [104]. In CAISO, which showed a lower cost of energy, reliability makes up a negligible proportion of total costs (<1%) [122]. Higher costs in markets with capacity remuneration were previously noted by [101], who showed in his model that a capacity market increased prices 55-61% accompanied by a 1.3-1.4% decrease in consumer surplus. He supported this theoretical case with data comparing prices in ERCOT with ISO-New England. If a capacity market also increases the relative penetration of conventionals, additional harm can be assessed.

Low carbon prices are present in the PJM regional greenhouse gas initiative states. Expanding carbon prices to other states would increase the cost of generation for fossil plants, further driving up capacity prices. Thus, carbon prices may not be a logical policy mechanism here; capacity markets ask consumers to pay a price for fossil fuels' intrinsic benefit of dispatchability while carbon prices charge even more for their intrinsic cost in terms of global warming potential. This may be further complicated by the expanded MOPR, as discussed next.

3.5.4 MOPR Expansion

Three scenarios for the expanded MOPR were included to allow some exploration of probable costs and implications, as well as providing a tool for further study. Pre-

vious versions of the FERC ruling were estimated to cost an additional \$1-7 billion⁵, a cost borne by consumers in addition to state level subsidies. The FERC has been concerned about the inclusion of subsidized energy sources in the market distorting prices [137]. This concern is illustrated in the scenarios without the MOPR, where NG CT is not profitable. The effects of the MOPR extension on the profitability of technologies in states subject to and not subject to RPS are shown in Figs. 3.5 and 3.6. Producers in states not subject to an RPS may benefit from the higher capacity prices regardless of technology. In states with an RPS, only lower cost technologies are bolstered.

High reserve margins of 20+% mean that capacity prices support the addition of plants whose electricity is seldom used, particularly if their marginal costs are higher than average. When reliability is considered a limiting factor for the expansion of VRE's (constraint-based optimization scenarios), NGCC plants are a rational choice. Still, ratepayers have not directly chosen these constraints. The additional cost of \$236-\$310/kw-yr for each NGCC plant is borne by consumers, who might make a different choice if they could. In this sense the expanded MOPR acts as a subsidy to counteract subsidies like RECs that bolster renewables. According to the recent report on the costs of hybrid systems [138], the cost of a 60 MW/240 MWh battery storage system that can be paired with a 100 MW PV system is \$91 million, which if divided over a lifetime of 15 years (see [139]), works out to just over \$100/kw-yr for the battery storage needed for pairing with solar.

3.5.5 Limitations

Considering two complex regions made a high degree of simplification necessary. Particular power generation projects in either area may be subject to different incentives and hurdles. The high sensitivity to many variables that cannot be known

⁵See [134] for an estimate of \$5.7 billion for a hypothesized version of the FERC ruling, contested by an industry group in [135] who estimated costs at "well below the \$2.2 billion annual cost" that they ascribe to subsidies to coal, nuclear and renewable plants. This caused a rebuttal that said costs might be higher than \$6.9 billion/year [136]

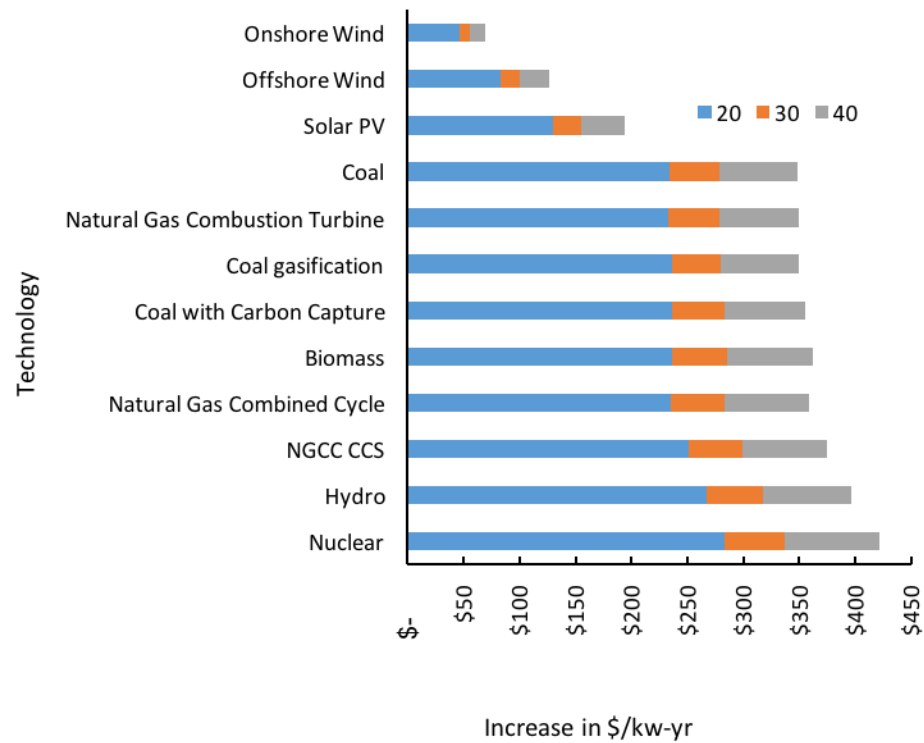


Fig. 3.5.: Increases in the NPV for each technology due to the expanded MOPR in states with no RPS, with no assumption made as to the ability of the asset to receive a winning bid. The color code refers to the lifetime of the asset, with more gains to the technology on a cumulative basis.

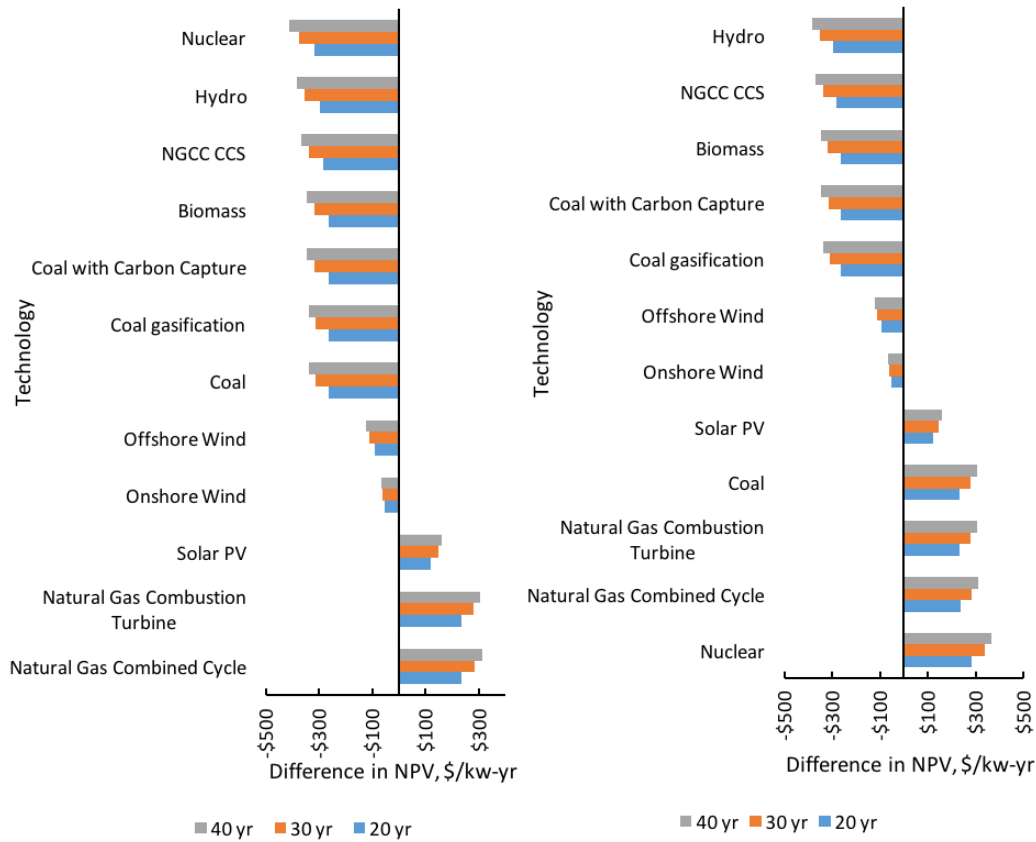


Fig. 3.6.: Two scenarios for the extension of the MOPR in states subject to RPS. On the left, only NGCC, NG CT, and solar PV plants win bids in the RPM auction, so their NPV is bolstered. On the right, supercritical coal and nuclear plants also win capacity income.

with high certainty suggests that policy options should be explored using scenarios. Installed costs are key, and have a high variability based on location. In PJM both NG CT and solar PV show as more profitable than wind, which has a higher level of planned implementation in the verification data. In 2017, however, solar costs were much higher, and the Renewable Electricity Production Tax Credit was still in effect for wind generation. The rapid drop in costs as renewable technology matures adds an option value to waiting, which is not taken into account here.

3.6 Conclusions

The movement to strengthen renewables in California reflects a set of assumptions that contrasts with the high value placed on reliability in the form of excess capacity in PJM. While California's policies resulted from referenda, however, the PJM capacity market reforms come from technocratic processes. The lack of clarity about tradeoffs explains controversy surrounding the recent FERC decision to apply the MOPR more broadly.

Since capacity markets have been adopted throughout most of the US, it is appropriate to ask whether additional markets should be added to value benefits that renewables are supposed to bring to the table, such as lower pollution, reduction of greenhouse gas emissions, early adoption of technology, and a hedge against volatile or high fuel prices. In a sense, RECs do this, but they are not universally adopted, and besides solar RECS, have had low prices. REC prices may decline further as renewables become more widely adopted. Considering the high price tag that PJM customers will be paying for the extension of the MOPR as well as the higher energy prices they are already paying with respect to energy only market customers, carbon taxes would further increase the amount that consumers have to pay for the good of reliability.

Many companies have announced contracts with renewable energy companies to achieve targets for renewables in their own energy mix [140]. This is unsurprising because solar PV and wind offer low costs as well as price risk reductions. The revenue structure in PJM gives an advantage to fossil resources due to their ability to serve as flexible peak demand. Storage associated with renewables could provide the same need (although long-term storage is still necessary in many cases), as could adaptive energy use by industry.

Profitability metrics account for a large portion of capacity adoption decisions. Work using portfolio approaches is also needed to better approach market outcomes. More transparency in California's reliability contracts would be helpful for verification

purposes. High sensitivity to many variables highlights the need for scenario-based approaches.

4. QUANTIFYING BARRIERS TO MARKET ACCEPTANCE OF RENEWABLES: A PORTFOLIO OPTIMIZATION APPROACH

4.1 Introduction and Background: Social Acceptance of Renewables and the Use of Portfolio Optimization

The perception of risks surrounding global warming have triggered large-scale investments in renewable energy and speculation about requirements for an energy system powered entirely by renewables [5,6]. Wüstenhagen et al. [14] grouped hurdles to the adoption of renewables into barriers to social, community and market acceptance. Market acceptance refers to the willingness of people in their capacity as consumers, firms and investors to adopt renewables. In the US, polling shows high public support for renewables. While barriers to the acceptance of particular projects may exist at a local and community level, that seems unlikely to explain the slow adoption of renewables. American utilities show lower adoption of renewables than the public would like, however. This makes it logical to explore a scenario in which market acceptance is the limiting factor for the spread of renewables.

Economic theory predicts that people adopt the best solution available based on available information. In the short term, however, market failures exist where particular problems have not yet been priced, and thus incentives present in the marketplace can lead to negative results. Sustainability is one such example, since the needs of future generations are heavily discounted by the market and governments (Solow, 1991). Ayres et al. pointed out that weak sustainability, the idea that natural and human capital are substitutable, ignores the biological nature of humankind [141]. Sustainability approaches typically consider a triple bottom line [26,142], and thus include economic, social and environmental concerns. Since sustainability is some-

times a vague concept, and can be either “weak” or “strong”, the assumptions made in assigning sustainability scores must be explicit as to what is and is not included. Considering that there is a strong social impetus to move towards more sustainable energy solutions means that market failures here are particularly problematic since they lead to equipment being installed today that will either be used for a long time (thus causing problems with carbon “lock-in”) or else cause stranded assets whose costs will largely be borne by the public.

The overall methodology is depicted in Fig. 4.1. First, cost and risk are used to select the most attractive portfolios from a market perspective. Then, the most sustainable portfolios, balancing the ability to meet current needs in an equitable and harmless manner with implications for future generations, are identified. This may be the first use of the portfolio optimization with sustainability, and offers a useful framework for identifying technologies that may be favored over the long-term. Because of concerns about the intermittent nature of variable renewable energy (VRE) and the current lack of long-term storage, scenarios with limits on VRE as 30%, 50% and 70% of the total portfolio are considered. The differences between these marketable and sustainable portfolios are considered to be barriers or boosts to market acceptance. Policies may be enacted to lower costs to eliminate barriers, and policies that currently allow market boosts may be vulnerable.

Optimal generating portfolios are found for two US regions: The Mid-Atlantic and California. The regions represent very different areas in terms of renewable and fossil resource potential and policies. Originally an acronym for Pennsylvania New Jersey Maryland, PJM is the regional transmission organization functioning in the Mid-Atlantic region of the US. PJM has been powered primarily by a mixture of coal, natural gas and nuclear with very little renewables. It covers parts of 13 states and the District of Columbia. The California Independent System Operator (CAISO) powers most of California and a small part of Nevada with a high penetration of renewables.

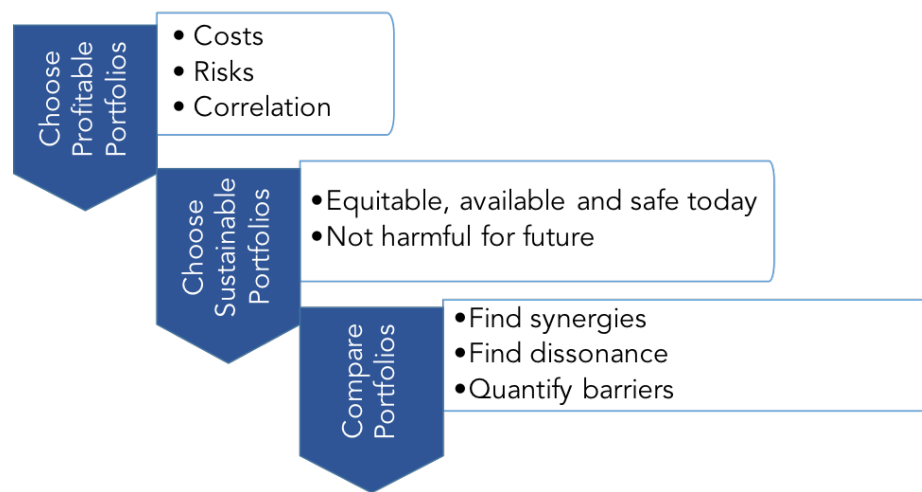


Fig. 4.1.: Summary of approach to quantifying barriers to market acceptance of renewables and identifying desirable portfolios from market and sustainability perspectives taken in this paper.

4.2 Methods

4.2.1 Data

The potential renewable resources available to the two regions considered are presented in table While there are no limits on the amount of coal or natural gas available per year, PJM states have extensive coal mining and gas drilling activity and reserves, whereas California does not. California mandates 100% renewables for electricity by 2045, whereas PJM has varying renewable portfolio standards. In California, new nuclear power plants cannot be built until a spent fuel disposal method has been enacted. The total generation in California's 2018 energy mix was 285,488 GWh, which, if all units ran at 100% capacity factor, would require 32,589 MW of capacity. Due to the short distance the continental shelf extends beyond the coastline of most of California, the offshore wind resource is located mostly in deeper waters, which make its development much more expensive. Likewise, while California has a very high potential for onshore wind, the resources are concentrated in less desirable areas (according to National Renewable Energy Laboratory classification, techno-resource groups 6-10). Table shows that onshore wind, offshore wind, solar PV, or solar thermal have the potential to meet electricity needs, whereas the other technologies can make only a partial contribution. Still, additions in any one year could be made up entirely of any one of the technologies.

In PJM, the total generation for 2018 was 806,546 GWh. Onshore wind, any of the offshore wind types, or solar photovoltaic (PV) could meet 100% of the total needs, but new hydropower could make up only 9% of the total matrix and biopower could make up only 18% of the total. Note that 70% of the offshore wind potential for PJM is from North Carolina and Michigan, however. Onshore wind resources come from the higher cost techno-resource groups, as in California.

Table 4.1.: Potential technical resources for renewable technologies in regions. These are conservative estimates since they cover the entire states: NV and CA in CAISO, and DE, IL, IN, KY, MD, MI, NJ, NC, OH, PA, TN, VA, WV and DC for PJM. The solar PV figures are an underestimate since they are based on technical potential from 2012.

	CAISO			PJM			CF
	Potential		% CA	Potential		% PJM	
	GW	TWh	2018	GW	TWh	2018	
Onshore Wind ^a	771	2,365	100%	1,131	3,467	100%	0.35
Offshore Wind ^b (S)	4	17	6%	440	1,734	100%	0.45
Offshore Wind ^b (M)	10	41	14%	259	1,022	100%	0.45
Offshore Wind ^b (D)	573	2,259	100%	424	1,671	100%	0.45
Solar PV ^c	7,864	17,741	100%	21,223	34,537	100%	
Solar Thermal	5,251	23,000 ^d	100%	-	-	0%	0.5
Geothermal ^e	6	45	16%	-	-	0%	0.9
Hydropower ^f	4	20	7%	14	73	9%	0.6
Biomass ^c	4	29	10%	17	144	18%	

^a From [143]

^b From [144]

^c From [145]

^d From [146]. California figure only.

^e From [147]

^f From [148, 149]

4.2.2 Portfolio optimization in energy planning literature

Portfolio optimization was introduced into energy planning literature by Shimon Awerbuch in a series of papers (although it had been used sporadically before his work). The procedure used by Awerbuch is summarized elegantly in the review of

portfolio optimization approaches by de Llano Paz et al. [150]. The total risk of a portfolio can be estimated using equation 4.1 from [151]:

$$R_{portfolio} = \sqrt{\sum_{i=1}^N \sum_{j=1}^N x_i x_j \rho_{ij} \sigma_i \sigma_j} \quad (4.1)$$

Where x refers to the respective weights of items i and j in the total portfolio, ρ refers to the correlation between the two items, and σ is the calculated risk for each item. In the case of this work, the items are technologies. The x value is found by optimization, or if the value is known for an existing or hypothetical portfolio, it can be used with equation 4.1 to find the score. Quantification of risk and expected return is discussed in sections 4.2.3 and 4.2.4, after the data collection process.

4.2.3 Return

Return is frequently modeled as the inverse of cost, although internal rate of return and net present value have also been used [150]. In this work, returns are approximated by levelized costs from the 2019 Annual Technology Baseline [152], which is appropriate since planners typically use the cost side [153]. Previous work has shown that the revenue side significantly changes the return of technologies [154]. Still, return can give either positive or negative values, so does not allow for easy comparisons between the technologies [150].

4.2.4 Quantifying Technology Cost Risk

Each technology's costs can be divided into individual cost streams, each of which has its own variability but whose movements may also be correlated with the variability of other cost streams. Then, the total risk for a single technology can be calculated by equation 4.2, where s and t refer to the individual cost streams for a single technology:

$$\sigma_i = \sqrt{\sum_{s=1}^M \sum_{t=1}^M x_{i,s} x_{i,t} \rho_{i,st} \sigma_{i,s} \sigma_{i,t}} \quad (4.2)$$

The cost stream categories used by Awerbuch and Yang [22] as well as [151] are used: investment costs, operations and maintenance (O&M), CO2 and fuel. A model documented in [154] is used to estimate the proportion of costs $x_{i,s}$ in each category for each technology and region (x values are shown in Table D.1 of appendix D). The O&M category refers to all fixed costs, including insurance and ad valorem as well as fixed O&M. Variable O&M is excluded in interest of parsimony because of its very low proportion of total costs.

The volatility risk factor for a given cost used is the standard deviation of holding period returns [22, 117, 155]. Holding period returns are calculated by equation 4.3:

$$HPR = \frac{EV - BV}{BV} \quad (4.3)$$

HPR refers to holding period returns, EV is the ending value for the time period studied, and BV is the beginning value. The sample standard deviation is used in the calculations throughout this work. Table D.2 collects the risk factors for the cost categories examined.

In most cases the correlation between cost categories is assumed to be zero, and is 1 for the same category, giving the identity matrix for ρ except for nonzero values between the fuel and carbon categories. The correlations between the fuels and carbon have been calculated and are available in Table D.3 of appendix D. Using the cost proportions from Table D.1, the cost stream risks from Table D.2, and the correlations from Table D.3, the risks for each technology are calculated and are shown in Table D.4 of appendix D.

4.2.5 Correlation between Cost Categories and Technologies

Cost Categories

While section 4.2.4 provides all the information necessary to calculate the value for each technology, it is still necessary to calculate the correlation between technologies, ρ_{ij} in equation 4.1. As mentioned above, correlation between cost categories for a single technology can generally be ignored, with the exception of fuel/carbon costs. When two different technologies are considered, however, correlation is more complicated. Fuel costs for two different technologies may be negatively correlated or may have a correlation of zero. Likewise, O&M costs may not have a perfect correlation between technologies, since the composition of the cost as well as the component parts may vary between technologies. Still, the capital costs and carbon costs should be close to perfectly correlated. This means that between any two technologies, a correlation matrix can be constructed that resembles the four by four identity matrix, but can include values between -1 and 1 for fuel/fuel, fuel/carbon and O&M/O&M correlation. Values used for these matrices are shown in Table D.3 and Table D.5 of the supplemental data files (note that these tables can be used for both the correlations for a single technology, as used in section 4.2.4, and between technologies).

The correlation coefficients are calculated from publicly available data. The standard error is high for each since the time series are short. Still, it is easy to replicate, and values should be recalculated if future researchers wish to use this method.

Awerbuch and Yang defined the correlation between O&M for different fuel types, basing it on analysis of the data captured in the Form 1 collected by the US Federal Energy Regulatory Commission detailing operating expenses for generating plants [22]. This is tabulated in table 8.4 of the annual electricity report issued by the US Energy Information Administration. Still, this form provides cost data primarily for nuclear, fossil steam, hydro-electric and gas turbine plants. It does not include renewables. For renewables such as solar PV, a much shorter time frame for empirical data on costs is available.

For wind, O&M costs are most highly correlated with the age of the plants [156], demonstrating that it is not appropriate to compare empirical data on a developing technology’s operating costs with those of a mature technology in order to determine correlation for future projections. On one hand, the drivers of the costs are different since one is driven by the technological development. Still, labor costs likely experience similar trends between technologies. Also, O&M is used as a proxy for all fixed costs, which in some cases are dominated by insurance and ad valorem. Those are also similar between technologies unless there is an exemption (in the US, nuclear has a different framework for insurance, and solar has a 90% exemption from ad valorem in CAISO, one of the markets studied). Fossil generation with carbon capture and storage (CCS) have not yet been commercially implemented, so a 90% correlation with their corresponding fossil fuel type is assumed.

Thus, the correlation coefficients for O&M by technology are calculated from Form 1 data over the past 11 years, while the correlation between renewables technologies and all other technologies are assumed as 0.6, a moderate correlation. The O&M correlation factors are shown in Table D.5 of appendix D.

4.2.6 Deriving Single Values for Correlation

Having assembled the necessary data to construct correlation matrices between any two technologies, it is still necessary to estimate a single ρ_{ij} value. Three approaches to estimating correlation between different technologies were found in the literature. Garcia et al. assumed zero cross-technology correlations [157]. This is the simplest method of correlation, but it does not allow the benefits of portfolio optimization to be used. Awerbuch pointed out that one of the key advantages to renewables was their lack of correlation with fossil fuel based technologies [117]. This seems particularly relevant today since in the PJM market there has recently been almost a 1:1 correlation between natural gas prices and energy prices, so renewables may provide a shield against natural gas price volatility.

Arnesano et al. proposed using the determinants of the cost correlation matrices between each technology pair as the correlation factors for the technologies [151]. The determinant method has a weakness, in that if, for example, fuel/fuel correlation is equal to zero, as between renewables and natural gas, the determinant is zero, while there may still be high correlation in non-fuel costs. The correlation matrix resulting from the determinant method are similar to those of Garcia et al. [157], as in their work the correlation matrix consists primarily of near-zero correlations between all technology pairs except those using the same fuel type (the highest correlation coefficient between technologies not sharing the same fuel type in their matrix is 0.07).

De Llano Paz et al. assumed that correlations are additive, including any existing correlation and adding the term to the next existing correlation [158]. They assigned a technology risk factor without weighting by cost. They assumed that all correlations between cost types not equal to each other are zero, so only consider the correlation between O&M costs and between fuel costs that vary from 1. Earlier, the only nonzero, non-diagonal component was the correlation between CO₂/fuel costs. Still, this is not insignificant since in the case of natural gas, for example, the CO₂ costs are close to 20% of estimated costs in CAISO. Some complementary cost, such as decommissioning/waste management costs for nuclear plants, costs due to intermittency of wind and solar generation (not clear as to how these costs are determined), and transport/storage costs for CCS were also included. In this paper such costs are part of O&M (fixed) costs for these technologies. De Llano Paz et al.'s approach [158] does not directly generate a correlation matrix. This approach has the weakness of being quite complex, and as the correlation is calculated each time in the optimization, it is much less computationally efficient.

To counteract the complexity of the method outlined in De Llano Paz et al. and the frequent zero correlations in Arnesano et al., a fourth method is proposed, the scaled matrix method. The cost proportions of each technology are used along with the correlation matrix between the two technologies to generate a scalar value for the

correlation. Each technology has a vector of costs, $C_{t,i}$ and technology j has its own vector of costs, $C_{t,j}$. As mentioned previously, the cost types have correlations, which are shown in matrix $Ccorr_{i,j}$. A different Ccorr matrix is formed between every two technologies considered. Thus, ρ_{ij} for each pair is calculated by equation 4.4:

$$\rho_{ij} = C_{t,i} \times Ccorr_{i,j} \times C_{t,j}^\top \quad (4.4)$$

Correlation matrices for the problem considered here are included in the data files using the determinant method as described in Arnesano et al. [151] (Tables D.6 and D.7, appendix D) and using the scaled matrix method (Tables D.8 and D.9, appendix D).

4.2.7 Optimization Problem and Approach

The optimization problem for cost and risk is a minimization as follows:

$$\begin{aligned} \min \quad & F(x) \equiv \sqrt{\sum_{i=1}^N \sum_{j=1}^N x_i x_j \rho_{ij} \sigma_i \sigma_j}, \sum_{k=1}^N c_k x_k \\ \text{s.t.} \quad & x_1 + x_2 + \dots + x_N = 1 \\ & 0 \leq x_m \leq 1 \end{aligned} \quad (4.5)$$

In the case where the additive (de Llano – Paz) method is used, the objective function is:

$$\min \quad F(x) \equiv \sqrt{\sum_{t=1}^N x_t^2 \sigma_t^2 + \sum_{t_1=1}^N \sum_{t_2=1, t_1 \neq t_2}^N 2x_{t_1} x_{t_2} \rho_{t_1, t_2}^{O\&M} \sigma_{t_1}^{O\&M} \sigma_{t_2}^{O\&M}}, \sum_{k=1}^N c_k x_k \quad (4.6)$$

Since the risk values may be complex numbers, the maximum of the argument calculated in equation 4.6 or 0 is taken before calculating the square root.

4.2.8 Solution Methods

Metaheuristic approaches to these problems are used in order to capture a variety of solutions and to avoid bias. Three approaches and two solution methods were used. The two solution methods were the paretosearch and genetic algorithms (using NSGA II in MATLAB’s multiobjective optimization toolbox). The approaches were: beginning with randomly generated solutions, seeding solutions, and performing a hybrid approach using goal attain. The exploration of these methods is based on [159]. MATLAB prerelease version 2019b was used.

4.2.9 Sustainability

In the second thrust of the model, sustainability scores are calculated for each technology. The Brundtland definition of sustainable development looks to an equitable distribution of goods today that does not harm the wellbeing of future generations. So return is loosely conceptualized as factors that allow an equitable and efficient distribution of goods with minimal harm to people and the environment today. Risk is conceptualized as the factors that expose the environment and conditions for future generations to peril.

The sustainability analysis is modeled on the work of Cartelle Barros et al. [26], who conducted a thorough analysis of literature to determine indicators that enable the selection of a sustainable power generation system using an approach from multi-criteria decision making (MCDM). To avoid double counting, the upstream economic indicators used in their work were excluded. Environmental indicators that were collapsed into a single quantitative indicator were here expanded to include three categories. Water use (as further documented in section D.3, appendix D), and land use were added. Land use was recognized by Cartelle Barros [26] as an important indicator, and efforts to quantify this are detailed in chapter 5. An additional indicator for the price factor, representing the relative prices that different generating

technologies receive for their output, was included as well. Indicators were divided into the current and future categories (division is shown in appendix D, Table D.10).

In order to use the portfolio method, single scores for current sustainability and for risks to the future are needed. This requires normalizing and weighting the indicator values. As detailed further in [26] and Alarcon et al. [160], each indicator is assigned a distinctive value function. Once the parameters have been identified, the value function is evaluated by equation 4.7 [26]:

$$V_{i,x} = \frac{1 - \exp\left(-m_i\left(\frac{|P_{i,x}-P_{i,min}|}{n_i}\right)A_i\right)}{1 - \exp\left(-m_i\left(\frac{|P_{i,x}-P_{i,min}|}{n_i}\right)A_i\right)} \quad (4.7)$$

Where $V_{i,x}$ is the value of the indicator, i , for technology x ; m_i , n_i and A_i are shape parameters (see [160] for further description of these), and $P_{i,max}$ and $P_{i,min}$ refer to the range of values for the variable, with $P_{i,x}$ representing the value for the technology and indicator. Once values for each indicator category are evaluated, they must be weighted together according to equation 4.8:

$$V_x = \sum_{i=1}^N \alpha_i \times \beta_i \times \gamma_i \times V_{i,x} \quad (4.8)$$

Where α , β , and γ refer to weights attached to the category (economic, social or environmental), indicator with respect to others in the same category, and the indicator with respect to other indicators for the same phenomenon, respectively. Each phenomenon being measured, e.g. water, should have a total of 1. Likewise, the values within each category and values for all the categories must sum to 1.

4.2.10 Sustainability Optimization

Since the sustainability scores range from 0 (least sustainable) to 1 (most sustainable), the minimization problem is formed as shown in equation 4.9. The correlation matrix is the identity matrix for this analysis. Correlation is not appropriate in the

same way since costs cannot be defined in the same way as monetary costs, and it is not desirable to trade off any indicator category for another.

$$\begin{aligned}
\min \quad & F(x) \equiv -\sqrt{\sum_{i=1}^N \sum_{j=1}^N x_i x_j \rho_{ij} \sigma_i \sigma_j}, -\sum_{k=1}^N c_k x_k \\
\text{s.t.} \quad & x_1 + x_2 + \cdots + x_N = 1 \\
& 0 \leq x_m \leq 1
\end{aligned} \tag{4.9}$$

Paretosearch and genetic algorithms when not seeded never gave results above 50% for either sustainability objective. When both algorithms were seeded with good initial solutions, i.e. 100% of each technology with a score over 50% on either objective, or if subject to constraints, limited with the rest randomly coming from the other positive technologies, a variety of solutions that were over 50% in both objectives were obtained. Using a hybrid goal attain approach limited the variety of the solutions. Only seeded genetic algorithms provided both a variety of solutions and good scores.

4.3 Results

Results from the sustainability MCDM are shown in Table 4.2. Solar PV has the highest score for current sustainability. Wind, both onshore and offshore, have the highest scores for future sustainability, however. Coal has the lowest scores in the sustainability assessment, and no coal technology outscores any non-coal technology. All renewable technologies have scores above 0.5 for both current and future sustainability. Natural gas combined cycle (NGCC), natural gas combustion turbine (NGCT) and nuclear have scores above 0.5 for current sustainability metrics, but below 0.5 for future risks. When CCS is included, NGCC has a score above 0.5 in both regions, while in PJM it is still below 0.5 for future risks.

Market-based optimization results for PJM are shown in Fig. 4.2. Results for CAISO are shown in Fig. 4.3. These figures show similar low risk solutions for each

Table 4.2.: Sustainability scores closer to 1 are on a blue scale, darker blue meaning more sustainable. Lower scores are on a red scale, with lower scores shown in darker red.

	Current		Future Risks	
	PJM	CAISO	PJM	CAISO
Solar PV	0.903	0.962	0.74	0.739
Solar thermal	0.757	0.86	0.68	0.679
Nuclear	0.662	0.709	0.419	0.449
Onshore Wind	0.816	0.899	0.787	0.842
NGCC	0.713	0.696	0.316	0.49
NGCC CCS	0.71	0.726	0.369	0.544
NG CT	0.512	0.581	0.473	0.465
Coal 30 CCS	0.277	0.363	0.267	0.44
Coal 90 CCS	0.247	0.317	0.267	0.44
Biomass	0.675	0.694	0.625	0.655
Offshore Wind (S)	0.656	0.657	0.787	0.842
Offshore Wind (M)	0.635	0.652	0.787	0.842
Offshore Wind (D)	0.632	0.627	0.787	0.842
Mini Hydropower	0.55	0.645	0.759	0.816
Geothermal Flash	0.7	0.756	0.7	0.723
Geothermal Binary	0.661	0.696	0.614	0.637
Coal Supercritical	0.308	0.356	0.045	0.218
Coal IGCC	0.278	0.342	0.139	0.312

scenario, while limiting VRE's changed lowest cost scores significantly. For PJM, the proportion of renewables in (average) low cost scores ranged from 31-80%, and for low risk scores from 60-77%. In CAISO, the proportion ranged from 61-72% in low cost solutions and from 63-65% in low risk solutions.

Results from the sustainability analysis are shown in Fig. 4.4. In CAISO, all the sustainable solutions in the Pareto front were 100% renewables. In PJM, renewables ranged from 93-100% of the total in the average sustainable portfolios. The composition of lower risk portfolios is >40% biomass, >10% coal, >10% onshore wind (in some PJM scenarios; in all CAISO scenarios) and >10% hydropower in all PJM scenarios. The most cost sensitive scenarios are made up primarily of onshore wind, with NGCC generally replacing it in the constrained scenarios in both regions. Sustainable solutions in PJM are made up only of solar PV, onshore wind, NGCC, NGCC with CCS, biomass and offshore wind. Sustainable solutions in CAISO are composed only of solar PV, onshore wind, offshore wind, solar thermal and geothermal.

4.4 Discussion

4.4.1 Best Solutions Based on Returns

Levelized costs and the scaled matrix method of measuring correlation were used as a reference case. Results from overnight costs are shown as well for comparison purposes. Using overnight costs makes 100% solar PV the lowest cost solution but gives a risk of 5.4%. Using levelized costs gave the lowest cost solution as 96% onshore wind, with 3% NGCC and 1% solar PV. Note that the large shift depending on the use of levelized versus overnight levelized costs gives a sense of how sensitive choices are to the method of cost approximation. The lowest risk solutions relied mostly on a mixture of hydro and biomass, with 4-20% coming from coal. In both cases, the xnew method gave the best values for the Pareto front, but gave only a small number of solutions.

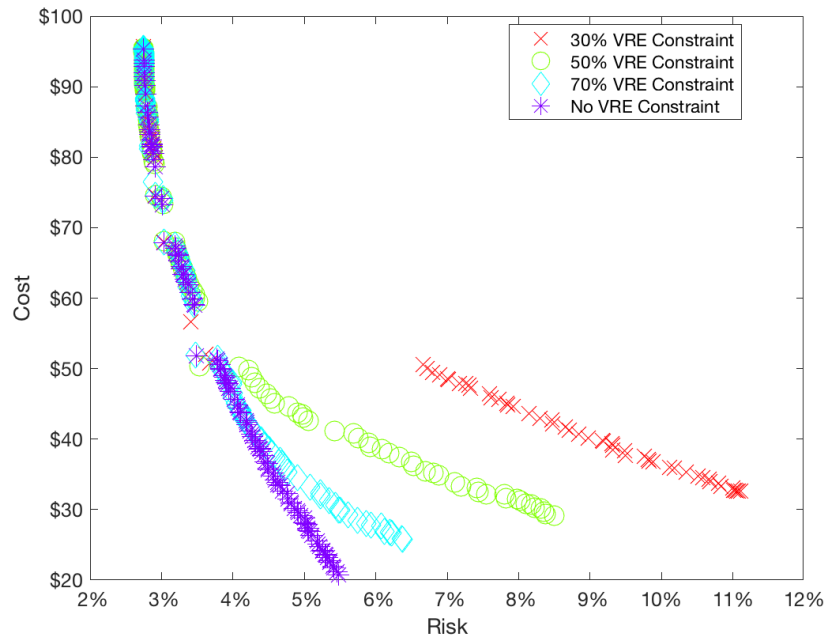


Fig. 4.2.: PJM portfolios with each constraint level for VREs differentiated by color and symbol: no constraint on VRE is shown with purple asterisks; a 70% constraint on VREs is shown with turquoise diamonds; a 50% constraint is shown with green circles; and a 30% constraint on VREs is shown with red exes.

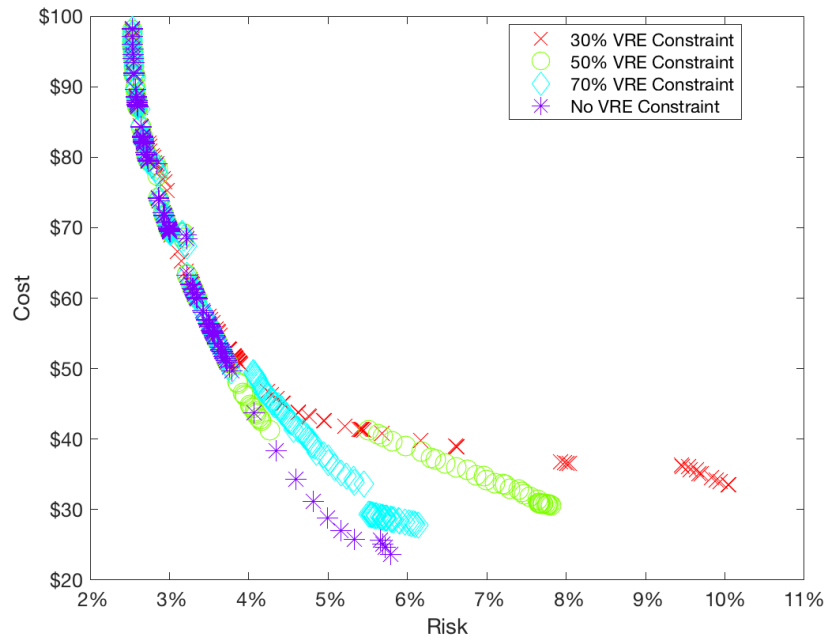


Fig. 4.3.: Pareto fronts for CAISO with each constraint level for VREs differentiated by color and symbol: no constraint on VRE is shown with purple asterisks; a 70% constraint on VREs is shown with turquoise diamonds; a 50% constraint is shown with green circles; and a 30% constraint on VREs is shown with red exes.

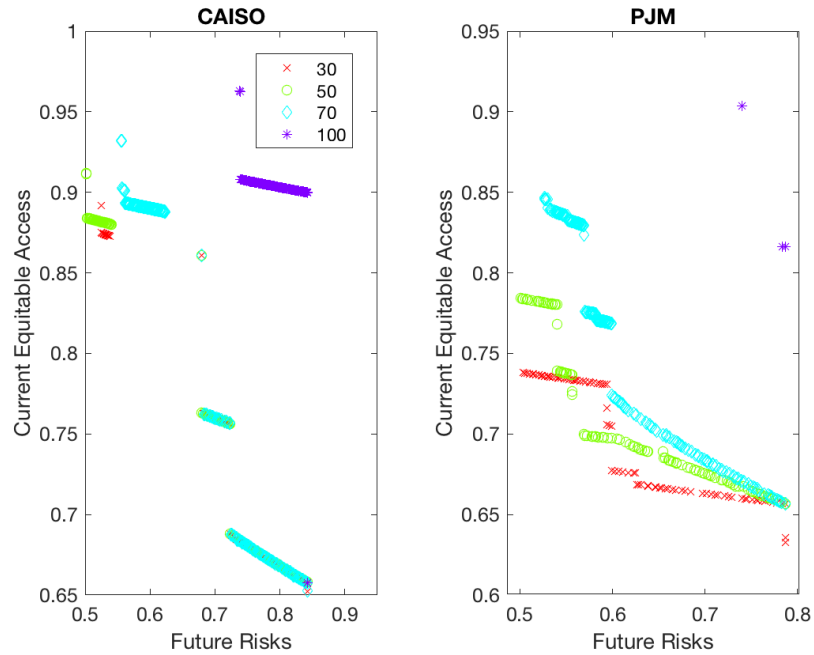


Fig. 4.4.: Sustainable portfolios for CAISO and PJM. The colors and symbols represent the percentage of VREs allowed in the scenario: no constraint on VRE is shown with purple asterisks; a 70% constraint on VREs is shown with turquoise diamonds; a 50% constraint is shown with green circles; and a 30% constraint on VREs is shown with red exes.

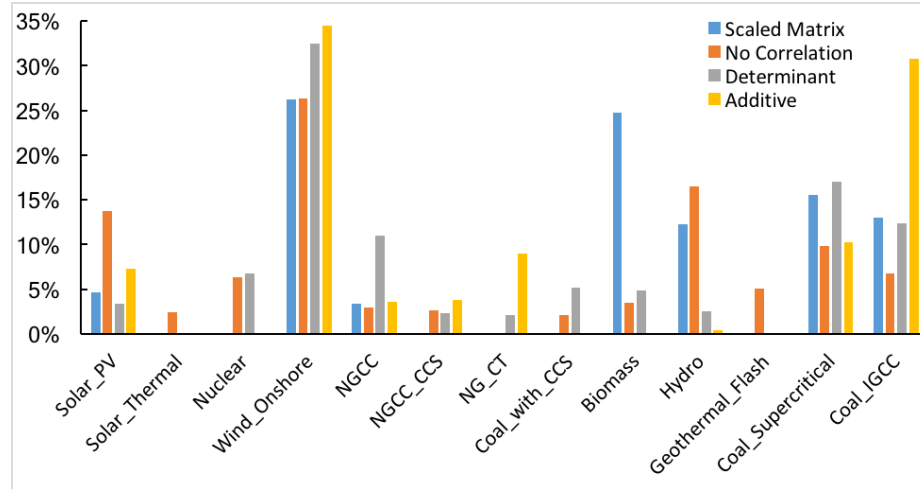


Fig. 4.5.: A comparison of the effect of correlation method on the proportion of each technology chosen in average portfolios. Results are for CAISO using leveled costs.

Nuclear comprises more than 2% of average portfolios only where VRE is constrained to 30% in CAISO. Offshore wind, solar thermal and geothermal do not appear in any of the lowest cost or risk portfolios. In all cases the combination of paretosearch and goal attain gave the closest approximation to the Pareto front. In some cases, however, this method gave very few solutions. This method also gave fewer low cost results and more low risk results.

Correlation has a strong effect on the portfolios chosen (see Fig. 4.5), and there is not a consensus method in the literature. Without correlation, all technologies except offshore wind appeared in the Pareto front results for CAISO's reference scenario. Including correlation (any method) eliminated solar thermal and geothermal from market solutions, and eliminated nuclear unless the determinant method was used. Including correlation also made solar PV and hydropower less attractive. Coal benefited from the inclusion of correlation (the additive method only slightly favored coal). Biomass benefited substantially from the scaled matrix correlation method.

The attractiveness of biomass here shows the strength of correlation in determining portfolios. The correlation of biomass is low with other technologies due to the lack of data for biomass prices. Coal, which fared quite poorly in an earlier study, never

showing up in the majority of portfolios minimizing environmental and monetary costs [154], also shows up much more frequently when correlation is included. NGCC shows up less frequently than its true representation due both to the lack of consideration of the revenue side in this study as well as the inclusion of cost risk. NGCC scores as the highest risk technology due to the relatively high volatility of natural gas fuel prices which are shown clearly in this technology which is forecast to run at a high capacity factor. In fact, this is also shown by the near-perfect correlation between natural gas prices and electricity prices, which reflects natural gas's role as the marginal supplier of electricity. NGCC does show up when VRE is limited, particularly in the lowest cost/high risk solutions. In a sense, this demonstrates the function of the Reliability Pricing Model in PJM which values the reliability from NGCC and other fossil plants more highly than the contribution from intermittent electricity sources. This may also suggest that investors don't expect to pay the price of their losses if natural gas prices rise again.

4.4.2 Sustainability

Recent work by Farfan and Breyer [161] offers a sustainability index for power generation giving all renewables a score of 1, but natural gas 0.25, oil (not considered in this paper) -0.25, and coal and nuclear -1. Besides nuclear, these scores roughly align with those from this earlier work.

When the optimization was run, the best solutions for each scenario tended to be clustered in groups with similar characteristics. For example the best solutions in PJM for current costs appearing in the Pareto front for the 30% VRE constraint included 63.4% offshore wind, 5% NGCC, 1% NGCC with CCS and 30% solar PV. The proportions varied slightly between the first three categories giving a range of scores. Therefore, the approximate reported values give a range of solutions.

Coal, nuclear and hydro did not appear in any of the best solutions for sustainability. This is the case even though hydro has scores above 0.5 in all categories so was seeded in solutions. Natural gas did not appear in any of the solutions for CAISO.

Since the sustainability optimization does not include correlation, there is some benefit for solutions made up exclusively of the lowest cost or risk technology. For example, it can be seen in Fig. 4.4 that the best solution frontier is made up of 100% solar PV and onshore wind, with 100% offshore wind showing up in constrained scenarios. The next frontier in PJM is composed mostly of solutions with a high proportion of offshore wind, supplemented by solar PV, onshore wind, and biomass. Still, one set of solutions has 20% NGCC, and one is 100% biomass, with another 70% solar PV.

Similar values for current and future sustainability scores in the case of onshore wind and solar PV, for example, are due to their positive profiles in many of the indicators used. Greenhouse gas emissions is a relatively high portion of the future risks category (the environmental category had a weight of 0.5 for the future score). The current category gives a high weight to social indicators, including primarily risk of accident, for which solar PV and onshore wind score very well, and to environmental indicators such as human health concerns for which solar PV and onshore wind also score very well. Both technologies are also low-cost, which also benefits them in the current category.

4.4.3 Sustainability versus Market

Here the market and sustainability solutions are contrasted by taking the average representation of each technology above and below the median risk and cost scores and comparing it with the average representation in sustainable solutions. The results in Figs. 4.6 and 4.7 show how the different scenarios affect the difference between sustainable and market-friendly solutions, forming barriers or boosts to market acceptance.

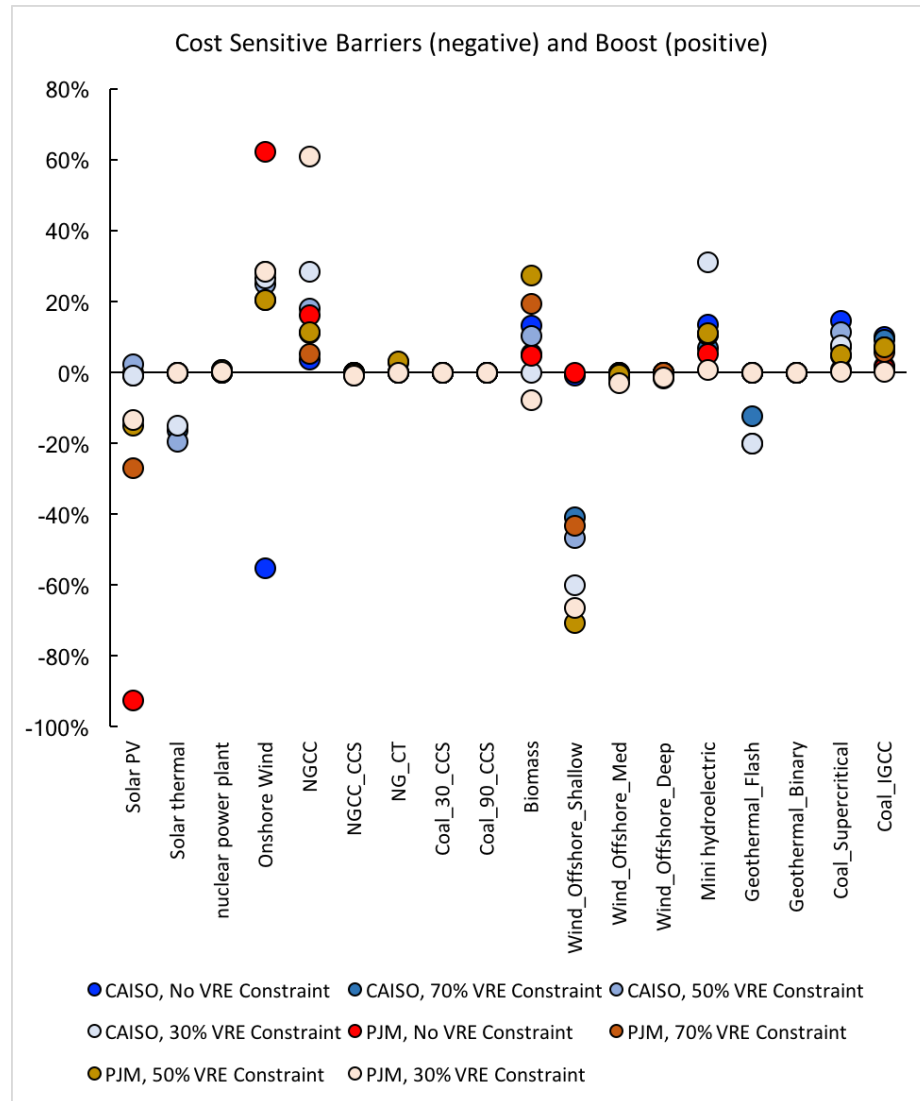


Fig. 4.6.: Differences between average sustainable portfolio values and average values from cost scenarios below the median value. Color coding shows scenario and region.

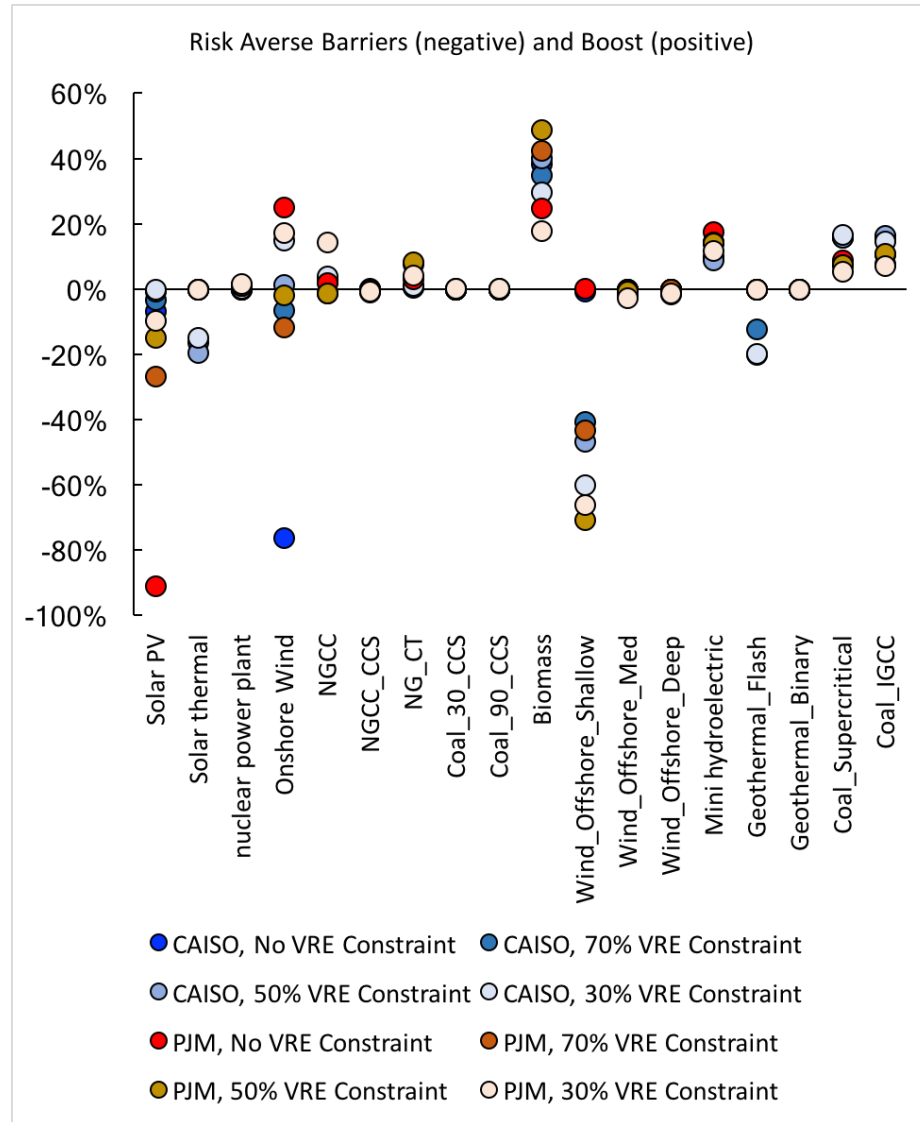


Fig. 4.7.: Differences between average sustainable portfolio values and average values from risk scenarios below the median value. Color coding shows scenario and region.

In a world with no constraints on VREs, sustainable portfolios are made up almost entirely of solar PV in PJM or onshore wind in CAISO. Thus, stakeholders who do not consider that there should be any constraints on VREs perceive a large barrier to market acceptance of solar PV or onshore wind. This barrier, however, may be due to the assumption and revenue considerations attached to scenarios where VREs are limited (note that both CAISO and PJM have mechanisms by which providers can be compensated for reliability, which tends to favor conventionals and renewables that are not intermittent).

If a stakeholder assumes that VREs should or must be constrained to account for the lower reliability/responsiveness that a simple cost or risk calculation does not show, offshore wind shows the strongest barriers in PJM and CAISO, with solar thermal and geothermal also showing barriers in CAISO and with solar PV still showing a barrier in PJM. Shallow offshore wind is most favorable due to its lower costs. While in PJM there would be enough shallow offshore wind capacity to meet any needs, California is much more limited in terms of shallow offshore wind potential. Sustainable and market type solutions are not totally independent of each other since levelized costs are important to both sets of criteria.

Market boosts if VREs are unconstrained in PJM are shown for both onshore wind (both cost sensitive and risk averse) and NGCC in cost sensitive scenarios and biomass, hydro and coal for risk averse scenarios. When VREs are unconstrained, CAISO also shows a small market boost for NGCC in both cases and higher boosts for biomass, hydro and coal in both cases (the boost for biomass is higher in the risk-averse case).

Offshore wind never appears in any of the market solutions. With no VRE constraints, solar PV and onshore wind do slightly less well in the market based scenarios in PJM, reaching 70% when levelized costs are used and 85% when overnight costs are used for the lowest cost solutions, rather than approaching 100% as in the case for the sustainability based solutions with no constraints. Still, they also go as low as 20% in the no constraint solutions, since the lower risk solutions rely more on biomass,

coal, and hydropower. Lowest cost solutions for scenarios with VRE constraints reach 67% NGCC, whereas the highest representation of NGCC in the sustainability optimization is 20%. Therefore, NGCC fares more favorably in the market than in sustainability-based analysis. When risk is taken into account, biomass appears quite favorable as an option in market scenarios. Higher risk scenarios have little biomass, so the barrier for biomass is present only if risk is ignored. NGCC with CCS is not present in most scenarios, but in sustainability it also appears only at low levels.

Interestingly, in CAISO while coal, NGCC and NG CT do show up in market based solutions, NG CT is actually more likely to be installed. CAISO has implemented many policies to aid renewables, and guarantees of 100% renewables represent a revenue risk to fossil fuels that is not captured in this model. Most of the technologies tended to skew in one direction, with the exception only of onshore wind. The technology was either better represented in the cost-risk based optimization than in the sustainability-based optimization, or vice versa. The degree varied slightly based on the region and cost or risk basis.

Biomass, coal and hydro benefited in the risk side of the analysis because their fuel sources and costs do not show high variability. While nuclear also benefited from this lack of variability, its overall risk score ended up as slightly higher than many of the other options, so in a dual objective optimization it did not score highly as compared to others. Nuclear is also hindered by the correlation method used (see Fig. 4.5); if the determinant method of correlation were used, its representation would be higher.

Ultimately, it is desirable for market incentives to match sustainability incentives. Therefore, where these results show boosts for a technology, this indicates that additional subsidies for these technologies may not be warranted. Where the results show a barrier, this indicates that it may be desirable to provide additional incentives to aid the development of the technology. VRE-constrained scenarios are included because the intermittency of VREs makes them undesirable for many planners, who are concerned about meeting reliability targets unless they are coupled with long-term storage.

4.4.4 Limitations

This work considers historical risk and correlation based on price history, which may not be indicative of future prices. High historical volatility of natural gas illustrates this well. Low natural gas prices due to hydraulic fracturing may continue, and many power generation investors seem to bet on that. Moreover, the use of correlation, while it offers a benefit in that it provides more information, may be controversial if this method of correlation is disputed. considering its high deployment despite past cost variability. Correlation in this work is based on historical data, and may not hold true in the future. Since Awerbuch’s work on portfolio approaches to power generation, the natural gas price has ceased to be well correlated with petroleum prices [118]. Still, correlation over time is difficult to predict. A lower risk value for natural gas technologies and a lower or negative value for correlations for natural gas based technologies would make them more attractive on the market side, enhancing the boost in market acceptance over its sustainability profile.

Levelized cost is an imperfect proxy for return. Previous work has shown that ranking by levelized costs does not perfectly align with profitability due to different prices available for technologies, capacity revenues, and subsidy revenues. Indeed, while using levelized cost in this work offers a favorable profile for onshore wind, previous work did not show onshore wind as a profitable technology in PJM. Cost, and particularly levelized costs, are important for planners but less useful for managers and investors [153].

This work does not look at retrofitting but instead at new installations, which is a limitation since much of the power generation infrastructure is already in place. Levelized costs from the ATB are used, which assume grid connection costs to be zero for most technologies. Grid connection costs can add a significant hurdle to some renewable development that is not included. Storage is rapidly emerging, and more analysis including storage will be helpful in the future.

Finally, one limitation of the sustainability model is that the desirability of technologies in this model scales linearly. Therefore, a technology's score has the same effect whether the technology occupies a large part of the total portfolio or not. Land use, for example, is more costly if expansion of renewables encroaches on other uses rather than being limited to marginal lands. Correlation should be explored further to account for this as the penetration of renewables increases. A second caveat for the sustainability model is that since access and equity are important considerations for meeting current needs, high current price barriers to technologies limit their attractiveness using this approach.

4.5 Conclusions

The results of this work suggest that offshore wind is the renewable technology facing the strongest barriers to market acceptance in the two study areas. They do not support the contention that market criteria represent barriers to CCS and nuclear plants. As opposed to earlier studies using the portfolio optimization methodology, this work shows a high representation of renewables in the most cost effective/lowest risk portfolios, particularly due to the precipitous drop in costs for solar PV and onshore wind.

NGCC is still significantly favored by market criteria. A holistic sustainability analysis of technologies leaves space for NGCC as well, which a narrower focus on climate change would not show. NGCC scores better in the current sustainability indicators than the future risks, so weighting more towards renewables. Still, the future will damage its score. If 100% renewable portfolios are desired, this work provides insight into where NGCC still performs favorably in terms of sustainability.

The inclusion of particular technologies depends on regional resources and costs. Solar PV and onshore wind were both attractive technologies, particularly from a sustainability and cost perspective. Assuming constraints based on concerns about intermittency highlights the attractiveness of other renewable technologies such as

offshore wind, solar thermal and geothermal. Concerns about risk make biomass a favorable option.

The method used allows the construction of an entire portfolio, considering correlations between costs as well as technologies. It contains a novel method for the calculation of overall sustainability and sustainable power generation portfolios. Growing attention has been placed on additional dimensions of sustainability beyond simply climate change in energy planning [28]. The holistic approach offered here can more accurately represent barriers to adoption of technologies. No single method for calculation of correlation was found in the literature, so a simple method was offered to improve estimates.

5. LAND USE FOR UNITED STATES POWER GENERATION: A CRITICAL REVIEW OF EXISTING METRICS WITH SUGGESTIONS FOR GOING FORWARD

5.1 Abstract

Renewable based energy systems have the potential to vastly increase the use of land devoted to energy, thus drastically changing landscapes and habitats, since conventional, fossil-based energy systems use a very small proportion of earth's land surface. Land use affects ecosystems, biodiversity, and geochemical cycles. It also affects people's well-being due to effects on views, noise, recreation, and quality of life. This means strong and transparent metrics to assess land use for energy systems are needed. This review considers some of the most influential papers and metrics in this category, namely ecological footprint, land use intensity and power density, attempting to make them transparent in terms of data used and calculations performed. We find that the literature frequently relies heavily on assessments that are decades old, many dating from the 1980's. The lack of transparency in the methods and even confusion in the units has led to the published metrics being applied incorrectly. Even within the same paper, the calculation is often performed several different ways, leading to errors and confusion on several orders of magnitude. We also attempt to provide a better assessment of land use by major electricity production technologies and fuels as well as an explanation and guide to commonly used metrics.

List of Abbreviations and Nomenclature

BTU British thermal unit

CSP concentrating solar-thermal power

GJ gigajoule

GW gigawatt

GW_e representative gigawatt of electricity

GWh gigawatt hour

ha hectare

km kilometer

kW kilowatt

kWh kilowatt hour

lb pound

LCA life-cycle assessment

m meter

MW megawatt

MWh megawatt hour

MW_i megawatts of installed nominal capacity

NARM North Antelope Rochelle Mine

PV photovoltaic

sq mi square mile

t tonnes (metric tons)

W_e representative Watt of electricity

W_i Watts of installed nominal capacity

5.2 Introduction

While quantification of global warming potential is highly advanced, many other metrics remain underdeveloped. Land use, with strong impacts on well-being of people and wildlife, is one such metric. As we begin the transition to systems based more heavily on renewables, these metrics will require the same level of treatment as those pertaining to climate change. Otherwise, they may provide unforeseen hurdles to energy transition. Land use in particular is important due to the world's increasing population and associated demands for food production, as well as its linkage to biodiversity.

5.2.1 Four conundrums

In assigning land change metrics that apply to both renewable and fossil sources of energy, we note four fundamental conundrums, which are explained below:

1. temporal scale;
2. system boundaries;
3. secondary effects and degradation; and
4. incomparability

All of these are sources of both unintentional and potentially intentional bias.

Temporal Boundaries

Land use metrics include an implicit time factor. If the factor is long enough, renewables always best conventionals. In the short term, however, that is not the case. Land use metrics sometimes refer to potential, that is how much of an energy source is present in a given area. However, it is important to bring them onto a level playing field by considering how much of that energy can be harnessed in a given

time period. In the case of fuels, extraction technologies and transportation networks limit the flow rate. Variable renewables, on the other hand, need to be tempered by a capacity factor that reflects the general operating conditions for existing technologies.

System Boundaries

For many energy system components, the total lease for a plant or mine site includes a proportion of land directly affected by construction or mining, while the rest may be only moderately disturbed or even untouched. Trainor et al. make a nice distinction between the landscape effect, which refers to the total scope of land used, e.g. lease boundaries, versus the land with a direct footprint, i.e. the site of the plant, roads constructed to provide permanent access, or the area disturbed by mining this year [162]. For coal extraction, for example, Colorado lists the number of permit acres included for coal mines, then the affected areas, then the disturbed acres for a given year (see [163]). None of the land use metrics explored consistently distinguish which of these figures should be used. This contributes to the large variations in assumed footprints in the literature.

Degradation versus Use; End of Life

Lingering effects on land are very different for each type of development, and include a temporal dimension with very high uncertainty. For example, mountaintop mining of coal may irrevocably change the landscape and diminish the quality of ecosystem services available, whereas biomass may be farmed today and replaced with a food crop next year with little difficulty (not to negate the food versus fuel debate as some forms of biomass require the use of dedicated agricultural land, whereas other types of extraction or renewable generation may use marginal lands). Advocates of nuclear state that going forward things will be better than the legacy of abandoned uranium mining sites. Renewables have simply not been around long enough to know what will happen when large numbers of solar panels and wind turbines reach the

end of their useful lives—will they become eyesores or leach toxic materials? Or will recovery and repurposing processes be instituted? This is related to the temporal question—what is the lifetime of a project in terms of its effects on the land?

Incomparabilities

The fourth difficulty is one found in all areas of life-cycle assessment (LCA), which is that environmental effects cannot really be compared between units; is it better to contaminate a stream than the air? Which species is it okay to lose? Who decides? In this sense, land use metrics must be well developed and are important for questions of environmental justice. This is particularly important considering that opposition can be particularly strong for certain land uses, as seen in recent protests over the Keystone pipeline.

5.2.2 Power Generation Units

This paper is focused on electricity. To that end, we apply prevailing efficiency conversions to fossil energy. Of course, fuels can also be burned for heat with a much higher efficiency. This means that beyond the comparison among electricity generation technologies, additional discussion regarding end uses is warranted. We do not consider this in our paper.

5.2.3 Looking forward and backward

Frequently people use metrics to look forward, considering the future land footprint from capacity expansion. This means that estimates should be based on the most competitive, prevalent or imminent technology. Still, it is also necessary to look backwards, particularly in the case of land use. As alluded to in section 5.2.1, many technologies have improved their land footprint going forward, but carry a legacy of contamination or failed clean-up. Since we cannot know what will happen at the end

of life for these assets, the past provides an important indication for the future, and provides a barrier to acceptance. Since sustainability metrics are frequently a key to people’s hesitation or resistance to embracing a given technology or process, past performance is important. Still, it does not make sense to use an obsolete technology to forecast future land use.

The rest of the paper is structured as follows: In section 5.3 we define the most commonly used metrics for land use. Section 5.4 details the application of these methods to dominant power generation technologies. The need for storage to be associated with solar photovoltaic (PV) and wind to provide the flexibility included in fossil -based generation and hydropower is briefly considered in section 5.4.9. Section 5.5 presents the results of our analysis, discussed in section 5.6. Section 5.7 briefly summarizes the major findings and presents suggestions for going forward.

5.3 Existing Methods

With the growing focus on the food energy water nexus and attention to the possible increase in land use for energy with a transition to renewables [35, 162], it is time to look more critically at metrics and data used to quantify land use for power generation. Multiple researchers have attempted to quantify land use by energy systems. We consider three frequently used metrics: ecological footprint [164], land use intensity [165], and power density [35]. First, we briefly document their calculations, basic equations, data used and units. We demonstrate strengths and weaknesses of each method. Studies by Gagnon et al. [34] and Hand et al. [166] are also frequently cited, although [34] is dated and neither study publishes their complete methodology, so we include their results for comparison in Figs. E.1 and E.2, appendix E.

5.3.1 Summary of Three Indicators

Ecological Footprint

The ecological footprint was developed in the 1990s by Wackernagel and Rees [164]. It measures our society's ability to stay within our "biocapacity," that is, the planet's biologically productive capacity. The metric is powerful because it simplifies the sustainability landscape into two important categories: land conversion (and thus effects on biodiversity), and global climate change. In their original book, Wackernagel and Rees estimated 80-100 gigajoule (GJ) fossil energy/hectare (ha) of land [164], which they obtained using three methods of estimating land use for fossil energy: 1) land needed to replace the fossil source using cultivated biomass, 2) land needed to sequester carbon dioxide emissions from the fossil fuel, and 3) land needed to recover the natural capital used up by fossil fuel combustion. They favored method 2 and used a ratio of 100 GJ/ha [164]. They noted that when electricity is considered, the land use is more than three times the listed rate, but they did not specify which rate they use. Their book listed ranges for different renewables and estimated 1 ha/1000 GJ for hydropower, and 1 ha/100-1000 GJ for solar PV [164]. The range they estimated for wind using only dedicated land is 1 ha/12,500-25,000 GJ [164].

Two main problems sometimes prevent the use of the ecological footprint in sustainability analyses: lack of data for end uses (it is primarily compiled according to state-level political organization), and the use of carbon sequestration land, which may represent double counting if another indicator measuring global warming potential is used. Since fossil fuel land use is measured by proxy, it is not comparable to renewable estimates used. Still, this method is notable in that it fully incorporates some of the tradeoffs we mention above, thereby addressing temporal and degradation issues.

Land Use Intensity

Fthenakis and Kim studied land use intensity for electricity systems in the US in a literature review based LCA [165], with results included in a summary figure. This was a particularly comprehensive work, but did not fully document the calculation method, relied on very old sources even at the time, and does not include all technologies considered relevant today. Their method as applied favors renewables through discounting land in the generation phase. Thus, its results and methods should be considered carefully in the context of other metrics to determine the best way of measuring land use.

Basic equation and definition(s)

The basic conceptual equation for the land use intensity metric is:

$$L = \frac{\textit{Discounted Total Installation Area}}{\textit{Yearly Generation} \times \textit{Asset Lifetime}} \quad (5.1)$$

Where L is the land use intensity, the discounted total installation area refers to the amount of land used for power generation (typically discounted to represent the direct footprint), the yearly generation was measured in gigawatt hour (GWh), and thirty years was used as the asset lifetime.

Data

Fthenakis and Kim conducted extensive literature review for their work, but many of their sources dated from the 1980's or 2000. Therefore, when their values are used, it is important to look closely at source data to make sure that it would still be representative of current conditions.

Units

The units used by Fthenakis and Kim were meter $(\text{m})^2/\text{GWh}$; thus, a lower number is better. The GWh is a levelized unit here. Production was calculated for the lifetime of the unit, and thus the land use was divided by the number of years the unit would be in service.

Pros and cons

This approach is strong in that the entire life cycle was considered. Efficiency metrics were consistently applied, ensuring that comparisons are done on the basis of electricity values. The use of lifetimes, however, make it difficult to do an apples-to-apples comparison. This is especially true for coal, where year discounting was not performed, thus overstating its land footprint with respect to renewables. The use of very old data makes it difficult to rely on their values, particularly in the case of natural gas, which has become dominant in the US since their article was published. The lack of data tables and equations in their work makes it difficult to understand their calculations. A lifecycle with units of land use per GWh is helpful, however.

Power Density

Smil laid out calculations and case studies for power density estimates in his 2015 book [35]. This appears to be the most in-depth examination of land use for power generation, and he makes a strong case for the adoption of his metric. Still, his analysis was not always implemented in a way that measures both renewables and conventionals on an equivalent basis and tends to favor conventionals.

Basic equation

The basic conceptual equation for power density is:

$$P = \frac{\textit{Yearly Generation}}{\textit{Discounted Total Installation Area}} \quad (5.2)$$

Data

While Smil [35] has fairly updated data, at times he uses power density estimates that come directly from other sources that have not used his method, so refer to total reserves rather than yearly generation.

Units

Smil's units for power density are annual power generated per earth's land surface area used, which for electricity are measured in W_e/m^2 .

Pros and cons

Smil's method is strong in that he suggests using annual generation, which is a more logical approach than assuming a lifetime and levelizing land use. Smil provides multiple case studies and solid theoretical bases for the calculations. Unfortunately, since equations and equivalencies are not always clearly spelled out, other researchers may fumble when trying to apply his method. Also, the ranges in the final results are very large. Some examples in the text substantially overstate the power density of common fossil sources by listing reserves. Fossil sources are generally not multiplied by an efficiency factor, so that the values are not comparable with the values for renewables. This is intentional since fuels can be burned for their heat value, and Smil's work includes discussion of end uses. The units in the power density metric make it more difficult to do lifecycle comparisons since the installation area is in the denominator.

5.3.2 Converting Between Power Density and Land Use Intensity

Both the land use intensity and power density metrics seek to provide a measure of actual generation of electricity or energy use with respect to area of land needed. It is easy to convert between the metrics. Equation 1, above, gave the conceptual equation for land use intensity. Here we show the basic numeric equation for land use intensity, L , in Fthenakis and Kim's work:

$$L = \frac{A}{C \times cf \times H \times y} \quad (5.3)$$

Equation 4 gives the basic equation for power density, P :

$$P = \frac{C \times cf}{A} \quad (5.4)$$

Where A is land area, C represents the nominal capacity of the power generation, whereas cf is a typical capacity factor. H is hours in the year (8760), taking capacity in megawatt (MW) to generation in megawatt hour (MWh). The assumed generating lifetime in years is given by y .

Most energy units are shown per MWh or MJ, but Smil uses W_e , similar to MJ/s. This unit can be obtained from MWh by dividing by H . Besides this factor and the temporal factor assumed lifetime, t , used in equation 5.3, power density and land use intensity are inverses of each other. Therefore, a value for L can be converted to P by the following equation:

$$P = \frac{10^9}{L \times H \times y} \quad (5.5)$$

The 10^9 figure in the denominator converts from representative gigawatt of electricity (GW_e) to W_e . Equation 6 converts power density to land use intensity:

$$L = \frac{10^9}{P \times H \times y} \quad (5.6)$$

For coal mining, however, Fthenakis and Kim omitted the lifetime (y). In this paper we omit the lifetime, so y can be excluded from equations 5.5 and 5.6.

5.4 Analysis of Major Power Generation Technologies

5.4.1 Solar

While not explicitly stated, Fthenakis and Kim calculate land use (L) for solar farms by equation 5.7 [165]:

$$L = \frac{pf}{I \times y \times \eta} \quad (5.7)$$

Where I is the annual irradiation, η is system efficiency, and pf is the packing factor, which refers to the spacing of units. The use of packing factor means that they consider the space needed by a hypothetical solar farm in its totality, excepting access roads and perimeters. They assumed a lifetime of 30 years, which reduces the total land footprint.

Smil's work assumes equivalencies. In his example of solar energy, he shows the power generation based on the solar resource present. Note that this is equivalent to equation 5.4 above, since irradiation includes area in the denominator. It is also equivalent to the conceptual equation for power density shown in equation 5.2.

$$P = I \times f \times \eta \quad (5.8)$$

The power density is given by the product of irradiation with a performance factor f (accounting for AC/DC conversion, typically 0.85) and an efficiency factor, η . Note that I already includes the capacity factor. If the actual annual production of a system is known, it can simply be divided by the land area covered to estimate the power density. These three methods are equivalent, although they all present simplifications (there can be high error in irradiation estimates, we are using average values for performance and efficiency factors, does not consider curtailment). Note the differences between these equations and those for land use intensity: equation 5.8 is similar to the inverse of the equation used in Fthenakis and Kim, but excludes both the packing factor (thereby including only panel area), and the assumed lifetime, so focuses only on annual generation rather than a levelized value.

In the US, the total installed capacity of solar PV is 71.3 gigawatt (GW) at the time of writing [167]. The most recent assessment of land use was based on installations present in 2012, when 2.1 GW had been constructed [168]. At that point the National Renewable Energy Lab found that large PV (>20 MW) used on average 7.9 acres/MW, whereas concentrating solar-thermal power (CSP) used 10 acres/MW. Direct area use was only slightly lower, 7.2 acres/MW for large PV and 7.7 acres/MW for CSP. For CSP this assumes a capacity factor of 32.6%, and they list 2.7 acres/GWh/year, and for PV a capacity factor of 26.5% is assumed, giving an average of 3.1 acres/GWh/year. This gives a power density of $9.1 \text{ W}_e/\text{m}^2$ for solar PV and 10.5 for CSP. The land use intensity is $1.26 \times 10^4 \text{ m}^2/\text{GWh}$ for solar PV and $1.09 \times 10^4 \text{ m}^2/\text{GWh}$ for CSP.

5.4.2 Wind

Onshore Wind

Fthenakis and Kim used equation 3 to determine the land transformation for wind farms assuming a 30 year lifespan. Land area was estimated from a 1997 document that assumed a 25 MW capacity wind farm with 2 rows of 25 turbines, each 500kilowatt (kW). Two capacity factors, 26% and 36%, result in land transformation intensities of 2780 and 2040 m^2/GWh . They mention that the indirect land use would be 5.5 m^2/GWh , less than 1% of the total land footprint. While the area used for the footprint is the total site area, they mention that wind turbines occupy a small portion of the total lands. Converting the figures from Fthenakis and Kim to power density units gives 1.37-1.87 W_e/m^2 .

Smil also provides a process for calculating power density, providing the equation for maximum power flux for a wind turbine:

$$p = \frac{1}{2} \rho A_w v^3 \quad (5.9)$$

Where p is the power, ρ is the air density, A_w is the working area swept by the turbine, and v is the wind speed. He points out that for the nominal power of a wind turbine, p must be corrected by an efficiency factor that considers materials used, called the actual power coefficient. Applying this coefficient gives a nominal capacity in Watts of installed nominal capacity (W_i). The working area term refers to the area cut by the turbine, so the product of π with the blade length squared. This means that a blade length must be assumed and multiplied out if the power density figure comes from a different source. The obtained power should be divided by the land area covered. To calculate power density, the power value must be multiplied by a capacity factor and divided by the true land surface area. Note that if the wind resource is known in W_e/m^2 , the fluctuation of wind during the year is already included.

Denholm et al. [169] estimated 25,438 MW of capacity in 8,778.9 kilometer (km)² of disturbed and undisturbed land, so the total footprint, in 2009. A capacity factor of 30% gives a total power density of 0.87 W_e/m^2 , or land use intensity of 1.3e6 m^2/GWh . Denholm et al. showed that the direct impact area when permanent structures are considered is roughly 1% of the total wind land use intensity [169]. The current National Renewable Energy Lab's Energy Analysis tool estimates 30 acres/MW, which is around 1/3 of the 85.3 acres/MW from the Denholm et al. study. The methodology is not provided, so it is difficult to know what assumptions led to this estimate. Still, since this is the most updated datum from governmental sources, we use this value. Assuming a capacity factor of 0.3 gives a land use intensity of 4.6e5 m^2/GWh and a power density of 2.47 W_e/m^2 .

If wind turbines can be installed on existing cropland or grazing land, their power density is very high. If they require dedicated land and buffers from habitation, the power density is low. Either way, the landscape is changed. Wind is notable in having a large difference between its landscape power density/land use intensity and its direct land footprint, which provides opportunities for innovation as long as the intrusion on human needs can be minimized.

Offshore wind

When offshore wind turbines are located sufficiently offshore as to not be visible from the beach, the human impact of their land use is almost nil. Still, the turbines may affect the surrounding water area. For example, Vanhellemont and Ruddick noted increased turbidity near offshore turbines, which can have effects on habitats of marine mammals and fish [170]. Erosion patterns near turbines may also differ, causing additional changes even far afield of the turbines [171]. The construction period as well as the decommissioning period may have their own effects on coastal ecosystems [172], and decommissioning in particular has not yet been carried out or thoroughly thought through [173]. We do not consider offshore wind separately since we found no studies that analyzed its land use.

5.4.3 Coal

The schematic in Fig. 5.1 shows the cradle to gate life cycle phases for power generation from coal. The fuel cycle requires indirect land use to power machinery and for construction of subterranean wooden supports in underground mines. Indirect land use is a significant $\sim 25\%$ factor in the land use for underground mines but insignificant $<1\%$ for other mining systems [165]. Ores are purified, typically onsite, in a process that involves significant loss of mass. Then they are transported to power plants, usually via rail. Power generation is the last step. The distributed nature of coal production, and variability in extraction technologies and coal ores, leads to very different estimates of land use (discussed further in section E.2, appendix E).

Mining and Extraction

Table 5.1 provides statistics presented in [35] and [165] on mining land use. There is not a particularly large difference between the numbers in the sources. Examination of original sources for this work, particularly [174], does not clarify whether the land

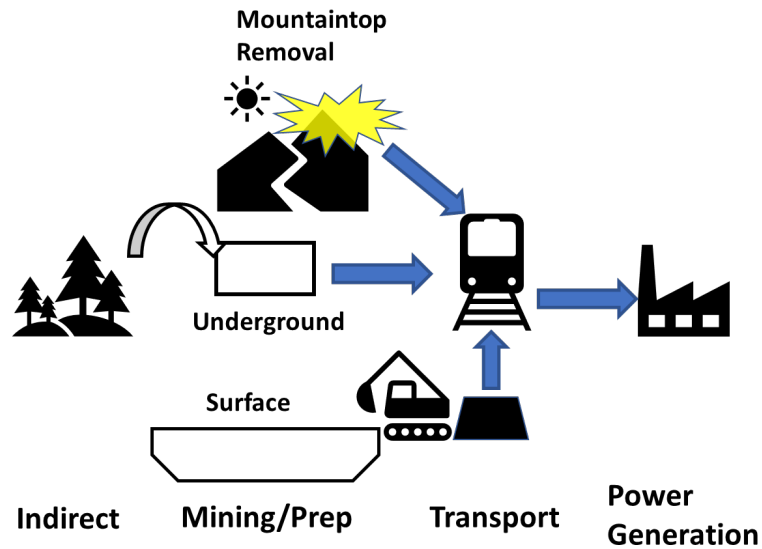


Fig. 5.1.: Schematic of major life cycle phases for power production from coal. Three major methods of extraction are used: mountaintop removal, underground mines, and surface mines. For underground mines, the indirect land use from wooden supports can be significant. Mined coal is typically transported by rail to power plants where it is burned for power generation. The major land use phase is mining, but rail transport makes up 6-53% of the land use according to Fthenakis and Kim [165]. The power generation phase is a very small part of the total land use.

represents the total footprint, affected area, or disturbed area. In section 3.3.1.1 we provide an in-depth analysis into the largest mine in the US, which leads us to surmise that the numbers here represent disturbed area, the smallest figure for land use. Some assumptions made in these calculations are loss during processing, which varies between 10-25%, and electricity conversion of 0.35. The lower heating value of coal varies by area. For eastern coal, the calculations in [165] use roughly 2.2 GWh/1000 t coal. For western coal, the conversion is roughly 1.8 GWh/1000 t coal. In 2012, the last year for which an annual report is accessible online, the Office of Surface Mining Reclamation and Enforcement assessed that just 75% of lands have been restored after coal mining [175].

Calculations for North Antelope Rochelle Mine in WY

Wyoming coal accounts for over 70% of Western production and nationally has the lowest land footprint [165] and [35]. The North Antelope Rochelle Mine (NARM), located in Wright, Wyoming and owned and operated by Peabody Energy, is the nation's largest coal mine. Its site covers 46,000 acres (p. 28, [175]) [$1.86 \times 10^8 \text{ m}^2$] with reserves of 1.7 billion tons [short tons, equivalent to 1.54 billion tonnes (metric tons) (t)] and heating value of 8,800 British thermal unit (BTU)/pound (lb) (20.47 MJ/kg) [176]. In 2018, NARM sold 98.4 million short tons of coal [89.3 million t]. Including the total area of the mine and using 2018 as a representative year, the ratio of land to mined coal is $2082 \text{ m}^2/1000 \text{ t}$. This is much higher than Fthenakis and Kim's Wyoming estimate of $90 \text{ m}^2/1000 \text{ t}$ [165], but less than half of the estimate of $5.15 \times 10^6 \text{ ha/million short tons}$ [$5676 \text{ m}^2/1000 \text{ t}$] from [162]. Smil cites two sources giving the density of the NARM as $12,000 \text{ W/m}^2$. Still, using Smil's method, the much lower value of 312 W/m^2 is obtained. Including an efficiency figure of 35% reduces the power density to $109 \text{ W}_e/\text{m}^2$. The corresponding land use intensity is $1,047 \text{ m}^2/\text{GWh}$ for mining alone. This represents a lower bound for land use by surface mining. Smil presents figures for Wyoming extraction from 1996-2009 at 4.37

Table 5.1.: Data on Mining land use found in the two principal source papers. Smil's numbers, which were given in W/m^2 , have been multiplied by an efficiency factor of 0.35 to convert to W_e/m^2 .

Mining System	Source	Vintage	Power Density	Land Use Intensity
			W_e/m^2	m^2/GWh
Surface mining, Western US	[165], Table 1	1983	815	140
Surface mining, Eastern US (a)	[165], Table 1	1989	368	310
Surface mining, Eastern US (b)	[165], Table 1	1983	79	1450
Northern Appalachia	[165], Table 1	1980	326	350
Central Appalachia	[165], Table 1	1980	317	360
Southern Appalachia	[165], Table 1	1980	200	570
Wyoming	[165], Table 1	1980	2655	43
Kansas	[165], Table 1	1980	136	840
US Average, Surface	[165], Table 1	1995	285	400
Underground mining, Eastern US	[165], Table 1	1983	49633	2.3
Underground mining, northern Appalachia	[165], Table 1	1980	243	470
Underground mining, central Appalachia	[165], Table 1	1980	224	510
Underground Mining, Southern Appalachia	[165], Table 1	1980	238	480
Underground mining, Utah	[165], Table 1	1980	476	240
Underground mining, US average	[165], Table 1	1985, 1995	571	200
Mountaintop removal, example 1	[35]		70	1631
Mountaintop removal, example 2	[35]		17.5	6523
Surface mining, Wyoming	[35]	1995-2009	3850	30
Tennessee, 2009	[35]	2009	122.5	932
Underground, low	[35]		700	163
Underground, high	[35]		5250	22
Nationwide	[35]		350	326

Gt from 25,700 ha of disturbed land, with a power density of almost 11,000 W/m² (3,850 W_e/m²). This suggests that the disturbed land is about 3% of the total for Wyoming surface mining.

Power Generation Stage

No official statistics are published on the size of the acreage of power plants. Fthenakis and Kim relied on the Characterization of Energy Types [174], already 30 years old when their paper was published. Smil provided details on some of the largest power plants operating in the US, contrasting their size with a postulated theoretical size. His theoretical size could reflect the possible direct impact bounds, whereas the true sizes he finds give a sense of the scope of the total landscape effect. In table 5.2, we provide the size in terms of installed capacity for two different capacity factors—0.5, representing today, and 0.8, representing the past.

Table 5.2.: Land use intensities for land for coal power plants assuming different capacity factors. We use the average from Fthenakis and Kim updated with a capacity factor of 0.5 as the representative value for coal power plant land use intensity.

Source	power generation (acre/MW _i)	cf = 0.5, m2/GWh	cf = 0.8, m2/GWh
Fthenakis and Kim (US average)	0.5	461.97	288.73
Fthenakis and Kim (US low)	0.3	273.51	170.95
Fthenakis and Kim (US high)	1.7	1568.85	980.53
Smil (low) - theoretical need	0.04	34.19	21.37
Smil (high) - theoretical need	0.06	59.32	37.07
Scherer (total land claim, Smil)	2.39	2205.28	1378.3
Bowen (total land claim, Smil)	0.26	241.43	150.89
Gibson (total land claim, Smil)	1.18	1093.71	683.57
Bull Run (total land claim, Smil)	0.18	164.87	103.05

Transport and Indirect Land Use

Fthenakis and Kim stated that 32% of the total ton-miles of shipping by US rail in 2001 was attributable to coal shipments. Allocating this proportion of the total rail miles to coal gives an estimate of an addition of 30 (East) or 80 (West) m²/GWh. Smil estimates that the transportation land footprint is negligible in comparison with the mining land footprint. Either way, we see that in the higher case of Fthenakis and Kim, it would add just another 5% to the total so far. Indirect land use ranges from 60 (West) - 175 (East) m²/1000 t according to Fthenakis and Kim, and using a conversion of 2.2 GWh/1000 t of Eastern coal and 1.8 GWh/1000 t of Western coal gives roughly 35-80 m²/GWh for this step, relevant only to underground operations. This is included below for the direct effect calculations.

Additional Considerations and Looking Forward

We have shown a broad swathe of estimates for land footprint throughout this section. Table 5.3 provides a single estimate. We use equations 10 and 11 to estimate the direct and landscape effect land use intensities for NARM (considered representative), underground, and mountaintop mining technologies as they are located in the US.

$$L_{D,tech} = aL_{P,tot} + b_{tech}L_{m,tot,tech} + T_r + Ind_{tech,r} \quad (5.10)$$

$$L_{L,tech} = qL_{m,tot,tech} + L_{P,tot} \quad (5.11)$$

Where a is the coefficient for power plant direct land use (assumed as 0.1), b_{tech} is the technology-specific coefficient for mining direct land use (0.1 for western surface mining and underground, 1 for mountaintop removal), T_r is the transportation term based on region r (30 for East, 80 for West), and Ind is the indirect land use term based on technology (0 for surface or mountaintop) and region (35 for West, 80 for

East), and q is the coefficient to transform direct land footprint to landscape level, which here was 1.5 for mountaintop, and 1 for underground and surface. The value assumed for $L_{m,tot}$ for underground mining is 1000 (from NARM estimate) and 4000 for mountaintop removal (average of two cases provided in Smil’s work, shown above in Table 1).

Table 5.3.: Our assessed land use intensities for the systems considered as well as a representative case. Mountaintop mining based systems have the highest land-use intensity, whereas the other systems are similar to each other, with the representative case doing slightly better.

Mining System	Landscape Effect Use Intensity	Land Land Use Intensity	Direct Effect In-	Landscape Effect Power Density	Direct Effect Power Density
Representative (NARM) (Sur- face, West)	1509		231	76	495
Underground	1462		259	78	441
Mountaintop	6462		4076	18	28

NARM is considered most representative due to its large market share and the positive economic profile of Wyoming coal. Currently, coal costs are much lower for the Powder River Basin than for other parts of the country, suggesting that only in Western states is there a clear economic case for coal. This might change if policy is enacted to preserve the coal industry, but so far there is no evidence of this. These estimates neglect allocation related to the use of coal ash waste products for cement production.

5.4.4 Natural Gas

Natural gas has become the dominant fuel source for power generation in the US, due to the dramatic expansion of shale gas plays over the past decade. Most new generation capacity in 2018 was powered by natural gas, and by 2015, half of US natural gas production was coming from “shale gas and tight oil plays” [177]. This is projected to increase over time to 70-80% of production for the foreseeable future. The largest producing shale for natural gas is Marcellus, over Pennsylvania, West Virginia and nearby areas.

Extraction by hydraulic fracturing allows very high recovery in the first year followed by hyperbolic decline [35]. Typical first year shale fields in Marcellus have a power density of around 2000 W/m², which declines to roughly 200 W/m² by their third year [35]. Thus, natural gas production is much different than the other fuels and power sources in this survey, with particularly thorny system boundaries. Moran et al. used GIS data to analyze the number of ha developed (completely converted from original state to housing for natural gas infrastructure) and modified (habitat is converted from original state, but not totally occupied by infrastructure) from 2004-2015 by shale gas and tight oil plays in the US [178]. Over the same period, 77.93 trillion cubic feet of dry natural gas was extracted from shale gas and tight oil plays, or 140.33 trillion cubic feet including tight gas as well [177]. Moran et al. estimate that 140,000 ha were developed with an additional 60,000 modified from original ecosystem states of temperate forest, grassland/pasture, woodlands and agricultural during the same period [178]. Assuming a heating value of 1030 BTU/ft³ (38.4 MJ/m³) and an efficiency of 43.3% for conversion to electricity, the power density estimates range from 582 W_e/m² (all terrain included and just shale gas and tight oil are counted) to 1496 W_e/m² if only developed terrain is included and tight gas is also included. All of these represent intermediate values in Smil’s estimates.

The transportation stage was not explored in Smil’s work [35] nor in Moran et al.’s analysis [178]. Fthenakis and Kim’s analysis apportions the highest contribution

to land use to the pipeline stage, however [165]. Considering that sustainability indicators should provide some measure of potential social opposition to a project, transportation should not be excluded here. In recent years, pipelines, which offer the safest transport method in terms of accidents, have faced strong opposition due primarily to the potential for accidents and siting considerations.

The US Department of Transportation’s Pipeline and Hazardous Materials Safety Administration data shows that in the recent past, around 30,000 miles are installed per decade, or around 3,000 miles per year (4,828 km) [179]. We use the estimate of Fthenakis and Kim that the buffer zone is 20 m wide. This gives an average of $9.66 \times 10^7 \text{ m}^2$ of land associated with pipeline constructed per year. The gas developments we have mentioned provided 54% of the natural gas produced in the US in the 12-year period from 2004-2015, so we will attribute the same proportion of the pipeline construction to this gas. This brings the estimates down to $443\text{--}1035 \text{ W}_e/\text{m}^2$. This is still well above the power density of coal from our calculations, but it is much lower than the upper bound of Smil’s estimate. Also, Fthenakis and Kim show natural gas as less land efficient than coal, but our analysis agrees with Smil’s in showing it to be more. Some of the natural gas currently produced from shale is a byproduct of oil production, especially in the Permian basin, where it may be flared or vented (this is being better controlled) due to low gas prices and low availability of pipelines, rather than sold. This means that there is some allocation need for natural gas land footprint, pointing out that part of the footprint goes to products from waste such as ethylene or more valuable products like oil. This will diminish the overall land footprint of natural gas, or increase its power density.

5.4.5 Biomass

The biomass used for electricity is mainly from wood, wood waste solids, black liquor, landfill gas and solid waste [180]. Both Fthenakis and Kim’s analysis as well as Smil’s analysis and others give very wide ranges for biomass and focus on crops,

particularly corn for ethanol. Land use issues for bioenergy from food crops differ from other land use issues since they also hinge on the food versus fuel debate. Here we focus on land use for wood and wood waste products. Neither paper evaluates wood waste products. Only Gagnon et al. show an estimate for power production from wood waste, included in Figs. E.1 and E.2 [34].

For woody biomass, we consider a yield on the order of 5-15 t/ha for temperate species such as willow and poplar [35,165]. Smil assumes a heating value of 19 GJ/t. This is further modified with an efficiency value, which we assumed as 30%. Using the high end (15 t/ha) gives $0.27 \text{ W}_e/\text{m}^2$. A lower bound of 5 t/ha with a lower heating value of 15 GJ/t and a lower efficiency value of 20% gives a power density of $0.05 \text{ W}_e/\text{m}^2$. This does not consider plant siting or indirect land use, which Fthenakis and Kim mentioned were a magnitude of difference smaller. Land use intensity values in Fthenakis and Kim of $101\text{-}136 \text{ m}^2/\text{GJ}$ [165] bracket our calculated value of $117 \text{ m}^2/\text{GJ}$, obtained by multiplying yield by heating value/efficiency. Still, both of these values should be considered high estimates for land use, since most biomass for power is derived from waste products, and thus does not require new land use.

5.4.6 Hydropower

Land use by hydro projects is extremely variable [35,165]. Fthenakis and Kim use a levelized equation, estimating the total power generated in a 30 year project lifetime [165]. A 30-year lifetime is very short for a hydropower project, however. Also, the results summary shows a much smaller land footprint for hydropower than the generic reservoir listed in Table 7 (which shows a transformation figure of $25,000 \text{ m}^2/\text{GWh}$, higher than any other generation technology by far) [165]. Note that hydro has effects downstream as well, not only at the reservoir. On the other hand, in the US, it has been performed so extensively that untouched waterways no longer remain.

Smil points out that since the power generation depends on the hydraulic head and water flow rate, deep water dams can have a smaller footprint in terms of size

of the reservoir, whereas shallow dams will have a larger reservoir and thus higher footprint [35]. The only US dam that Smil includes is the Grand Coulee Dam. The nameplate capacity is 6,809 MW, but the capacity factor generally used is 36%. The reservoir surface area is 125 square mile (sq mi) (324 km²). This gives a power density of 7.6 W_e/m². The famous Hoover dam has a nameplate capacity of 2,080 MW with capacity factor of 23% and reservoir area of 640 km², so a power density of 0.75 W_e/m².

The total surface area of dams in the 2018 national inventory of dams (does not include all dams, but best record we have) is 4.61 x 10⁷ acres [181]. In 2018, 292 billion kilowatt hour (kWh) of hydroelectricity was generated in the US from 79,893 MW of installed capacity (so a capacity factor overall of 0.417) [182]. This averages 0.18 W_e/m² or 6.39 x 10⁵ m²/GWh. While a large-scale hydropower plant or one with an exceptionally deep reservoir could have a high power density, the average power density is probably more representative for most projects or existing capacity that could be developed in the US. Hand et al.'s analysis assumes only run of the river generation, with a much lower land footprint (see Figs. E.1 and E.2) [166].

5.4.7 Geothermal

The sources that included land use for geothermal power (not included in [165]) typically rely on an analysis performed by DiPippo in 1991 [183] (for example Smil, p. 93 cites DiPippo, and then cites McDonald, who cited an MIT Energy Study whose estimates came from DiPippo). Copeland et al. look at records from the Bureau of Land Management, noting that 449,000 ha of federal lands were subject to lease for geothermal development [184]. Around 2,700 megawatts of installed nominal capacity (MW_i) existed in 2013 [185]. Capacity factor is generally around 0.7. This would give a power density of 0.42 W_e/m² or 2.4 W_e/m². This is much lower in density than literature estimates, however, since not all development would be complete. Copeland et al. estimate 1 exajoule per 208,333 ha, which is equivalent to 15.2 W_e/m², without

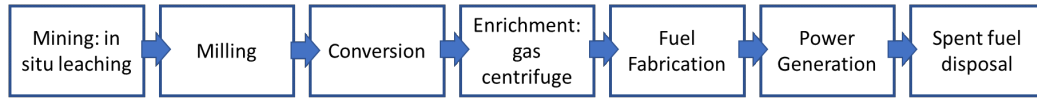


Fig. 5.2.: Nuclear energy process diagram

specifying whether this refers to disturbed or landscape effect [184]. Smil provides a landscape estimate for the Geysers as a power density of $21 \text{ W}_i/\text{m}^2$, and varies that to provide a direct footprint of $55 \text{ W}_i/\text{m}^2$. We use this pair of estimates (and a capacity factor of 0.7), since many geothermal projects seem to have a higher power density than that derived from overall leased land.

5.4.8 Nuclear

As in the case of all fuel-based power generation, nuclear energy requires a fuel cycle as well as transport before the generation stage. Fig. 5.2 shows the cradle to gate stages for nuclear power. Note that according to [165], only mining, milling, power generation and fuel disposal have a significant land footprint. Land use for nuclear energy has been the subject of much debate. In part this is due to dissent over the land requirement for uranium enrichment, with some sources [186] ascribing all and others [165] a large portion (30%) to the gas diffusion process, which is now obsolete (according to [187] all plants have now been shut down). Since the centrifuge process is much less energy intensive, the corresponding indirect land use is here assumed to be inconsequential.

Unlike coal and natural gas, 90% of uranium used for US power generation is imported [188]. Canada is the largest supplier, but Kazakhstan and Uzbekistan are also significant suppliers. In situ leaching is the major technology for uranium mining. Only one domestic uranium mill and one domestic enrichment plant are currently operational. This means that domestic land use impacts going forward are concentrated on the power generation stage. Fthenakis and Kim show graphically that the power plant is the largest land use stage for nuclear [165]. Together, mining,

milling and disposal account for a larger area than the power plant in their analysis, just under 2/3 of the total. So, total land use can be discounted by approximately 1/4 if just US territorial area is of interest.

Since no disposal sites have been commissioned in the US, most waste remains on site at power plants. Thus, we do not assign additional land footprint to the disposal stage. We do consider the entire land footprint for both the power plants and mining. Nuclear is the best example of how while the power plant may occupy just a small portion of the site, the siting of plants shows the much larger landscape effect perceived by the public.

If we assume that all future uranium needs come from imports and consider only domestic land use, and use a figure of 1.3 sq mi (3.4×10^6 m²) needed per 1000 MW installed capacity [189], running at a capacity factor of 90%, we get a power density of 267.3 W_e/m² and a land use intensity of 427 m²/GWh. If we assume that same reactor needs 200 t of mined uranium per year, extracted via in-situ leaching, it requires 1/5 of the total production of the Beverly Mine (800 ha total), so the production from 160 ha (0.6 sq mi). Assuming that mining and generation account for all land use gives a power density of 181.2 W_e/m² and land use intensity of 630 m²/GWh.

Smil includes one US mine, Crow Butte, whose license covers 1,320 ha but with only 440 disturbed [35]. Using the disturbed acreage, a power conversion assumption of 42.2 GWh/t and total extraction of 3800 t in 11 years, the power density is 380 W_e/m². To be consistent with other calculations, the total mine area should be used, which gives the lower power density of 126 W_e/m². Looking backwards presents a different story, however. In the US, there are thousands of abandoned uranium mines, typically abandoned when production became uneconomical with no safeguards put in place at the time. This is part of nuclear power's legacy in the US.

5.4.9 Storage

Reliance on variable renewables makes storage and auxiliary services separate elements. This may be transformative particularly in markets, since high prices result in part from the need to generate and use electricity in tandem. Storage was not included in any of the major sources we surveyed. There are a variety of estimates of how much storage capacity needs to be included per MW of renewable energy to make it comparable to fossils in terms of flexibility. Cebulla et al. find that the amount of storage depends on the amount of penetration of variable renewables [190]. They found that solar requires a higher amount of storage capacity than wind based systems. With a penetration of 80% VRE in the US, they estimated 3 TWh of storage needs, which, assuming an annual net generation of 4.178×10^9 MWh [191], amounts to less than 0.1% of generation from storage.

The two dominant storage options are hydro pumped storage and batteries. Lithium ion is the leading battery technology, but other technologies are being actively developed. Some people also anticipate a hydrogen economy to surpass difficulties such as cloudy and cold winter days with no wind. Immendoerfer et al. estimated 1×10^5 m²/GWh for pumped storage and 8×10^4 m²/GWh for batteries [192]. For pumped storage, land use concerns have been high [192], in part because pumped storage typically affects pristine greenfields. Note that the land use impact for electricity from storage is higher than all land use impacts except biomass and hydro. Still, only a portion of the storage land use (say 0.1%) would be allocated to one GWh of renewable energy. These discounted numbers are still higher than the total direct land footprint for onshore wind, nuclear, coal and natural gas, so they are not insignificant.

It is not clear whether the values in [192] will be appropriate for mature battery technologies since they are scaled up by almost 2,000. If current battery installations are more power dense and more efficient, the proportion of land use from the production phase may become more relatively important. The largest battery currently planned is the Manatee Energy Storage Center in Florida, which covers 40 acres and

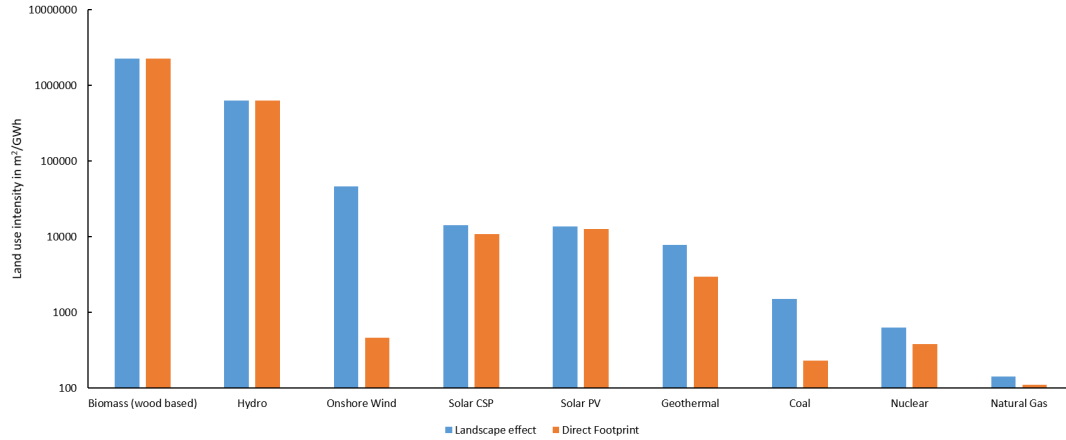


Fig. 5.3.: Land use intensities for technologies considered, shown in m^2/GWh . While natural gas is least land-intensive in both metrics, wind is much more attractive if only the direct footprint is considered.

is rated at 409 MW or 900 MWh [193]. This equates to a land use density of $1.8 \times 10^5 \text{ m}^2/\text{GWh}$, roughly double the estimates by Immendoerfer et al [192]. This area requires further study since much storage infrastructure is planned for the coming years.

5.5 Results

Figs 5.3 and 5.4 show the results of our analysis. Fig. 5.3 shows the results from our calculations in land use intensity (m^2/GWh). Fig. 5.4 shows the results in power density (W_e/m^2). In both landscape-level and direct footprints, natural gas shows the lowest land use intensity/highest power density. This assessment is based on current US practices. Electricity from biomass assumes wood plantations. Logarithmic scales are used to show the true variation between technologies. Measuring direct footprint shifts wind power and coal into better profiles versus landscape effect. These measurements are placed in context in Figs. E.1 and E.2, appendix E.

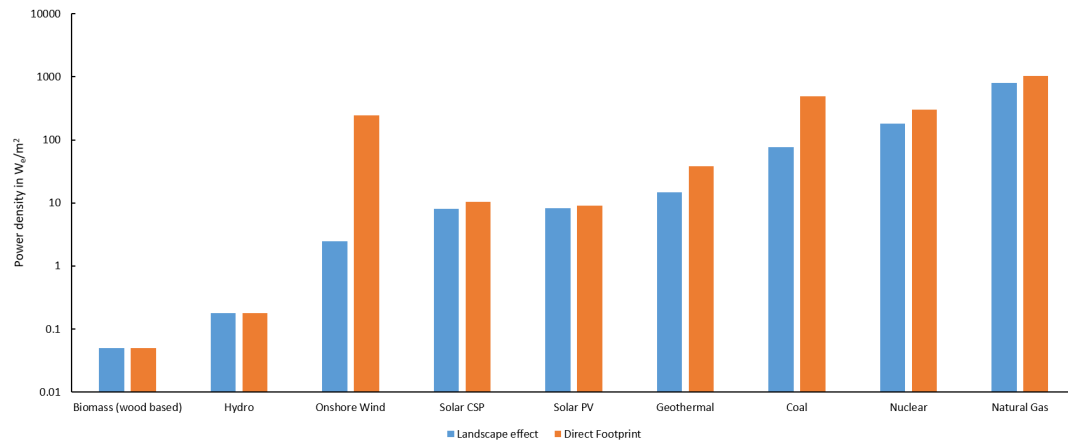


Fig. 5.4.: Power densities in W_e/m^2 for technologies considered. Note that the density is higher when only the direct footprint is considered.

5.6 Discussion

Natural gas has, by far, the highest power density/lowest land use intensity in our analysis. This can be seen in Figs. 5.3 and 5.4, as well as our literature review in Figs. E.1 and E.2, appendix E. The only low carbon technology whose land use intensity approaches that of natural gas is nuclear (in fact Smil's results group thermal power generation together, showing the similarity of the land footprint of these technologies [35]). The direct footprint of wind approaches the land footprint of conventional fossil sources. Some projects now look at combining solar panels with farming by raising the panels (see [194]). Likewise, biomass from wood wastes and hydro from run of river projects have a low footprint, but will remain marginal in their total contribution to power generation. While geothermal and solar CSP have relatively low land footprints, it may be more difficult to reduce them further. The large landscape effect of renewables suggest the potential resistance to greater use of renewables. Even when it is possible to allow combined uses, locking a field in as a wind farm does not provide the same flexibility or options for higher value future uses as a piece of farmland with no wind turbines present. Still, opportunities to mitigate effects on land and allow combined use may aid acceptance. Planning for end-of-life will also influence acceptance.

A qualitative approach to land disturbances may tell a different story, which is in part why the ecological footprint and Fthenakis and Kim's work sought to penalize conventionals further for greenhouse gas emissions and discount the major land use stage for renewables by levelizing according to lifetimes. Metrics that allow this multi-dimensional approach are still lacking.

5.6.1 Temporal Scale

Land is a finite resource, which will be under increasing pressure with population growth over the coming decades. One temporal scale of critical import, then, is the footprint, that is, land that must be dedicated to the energy system at any point

in time. This scale requires a level playing field for the various technologies. A second temporal dimension must also be considered, the question of land quality—if we shut the plant down tomorrow, have we diminished the capacity in the future to re-wild the land or to use it for something else? This temporal dimension is related to degradation and secondary effects and is discussed below in section 5.6.3.

The time horizon for fossil fuel reserves to diminish is usually much longer than our planning horizon. It is functionally equivalent to have something persist for 50 years or forever. But renewables are attractive in part because the same plot of land can be used indefinitely. Trainor et al. demonstrates a crossover point for technologies in Fig. 3 of their paper [162]. Fthenakis and Kim provide a graphical example of how timescales work with renewables, but those values are already outdated.

In [165] land use is leveled by total production over time. As soon as we want to use renewable resources, however, we must establish the farm on a given plot of land. Then the resource is meted out annually. On the other hand, once the lifetime of this farm runs out, we can refurbish and continue reaping the dividends. To make this point further, since solar power will be available every year, any lifetime could be chosen, allowing us to say that solar power requires essentially no land area. This is useless in terms of planning and assessing the snapshot of land footprints.

If fossil reserves can be known with certainty, we can calculate a ratio of energy per land area that will never be exceeded, an upper limit for the maximum power density for a given energy reserve. Using that as a measure of power density that is somehow comparable with that of renewables, however, is problematic since we do not have an instantaneous method of extracting and transporting the energy for its final use. An appropriate measure for power density, then, must be harmonized with our technological capabilities, that is what is installed on the ground and can be extracted in a given time period.

5.6.2 System Boundaries

Land use has vital consequences for nature. Since there is an inherent difficulty in determining the correct spatial boundaries for land use for power generation, it is important to consider the use of the metric. Developing land adds noises, odors and aesthetics that may be unpleasant. It replaces natural surfaces with impervious surfaces, which change runoff patterns. It removes vegetation, which provides habitat while regulating the climate. It takes away recreational space and views. It may fragment habitat or introduce invasive species. Sometimes habitat is eliminated altogether, or corrupted with pollution into waterways or air. In some cases, changes are permanent; a forest is degraded into a different ecosystem that can no longer provide the same services to people or animals, or even needs to be reclaimed. Other times, development involves only slight or temporary modifications to the land, leaving land similar to its original state. This means that two dimensions, spatial boundary and extent of damage, need to be considered.

In terms of area affected by development, Trainor et al. noted that even landscape footprint based on total area may be a conservative estimate [162]. People unhappy when offshore wind turbines mar the view from their beaches are far from the direct footprint of the turbine, but still perceive the landscape effect far beyond the area of the wind lease. Once a road divides formerly intact wilderness, habitat is fragmented on either side of the road itself. Thus, the total area is a conservative proxy for the true value, which cannot be easily measured. That means that empirical data is also the best measure of land footprints, since the size of the average building or panel does not convey the purchased area. For this reason, our results reflect both the direct footprint and landscape effect to the extent possible.

Still, as better metrics measuring biodiversity effects and ecosystem services are devised, they will vary for technologies even when the land use area is the same. More study is needed to construct this, but work must be done to understand what types of ecosystem services are affected by development for different energy types, as well

as how development affects biodiversity. In part this is what qualitative indicators like those described and used in [26, 195] seek to achieve, but it should be possible to improve them and quantify them. The lack of these indicators applied to power generation are part of what have made projects such as the Keystone pipeline so controversial, since this project affects cultural ecosystem services.

Indicators linking biodiversity to development for power generation have so far have been slow to develop. Bird mortality related to wind farms has frequently been discussed, but bird deaths related to natural gas extraction have scarcely been studied [196]. Sovacool performed a comparative study between power generation technologies, finding fossil technologies more lethal than wind energy [197]. This analysis, however, ascribed the lion's share of avian mortality to climate change. This places these issues in context, but the rest of his analysis suggests that direct mortality from fossil fuels and wind power is similar [197]. Since development from the two energy sources is similar [196], further research should enable us to quantify this and other effects on species loss. Jones and Pejchar point out the complexity of comparing mortality in wind versus oil and gas development, since it depends on the condition of the land before development and the length of time that energy is utilized from the installation [198]. No two developments are the same, even when the same energy source is used.

As Jones et al. [196] point out, it is possible to identify links between ecosystem services, biodiversity and land use. They look at wildlife mortality and population, loss and fragmentation of habitats, noise and light pollution, spread of invasive species, decrease in carbon stocks, and effects on freshwater including from impervious surfaces. Their study found that there were simply not many studies on these issues. For example, they found 79 studies on wildlife mortality in wind farms, but these spanned only 13 states in the US. They noted that most data on mortality in wind farms was proprietary. On the other hand, despite areas of concern, they found only 12 studies on wildlife mortality related to oil and gas exploration. Their study focused only on the exploration phase for gas and oil, and the wind farm operations and construction

phases for wind farms, so ignored pipelines and power plants. In fact, in a detailed review of papers on wildlife mortality across energy sources, Loss et al. found that it is not possible currently to draw on sufficient literature to compare wildlife mortality by energy technology [199].

5.6.3 Secondary effects, land degradation and end of life

Beyond the energy footprint snapshot and the additional question of its spatial boundaries, there is an additional question of reversibility. In some cases, contamination, acidification, forest deterioration caused by mining or accidents can cause long-lasting harm. In a sense, when we mine energy resources, we are passing the land use effects on to future generations if we know that restoration will be time-intensive or that damage may be permanent. For different fuel or technology sources, the level of damage differs. This legacy type effect is one of the largest barriers to acceptance of certain types of development, for example nuclear power plants. End of life for renewables can present a similar hurdle, since wind and solar farms may remain after being decommissioned, which has been a source of controversy in the past [200]. Essentially this means that once the snapshot land footprint during the asset's productive lifetime is captured, it is still necessary to capture the land footprint after that lifetime. This involves studying how long structures remain after being taken out of use, and measuring how long ecosystems services are affected at end of life. This can be an additional metric, since it can add up to a much higher amount of land than accounted for by installations on the ground, and could conceivably include double-counting. While Fthenakis and Kim mention secondary effects and end-of-life, they do not include these times in their land-use intensity metric [165]. It is likewise excluded from the other sources considered here.

Moving forward with nuclear requires inattention to mines or faith that future mines and processing sites will be dealt with differently than in the past. Hydraulic fracturing carries a large stigma with future damage to waterways. Coal mining

has seriously degraded mountainous areas and has poisoned water sources. Fuel based power generation, thus, is tied to much historic contamination. In this sense, renewables have an opportunity. Still, renewables are tied to mining as well, in rare earth metals needed for their fabrication (see op-ed in [201]), and storage is tied strongly to lithium mining. Still, the land footprint from these mines should be much smaller than the footprint of the use phase of these technologies. At the very least, long term legacies from mining, extraction and end of life should be considered in qualitative metrics.

5.6.4 Incomparabilities

Renewable plants are more viable where those resources are plentiful. Extraction also occurs at sites where fossil resources are accessible. Moran et al. approach this type of incomparability by using calculations from de Groot et al. that place monetary value on ecosystem services based on the characteristics of the landscape, i.e. forest, desert [178]. They note, for example, the high impact of shale gas extraction on temperate grasslands and forests [178]. This methodology has promise as a way of valuing damages which are always site-specific. This type of site-specific analysis will continue to be important, and is excluded in these large-scale metrics.

5.7 Conclusions

The purpose of this paper was to clarify and evaluate the metrics extant in the literature for measuring land use of power generation systems. These are frequently cited with superficial or misleading discussion of their differences. In the source papers, the methodology is not always laid out in such a way as to make them usable for researchers who might wish to use their metrics with updated data. We have attempted to clarify them for others and in the process have formulated the following recommendations:

- There is a need for up to date studies using current conditions – many of the existing assessments rely heavily on data that is almost 40 years old. No studies have been done for geothermal (since 1991) or offshore wind. The most recent solar study in the US was completed when the installations were a fraction of current installed capacity.
- If using the land use intensity metric as defined in [165], make sure that generating lifetime for renewables has been factored out, or explain why it is used and make conversions to all technologies.
- Metrics for land use should be based on annual power generation, whether annual W_e or annual Wh_e . This allows an equal playing field for technologies by basing the land use on the snapshot of the area of earth's surface that must be utilized at any point for annual generation.
- Since in many cases the entire land use is relevant in terms of effects on biodiversity, nature and landscape, the entire footprint, or landscape effect, should be assessed. A qualitative or additional scaled indicator can be factored in to give a sense of the relative impact on the land. Another distinct calculation can be included with a direct footprint as suggested by [162]. To account for slow land reclamation for coal mining, we recommend including an extra $1/3$ to all mining land footprints, since there is an additional burden from unreclaimed lands. Further study is needed on the question of land degradation and end of life, including a separate metric evaluating this, for all generation technologies.
- More work is necessary on an ecosystem services effect indicator for power generation systems, measuring the effects of the land footprint on the environment.

Land use has appeared to some a strange benchmark for power generation [186]. This is most likely due to the relatively small land footprint of energy systems as they exist today [35]. Converting our energy and materials systems away from petroleum, however, will most likely require a large increase in the land footprint [35]. This

will likely lead to new challenges for adoption, particularly in terms of community acceptance (see [14]). At the same time, the larger land footprint does not necessarily translate into worse outcomes for biodiversity or availability of ecosystem services. Further research is needed to understand these outcomes to more fully understand environmental consequences of the energy transition.

6. CONCLUSIONS AND IMPLICATIONS FOR FUTURE WORK

6.1 Overview

A framework was developed to quantify market barriers and boosts for different power generation technologies in two regional US markets: CAISO and PJM. The approach leverages on mean variance portfolio optimization by including risks and costs both in terms of dollars and sustainability. This is the first application of the portfolio optimization approach with sustainability, and the ability to view solutions in light of how they fare in terms of meeting current needs versus risks for the future is important in terms of transparency and dialogue. The framework demonstrated that offshore wind faces market barriers, but that onshore wind and solar PV only show strong barriers if it is assumed that VRE can make up 100% of the power generation mix. This may be a good assumption in PJM, where VRE makes up a very small part of the current portfolio. Still, including the revenue side for solar PV might eliminate the barrier since highly-priced SRECs are available in many PJM states. The approach here offers innovations in terms of correlation calculations, the adoption of the portfolio approach to sustainability analysis for power generation, and a useful diagnostic tool for the identification of market barriers and boosts for technologies.

The work demonstrated the difference in regions with high renewable resources versus those with lower resources, since CAISO showed market barriers for solar thermal and geothermal. One major advantage of the model is its ability to provide a range of good solutions, accessing the feasible but dominated space found to be important by [40, 42]. Correlation methods used are found to have a high impact on the resulting portfolios chosen, and a method was chosen to better represent the

relative cost proportions for each technology with the benefit of still being efficient for calculations.

The first thrust of this research showed that population growth is expected to drive increased electricity and transportation demand in Indiana cities (Ch 2). Heating is expected to play a smaller part in the total energy bundle due to climate change. These results confirm the importance of focusing on the electricity sector, since electric transport is expected to rise. The changes to Indiana's climate with the strongest impact on heating and cooling happen by 2050, with cooling demand rising in northern cities as the climate becomes more homogeneous in the state. Efficiency increases in cooling technologies are likely to ameliorate the increased cooling demand from electricity.

The second thrust involved an analysis of costs and prices for technologies in both CAISO and PJM (see chapter 3). The study confirmed that NPV tracked more closely with generation capacity expansion than did LCOE. It provided useful tools for exploring capacity market regulation changes, and showed that capacity markets bolster natural gas in PJM, which is likely to be exacerbated by the planned MOPR expansion. It suggested that markets for other aspects of renewables may be more favorable incentives than carbon pricing, which would add to the already high cost of energy in PJM and drive up the cost of new entry to the RPM.

Results of the third thrust show that renewables made up the majority of unconstrained scenarios even for market-based optimization. This was due to risk assessment that favored biomass, and low costs for solar PV and wind. Solar PV and wind were both attractive technologies, particularly from a sustainability and cost perspective. Assuming constraints based on concerns about intermittency highlights the attractiveness of other renewable technologies such as offshore wind, solar thermal and geothermal. The work highlighted the market attractiveness and relatively benign sustainability profile of natural gas profile. It did not support the argument that carbon capture and storage or nuclear power are subject to market barriers, since their outcomes in the market and sustainability optimizations were nearly identical.

Land use metrics were critically reviewed in chapter five. More work is necessary in this area, since there is still disagreement over the appropriate temporal scale and system boundaries. Much of the seminal work on this area is dated and does not accurately reflect current technologies and processes. Also, metrics do not yet accurately reflect effects on biodiversity and resource degradation. Offshore wind has not been surveyed in terms of land use. Still, an approach was suggested that used the land use intensity metric from [165] but omits the temporal discounting on renewables. Calculations were performed on fossil and renewable power generation that can be used for sustainability assessments as performed in the tool offered in chapter four.

6.2 Limitations

This model is currently available only for CAISO and PJM, and still requires running the experiments manually. It is not fully integrated with storage options that are still emerging. The results from chapters three and four point to the need for viable long-term storage options. For areas like PJM, hydro is not a viable option for winter conditions, and winter conditions will require either a very high amount of storage or else novel frameworks such as hydrogen that have not been proposed or explored. In PJM, capacity markets require consideration of a ten hour period for storage. Still, for winter peaks, storage needs may be high if VRE penetration were high. For now, constraints on VRE have been manually added to simulate this concern. This is not ideal since such constraints lead to much of the debate over integrated resource plans that override cheap VRE options in favor of leaving fossil plants open. Much work on carbon capture and storage and nuclear is based on the lack of storage and the unsuitability of intermittent VRE to act as a main power source. The work in chapters three and four does not lend support to these arguments, since neither technology choice fares well in terms of sustainability or

favorably in constrained scenarios. Still, without better storage options, these may seem more attractive.

The sustainability assessment needs further development as well. Indicators for water use were left as categorical indicators because of lack of specific data and a large bound on values for each technology. Land use metrics need further development since they do not account fully for biodiversity impacts, which is one of the chief motivators for their use. It is important to continually update the parameters for the model, because cost is very important to equity and accessibility concerns. Still, this means that lower costs for a technology not currently favorable can change the sustainability perspective as well in this model on the current needs objective. On the cost side, the emerging nature of renewable technologies makes data series short and uninformative, adding uncertainty.

Adoption of renewable energy affects the demand of petroleum and fossil resources, rather than the supply side [202]. Carbon leakage refers to price effects from decreased demand for fossil fuels in a specific place and time leading to an increase in demand in other places. Carbon leakage effects have been widely noted both in theory and actuality from unilateral actions to combat climate change. Sinn [202] pointed out that all policies on the demand side are limited in their potential to reduce global warming since the small group of global actors controlling supply of fossil resources can increase extraction in the short term if they perceive a benefit to themselves to doing so and greater risks to leaving the fossil resources in the ground. Such actions decrease prices in the short term, leading to higher usage, an intertemporal carbon leakage effect. The other issue that arises with demand side interventions is the rebound effect, usually considered when discussing efficiency improvements, but with a potential here as well. As the penetration of renewables increases, these limitations may be felt in terms of the resulting decrease in greenhouse gas emissions.

6.3 Impact on Field of Power Generation

In many geographic areas, market acceptance may be the limiting factor in the spread of renewables. The framework proposed in chapter four offers a short term analytical tool for finding discrepancies between market prognosis and sustainability of technologies. This is helpful for the design of long-term energy models, which may need to anticipate the likelihood of policies being enacted that specifically affect those technologies. It is also helpful to show stakeholders and policymakers areas that may be sources of disagreement and may require policy support.

For this to be a more helpful tool, more work could be done on the market side to incorporate profit metrics and the revenue side rather than costs. Work on the front end to make a graphical user interface and allow user input and weighting of preferences could allow this to be used by stakeholders in the integrated resource planning process, to help utilities understand the concerns and preferences of stakeholder groups and to increase transparency around scenario design.

6.4 Impact for other fields

An approach for sustainability assessments that transparently balances current and future generations is helpful for other industrial technologies and processes as well. Such a transparent approach may enable rapid diagnosis of policy mechanisms or movements that can find wide appeal. Much of the most heated debate on environmental policy issues has to do with trade-offs between meeting current needs equitably and sacrificing the comfort of future generations. This tool can allow the location on the curve to be clearly seen, so that stakeholder preferences can be more transparent. Social cost of carbon is another approach in the same vein. Eventually this tool should be able to show the location of a particular product or industry with reference to a Pareto front of best possible solutions as in Fig 6.1. As such it could be used in industry communication with customers, and could also be considered as part of a firm's strategic planning and core values discussions.

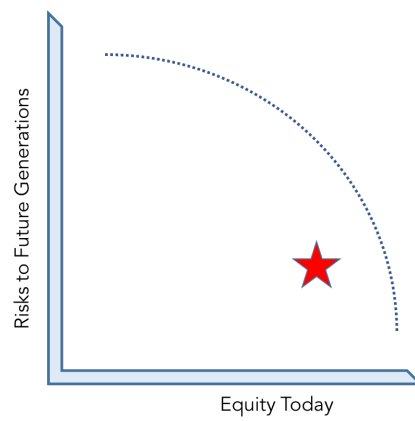


Fig. 6.1.: Illustration of a product with respect to hypothetical Pareto front according to sustainability criteria

REFERENCES

REFERENCES

- [1] D. Arent, C. Arndt, M. Miller, F. Tarp, and O. Zinaman, “Introduction and synthesis,” *The Political Economy of Clean Energy Transitions*, p. 1, 2017.
- [2] S. J. Liebowitz and S. E. Margolis, “The troubled path of the lock-in movement,” *Journal of Competition Law and Economics*, vol. 9, no. 1, pp. 125–152, 2013.
- [3] G. C. Unruh, “Understanding carbon lock-in,” *Energy policy*, vol. 28, no. 12, pp. 817–830, 2000.
- [4] A. McCrone *et al.*, “Global trends in renewable energy investment 2018,” Frankfurt School-UNEP Centre/BNEF, Tech. Rep., 2018.
- [5] G. Turner, “How much renewable energy will the global economy need?” in *Renewable Energy Finance: Powering the Future*, C. W. Donovan, Ed. London: Imperial College Press, 2015, pp. 47–76.
- [6] J. Skea, “The clean energy imperative,” in *Renewable Energy Finance: Powering the Future*, C. W. Donovan, Ed. London: Imperial College Press, 2015, pp. 17–46.
- [7] M. Sugiyama, “Climate change mitigation and electrification,” *Energy policy*, vol. 44, pp. 464–468, 2012.
- [8] S. Lechtenböhmer, L. J. Nilsson, M. Åhman, and C. Schneider, “Decarbonising the energy intensive basic materials industry through electrification—implications for future eu electricity demand,” *Energy*, vol. 115, pp. 1623–1631, 2016.
- [9] “Primary energy production by source,” http://www.eia.gov/totalenergy/data/monthly/pdf/sec1_5.pdf, April 2019.
- [10] “More than 60% of electric generating capacity installed in 2018 was fueled by natural gas,” <https://www.eia.gov/todayinenergy/detail.php?id=38632>, March 2019.
- [11] K. Hubacek and G. Baiocchi, “Fossil fuel assets may turn toxic,” *Joule*, vol. 2, no. 8, pp. 1407–1409, 2018.
- [12] A. Mills, R. Wiser, and J. Seel, “Power plant retirements: Trends and possible drivers,” Lawrence Berkeley National Laboratory, Tech. Rep., 2017.
- [13] BP, “Bp statistical review of world energy,” British Petroleum, Tech. Rep., 2018.

- [14] R. Wüstenhagen, M. Wolsink, and M. J. Bürer, "Social acceptance of renewable energy innovation: An introduction to the concept," *Energy policy*, vol. 35, no. 5, pp. 2683–2691, 2007.
- [15] C. W. Donovan, "Introduction to renewable energy finance," in *Renewable Energy Finance: Powering the Future*, C. W. Donovan, Ed. London: Imperial College Press, 2015, pp. 3–15.
- [16] M. Mazzucato and G. Semieniuk, "Financing renewable energy: Who is financing what and why it matters," *Technological Forecasting and Social Change*, vol. 127, pp. 8–22, 2018.
- [17] S. Ghosh and R. Nanda, "Venture capital investment in the clean energy sector," *Harvard Business School Working Papers*, vol. 11-020, 2010.
- [18] B. Steffen, "The importance of project finance for renewable energy projects," *Energy Economics*, vol. 69, pp. 280–294, 2018.
- [19] P. Sopher, "Early-stage venture capital for energy innovation," International Energy Agency, Tech. Rep., 2017.
- [20] R. Wüstenhagen and E. Menichetti, "Strategic choices for renewable energy investment: Conceptual framework and opportunities for further research," *Energy Policy*, vol. 40, pp. 1–10, 2012.
- [21] R. Gross, W. Blyth, and P. Heptonstall, "Risks, revenues and investment in electricity generation: Why policy needs to look beyond costs," *Energy Economics*, vol. 32, no. 4, pp. 796–804, 2010.
- [22] S. Awerbuch and S. Yang, "Efficient electricity generating portfolios for europe: maximising energy security and climate change mitigation," *EIB Papers*, vol. 12, pp. 8–37, 2007.
- [23] S. Abbasi and N. Abbasi, "The likely adverse environmental impacts of renewable energy sources," *Applied energy*, vol. 65, no. 1-4, pp. 121–144, 2000.
- [24] N. Onat and H. Bayar, "The sustainability indicators of power production systems," *Renewable and Sustainable Energy Reviews*, vol. 14, no. 9, pp. 3108–3115, 2010.
- [25] M. Z. Jacobson, "Review of solutions to global warming, air pollution, and energy security," *Energy & Environmental Science*, vol. 2, no. 2, pp. 148–173, 2009.
- [26] J. J. C. Barros, M. L. Coira, M. P. De la Cruz López, and A. del Caño Gochi, "Assessing the global sustainability of different electricity generation systems," *Energy*, vol. 89, pp. 473–489, 2015.
- [27] J. J. C. Barros, M. L. Coira, M. P. de la Cruz López, A. del Caño Gochi, and I. Soares, "Probabilistic multicriteria environmental assessment of power plants: A global approach," *Applied Energy*, vol. 260, p. 114344, 2020.
- [28] T. Hooper, M. C. Austen, N. Beaumont, P. Heptonstall, R. A. Holland, I. Ket-sopoulou, G. Taylor, J. Watson, and M. Winskel, "Do energy scenarios pay sufficient attention to the environment? lessons from the uk to support improved policy outcomes," *Energy Policy*, vol. 115, pp. 397–408, 2018.

- [29] IEA, “World energy outlook,” International Energy Agency and Organisation for Economic Co-operation and Development, Tech. Rep., 2009.
- [30] —, “World energy outlook,” International Energy Agency and Organisation for Economic Co-operation and Development, Tech. Rep., 2017.
- [31] R. K. Pachauri, M. R. Allen, V. R. Barros, J. Broome, W. Cramer, R. Christ, J. A. Church, L. Clarke, Q. Dahe, P. Dasgupta *et al.*, *Climate change 2014: synthesis report. Contribution of Working Groups I, II and III to the fifth assessment report of the Intergovernmental Panel on Climate Change*. Ipcc, 2014.
- [32] C. A. Kennedy, I. Stewart, A. Facchini, I. Cersosimo, R. Mele, B. Chen, M. Uda, A. Kansal, A. Chiu, K.-g. Kim, C. Dubeux, E. Lebre La Rovere, B. Cunha, S. Pincetl, J. Keirstead, S. Barles, S. Pusaka, J. Gunawan, M. Adegbile, M. Nazariha, S. Hoque, P. J. Marcotullio, F. González Otharán, T. Genena, N. Ibrahim, R. Farooqui, G. Cervantes, and A. D. Sahin, “Energy and material flows of megacities,” *Proceedings of the National Academy of Sciences*, vol. 112, no. 19, pp. 5985–5990, 2015. [Online]. Available: <http://www.pnas.org/lookup/doi/10.1073/pnas.1504315112>
- [33] S. Singh and C. Kennedy, “Estimating future energy use and CO₂ emissions of the world’s cities,” *Environmental Pollution*, vol. 203, pp. 271–278, 2015. [Online]. Available: <http://dx.doi.org/10.1016/j.envpol.2015.03.039>
- [34] L. Gagnon, C. Belanger, and Y. Uchiyama, “Life-cycle assessment of electricity generation options: The status of research in year 2001,” *Energy policy*, vol. 30, no. 14, pp. 1267–1278, 2002.
- [35] V. Smil, *Power density: a key to understanding energy sources and uses*. MIT Press, 2015.
- [36] L. Wachs and S. Singh, “Projecting the urban energy demand for indiana, usa, in 2050 and 2080,” *Climatic Change*, pp. 1–18, 2020.
- [37] S. Pfenninger, A. Hawkes, and J. Keirstead, “Energy systems modeling for twenty-first century energy challenges,” *Renewable and Sustainable Energy Reviews*, vol. 33, pp. 74–86, 2014.
- [38] “Global energy assessment: toward a sustainable future,” Global Energy Assessment, Cambridge, UK, and Laxenburg, Austria, Tech. Rep., 2012.
- [39] R. Loulou and M. Labriet, “Etsap-tiam: the times integrated assessment model part i: Model structure,” *Computational Management Science*, vol. 5, no. 1-2, pp. 7–40, 2008.
- [40] E. Trutnevyte, “Does cost optimization approximate the real-world energy transition?” *Energy*, vol. 106, pp. 182–193, 2016.
- [41] A. Der Kiureghian and O. Ditlevsen, “Aleatory or epistemic? does it matter?” *Structural Safety*, vol. 31, no. 2, pp. 105–112, 2009.
- [42] J. F. DeCarolus, “Using modeling to generate alternatives (mga) to expand our thinking on energy futures,” *Energy Economics*, vol. 33, no. 2, pp. 145–152, 2011.

- [43] R. E. Klosterman, "Simple and complex models," *Environment and Planning B: Planning and Design*, vol. 39, no. 1, pp. 1–6, 2012.
- [44] P. L. Joskow, "Capacity payments in imperfect electricity markets: Need and design," *Utilities Policy*, vol. 16, no. 3, pp. 159–170, 2008.
- [45] —, "Comparing the costs of intermittent and dispatchable electricity generating technologies," *American Economic Review*, vol. 101, no. 3, pp. 238–41, 2011.
- [46] M. Kohansal, A. Sadeghi-Mobarakeh, and H. Mohsenian-Rad, "A data-driven analysis of supply bids in california iso market: Price elasticity and impact of renewables," in *2017 IEEE International Conference on Smart Grid Communications (SmartGridComm)*. IEEE, 2017, pp. 58–63.
- [47] "2017 state of the market report," PJM, Tech. Rep., August 2018.
- [48] Data Driven Yale, NewClimate Institute, PBL, "Global climate action of regions, states and businesses," Data Driven Yale, NewClimate Institute, PBL, Tech. Rep., 2018. [Online]. Available: <http://bit.ly/yale-nci-pbl-global-climate-action>
- [49] M. A. Schilling and M. Esmundo, "Technology s-curves in renewable energy alternatives: Analysis and implications for industry and government," *Energy Policy*, vol. 37, no. 5, pp. 1767–1781, 2009.
- [50] C. M. Christensen, "Exploring the limits of the technology s-curve. part i: component technologies," *Production and operations management*, vol. 1, no. 4, pp. 334–357, 1992.
- [51] —, "Exploring the limits of the technology s-curve. part ii: Architectural technologies," *Production and Operations Management*, vol. 1, no. 4, pp. 358–366, 1992.
- [52] R. U. Ayres, "Toward a non-linear dynamics of technological progress," *Journal of Economic Behavior & Organization*, vol. 24, no. 1, pp. 35–69, 1994.
- [53] J. H. Cochrane, *Asset Pricing*, revised ed. Princeton University Press, 2009.
- [54] W. Short, D. J. Packey, and T. Holt, "A manual for the economic evaluation of energy efficiency and renewable energy technologies," National Renewable Energy Laboratory (NREL), Tech. Rep., 1995.
- [55] T. Helms, S. Salm, and R. Wüstenhagen, "Investor-specific cost of capital and renewable energy investment decisions," in *Renewable Energy Finance: Powering the Future*, C. W. Donovan, Ed. London: Imperial College Press, 2015, pp. 77–101.
- [56] V. Datar and S. Mathews, "European real options: An intuitive algorithm for the black-scholes formula," *Journal of Applied Finance*, 2004.
- [57] M. Collan, R. Fullér, and J. Mezei, "A fuzzy pay-off method for real option valuation," in *Business Intelligence and Financial Engineering, 2009. BIFE'09. International Conference on*. IEEE, 2009, pp. 165–169.

- [58] K. C. Seto, S. Dhakal, A. Bigio, H. Blanco, G. C. Delgado, D. Dewar, L. Huang, A. Inaba, A. Kansal, S. Lwasa, J. McMahon, D. Müller, J. Murakami, H. Nagrenda, and A. Ramaswami, *Climate Change 2014: Mitigation of Climate Change. Contribution of Working Group III to the Fifth Assessment Report of the Intergovernmental Panel on Climate Change*. Cambridge University Press, 2015, ch. 12. Human Settlements, Infrastructure, and Spatial Planning, pp. 923–1000.
- [59] A. Schneider, M. A. Friedl, and D. Potere, “A new map of global urban extent from MODIS satellite data,” *Environmental Research Letters*, vol. 4, no. 4, 2009.
- [60] E. R. Masanet, D. Poponi, T. Bryant, K. Burnard, P. Cazzola, J. Dulac, A. F. Pales, J. Husar, P. Janoska, L. Munuera, U. Remme, J. Teter, and K. West, *Energy Technology Perspectives 2016 - Towards Sustainable Urban Energy Systems*. International Energy Agency, 2016.
- [61] L. Parshall, K. Gurney, S. A. Hammer, D. Mendoza, Y. Zhou, and S. Geethakumar, “Modeling energy consumption and CO₂ emissions at the urban scale: Methodological challenges and insights from the United States,” *Energy Policy*, vol. 38, no. 9, pp. 4765–4782, 2010. [Online]. Available: <http://dx.doi.org/10.1016/j.enpol.2009.07.006>
- [62] M. Watts, “Commentary: Cities spearhead climate action,” *Nature Climate Change*, vol. 7, no. 8, pp. 537–538, 2017. [Online]. Available: <http://dx.doi.org/10.1038/nclimate3358>
- [63] L. Raymond, D. Gotham, W. McClain, S. Mukherjee, R. Nateghi, P. V. Preckel, P. Schubert, S. Singh, and E. Wachs, “Projected climate change impacts on indiana’s energy demand and supply,” *Climatic Change*, Jan 2019. [Online]. Available: <https://doi.org/10.1007/s10584-018-2299-7>
- [64] US Census Bureau, “2010 Census Urban and Rural Classification and Urban Area Criteria,” Washington, DC, 2012. [Online]. Available: <https://www.census.gov/geo/reference/ua/urban-rural-2010.html>
- [65] A. M. Thomson, K. V. Calvin, S. J. Smith, G. P. Kyle, A. Volke, P. Patel, S. Delgado-Arias, B. Bond-Lamberty, M. A. Wise, L. E. Clarke, and J. A. Edmonds, “RCP4.5: A pathway for stabilization of radiative forcing by 2100,” *Climatic Change*, vol. 109, no. 1, pp. 77–94, 2011.
- [66] K. Riahi, S. Rao, V. Krey, C. Cho, V. Chirkov, G. Fischer, G. Kindermann, N. Nakicenovic, and P. Rafaj, “RCP 8.5-A scenario of comparatively high greenhouse gas emissions,” *Climatic Change*, vol. 109, no. 1, pp. 33–57, 2011.
- [67] J. Ritchie and H. Dowlatabadi, “The 1000 GtC coal question: Are cases of vastly expanded future coal combustion still plausible?” *Energy Economics*, vol. 65, pp. 16–31, 2017. [Online]. Available: <http://dx.doi.org/10.1016/j.eneco.2017.04.015>
- [68] US Energy Information Administration, “Indiana: State Profile and Energy Estimates,” 2017. [Online]. Available: <https://www.eia.gov/state/?sid=IN>

- [69] M. a. McNeil and V. E. Letschert, “Future air conditioning energy consumption in developing countries and what can be done about it: the potential of efficiency in the residential sector,” Lawrence Berkeley National Laboratory, Tech. Rep., 2008. [Online]. Available: <https://escholarship.org/uc/item/64f9r6wr>
- [70] M. Isaac and D. P. van Vuuren, “Modeling global residential sector energy demand for heating and air conditioning in the context of climate change,” *Energy Policy*, vol. 37, no. 2, pp. 507–521, 2009.
- [71] L. G. Fishbone and H. Abilock, “Markal, a linear-programming model for energy systems analysis: Technical description of the bnl version,” *International journal of Energy research*, vol. 5, no. 4, pp. 353–375, 1981.
- [72] C. Heaps, “Long-range energy alternatives planning (LEAP) system,” 2016, software version: 2018.1.8. [Online]. Available: <https://www.energycommunity.org>
- [73] K. R. Gurney, D. L. Mendoza, Y. Zhou, M. L. Fischer, C. C. Miller, S. Geethakumar, and S. de la Rue du Can, “High resolution fossil fuel combustion co2 emission fluxes for the united states,” *Environmental science & technology*, vol. 43, no. 14, pp. 5535–5541, 2009.
- [74] M. A. Brown and E. Logan, “The Residential Energy and Carbon Footprints of the 100 The Residential Energy and Carbon Footprints of the 100 Largest U . S . Metropolitan Areas,” 2008, white paper.
- [75] M. Sivak, “Potential energy demand for cooling in the 50 largest metropolitan areas of the world: Implications for developing countries,” *Energy Policy*, vol. 37, no. 4, pp. 1382–1384, 2009.
- [76] L. W. Davis and P. J. Gertler, “Contribution of air conditioning adoption to future energy use under global warming,” *Proceedings of the National Academy of Sciences*, vol. 112, no. 19, pp. 5962–5967, 2015. [Online]. Available: <http://www.pnas.org/lookup/doi/10.1073/pnas.1423558112>
- [77] US Energy Information Administration, “2015 Residential Energy Consumption Survey,” 2017.
- [78] D. J. Sailor and A. A. Pavlova, “Air conditioning market saturation and long-term response of residential cooling energy demand to climate change,” *Energy*, vol. 28, no. 9, pp. 941–951, 2003.
- [79] M. Lokhandwala and R. Nateghi, “Leveraging advanced predictive analytics to assess commercial cooling load in the U.S.” *Sustainable Production and Consumption*, vol. 14, pp. 66–81, 2018. [Online]. Available: <https://www.sciencedirect.com/science/article/pii/S2352550918300083>
- [80] D. J. Sailor and J. R. Muñoz, “Sensitivity of electricity and natural gas consumption to climate in the U.S.A. - Methodology and results for eight states,” *Energy*, vol. 22, no. 10, pp. 987–998, 1997.
- [81] R. Nateghi and S. Mukherjee, “A multi-paradigm framework to assess the impacts of climate change on end-use energy demand,” *PLoS ONE*, vol. 12, no. 11, p. e0188033, 2017. [Online]. Available: <http://journals.plos.org/plosone/article/file?id=10.1371/journal.pone.0188033{&}type=printable>

- [82] J. A. Dirks, W. J. Gorrisen, J. H. Hathaway, D. C. Skorski, M. J. Scott, T. C. Pulsipher, M. Huang, Y. Liu, and J. S. Rice, "Impacts of climate change on energy consumption and peak demand in buildings: A detailed regional approach," *Energy*, vol. 79, no. C, pp. 20–32, 2015. [Online]. Available: <http://dx.doi.org/10.1016/j.energy.2014.08.081>
- [83] H. Wang and Q. Chen, "Impact of climate change heating and cooling energy use in buildings in the united states," *Energy and Buildings*, vol. 82, pp. 428–436, 2014.
- [84] M. A. McNeil, V. E. Letschert, and S. de la Rue du Can, "Global Potential of Energy Efficiency Standards and Labeling Programs," Ernest Orlando Lawrence Berkeley National Laboratory, Tech. Rep. June, 2008. [Online]. Available: <https://eaei.lbl.gov/sites/all/files/lbnl-760e.pdf>
- [85] U. E. I. Administration, "Annual energy outlook," US Department of Energy, United States Government Printing Office: Washington, DC, Tech. Rep., 2017.
- [86] G. Iyer, L. Clarke, J. Edmonds, P. Kyle, C. Ledna, H. Mcjeon, and M. Wise, "GCAM-USA Analysis of U . S . Electric Power Sector Transitions," Pacific Northwest National Laboratory - US Department of Energy, Tech. Rep. May, 2017.
- [87] F. Rong, L. E. Clarke, and S. J. Smith, "Climate Change and the long term evolution of the US Building sector," Pacific Northwest National Laboratory, US Department of Energy, Tech. Rep. April, 2007. [Online]. Available: http://www.pnl.gov/main/publications/external/technical{_-}reports/PNNL-16869.pdf
- [88] U. E. I. Administration, "Annual energy outlook," US Department of Energy, United States Government Printing Office: Washington, DC, Tech. Rep., 2018.
- [89] A. Hamlet, K. Brun, S. Robeson, M. Widhalm, and M. Baldwin, "Impacts of climate change on the state of Indiana: future projections based on statistical downscaling," *Climatic Change*, 2018 This issue.
- [90] STATS Indiana, "Population Projections By Age and Sex for Indiana Counties and Regions, 2010-2050," STATS Indiana, Tech. Rep., 2012. [Online]. Available: www.stats.indiana.edu/topic/projections.asp
- [91] S. Angel, J. Parent, D. L. Civco, and A. M. Blei, "Atlas of Urban Expansion Data," Lincoln Institute of Land Policy, Tech. Rep., 2012.
- [92] US Census Bureau, "Indiana : 2010 Population and Housing Unit Counts," Washington, DC, 2012. [Online]. Available: <https://www.census.gov/prod/cen2010/cph-2-16.pdf>
- [93] —, "Quickfacts database," 2017.
- [94] M. Douglas and G. Runger, *Applied statistics and probability for engineers*. John Wiley & Sons, 2010.
- [95] US Energy Information Administration, "Commercial Buildings Energy Consumption Survey (CBECS)," 2012. [Online]. Available: <https://www.eia.gov/consumption/commercial/>

- [96] J. Arbib and T. Seba, “Rethinking Transportation 2020-2030,” RethinkX, Tech. Rep., May 2017.
- [97] E. Trutnevyte, W. McDowall, J. Tomei, and I. Keppo, “Energy scenario choices: Insights from a retrospective review of uk energy futures,” *Renewable and sustainable energy reviews*, vol. 55, pp. 326–337, 2016.
- [98] S. Reichelstein and A. Sahoo, “Time of day pricing and the levelized cost of intermittent power generation,” *Energy Economics*, vol. 48, pp. 97–108, 2015.
- [99] “Cost of generation model version 3.98,” 2016.
- [100] K. Eurek, W. Cole, D. Bielen, N. Blair, S. Cohen, B. Frew, J. Ho, V. Krishnan, T. Mai, B. Sigrin, and D. Steinberg, “Regional energy deployment system (reeds) model documentation: Version 2016,” National Renewable Energy Laboratory, Tech. Rep., 2016.
- [101] R. Bajo-Buenestado, “Welfare implications of capacity payments in a price-capped electricity sector: A case study of the texas market (ercot),” *Energy Economics*, vol. 64, pp. 272–285, 2017.
- [102] A. Bublitz, D. Keles, F. Zimmermann, C. Fraunholz, and W. Fichtner, “A survey on electricity market design: Insights from theory and real-world implementations of capacity remuneration mechanisms,” *Energy Economics*, vol. 80, pp. 1059–1078, 2019.
- [103] “Us average annual wind speed at 80 meters,” <https://windexchange.energy.gov/maps-data/319>, 2010.
- [104] L. Monitoring Analytics, “State of the market report for pjm,” PJM, Tech. Rep., 2019.
- [105] B. Kroposki, B. Johnson, Y. Zhang, V. Gevorgian, P. Denholm, B.-M. Hodge, and B. Hannegan, “Achieving a 100% renewable grid,” *IEEE Power and Energy Magazine*, vol. March/April, pp. 61–73, 2017.
- [106] “Macrs asset life table,” 2019.
- [107] G. Barbose, “Us renewables portfolio standards: 2018 annual status report,” Lawrence Berkeley National Laboratory, Tech. Rep., 2018.
- [108] “Mopr floor offer prices for 2022/2023 bra (\$/mw-day in icap mw terms),” PJM, Tech. Rep., 2019.
- [109] NREL, “Annual technology baseline,” *National Renewable Energy Laboratory*, 2018. [Online]. Available: <https://atb.nrel.gov/>
- [110] J. D. Rhodes, C. King, G. Gulen, S. M. Olmstead, J. S. Dyer, R. E. Hebner, F. C. Beach, T. F. Edgar, and M. E. Webber, “A geographically resolved method to estimate levelized power plant costs with environmental externalities,” *Energy Policy*, vol. 102, pp. 491–499, 2017.
- [111] EC European Commission and others, “Characterization factors of the ilcd recommended life cycle impact assessment methods, database and supporting information,” EC, Tech. Rep., 2012.

- [112] “Electricity monthly update,” US Energy Information Administration, Tech. Rep., 2018.
- [113] M. Bolinger and J. Seel, “Utility scale solar 2018 edition public data file,” 2018.
- [114] “Pjm quadrennial review: Discount rate,” Energyzt Advisors, LLC, Tech. Rep., 2018.
- [115] S. Newell, J. M. Hagerty, J. P. Pfeifenger, B. Zhou, E. Shorin, P. Fitz, S. Gang, P. Daou, and J. Wroble, “Pjm cost of new entry: Combustion turbines and combined-cycle plants with june 1, 2022 online date,” Brattle Group, Tech. Rep., 2018.
- [116] M. Goedhard, T. Koller, and D. Wessels, *Valuation: Measuring and managing the value of companies*. John Wiley & Sons, 2015.
- [117] S. Awerbuch, “Market-based irp: It’s easy!!!” *The Electricity Journal*, vol. 8, no. 3, pp. 50–67, 1995.
- [118] D. Hulshof, J.-P. van der Maat, and M. Mulder, “Market fundamentals, competition and natural gas prices,” *Energy Policy*, vol. 94, pp. 480–491, 2016.
- [119] “Wholesale gas price survey: 2018 edition,” International Gas Union, Tech. Rep., 2018.
- [120] B. Bernanke, “The relationship between stocks and oil prices,” 2016.
- [121] R. Weron, “Electricity price forecasting: A review of the state-of-the-art with a look into the future,” *International journal of forecasting*, vol. 30, no. 4, pp. 1030–1081, 2014.
- [122] D. of Market Monitoring, “2017 annual report on market issues & performance,” California Independent System Operator, Tech. Rep., 2018.
- [123] “Weekly commentary: Cca prices increase significantly as the front changes from april 19 to may 19,” April 2019.
- [124] “Form eia-860 detailed data with previous form data (eia-860a/860b),” September 2018.
- [125] S. Brant, E. Dupré, M. Kito, and J. Iklé, “2018 resource adequacy report,” California Public Utilities Commission Energy Division, Tech. Rep., 2019. [Online]. Available: <https://www.cpuc.ca.gov/RA/>
- [126] J. Gerdes, “How sdg&e plans to quit the electricity procurement business,” *www.greentechmedia.com*, February 2019. [Online]. Available: <https://www.greentechmedia.com/articles/read/sdge-quit-electricity-procurement-business#gs.N2DafIXv>
- [127] J. Bowring, “Capacity markets in pjw,” *Economics of Energy & Environmental Policy*, vol. 2, no. 2, pp. 47–64, 2013.
- [128] P. C. Bhagwat, L. J. de Vries, and B. F. Hobbs, “Expert survey on capacity markets in the us: Lessons for the eu,” *Utilities Policy*, vol. 38, pp. 11–17, 2016.

- [129] N. Fabra, “A primer on capacity mechanisms,” *Energy Economics*, vol. 75, pp. 323–335, 2018.
- [130] H. Höschle, C. De Jonghe, H. Le Cadre, and R. Belmans, “Electricity markets for energy, flexibility and availability—impact of capacity mechanisms on the remuneration of generation technologies,” *Energy Economics*, vol. 66, pp. 372–383, 2017.
- [131] A. Silverstein, R. Gramlich, and M. Goggin, “A customer-focused framework for electric system resilience,” Grid Strategies LLC, Washington DC, Tech. Rep., 2018.
- [132] H. Messera, “Distributed generation: Cleaner, cheaper, stronger-industrial efficiency in the changing utility landscape,” Pew Charitable Trusts, Tech. Rep., 2015.
- [133] PJM, “Electric storage resource participation model (additional hybrid resource questions addressed),” Tech. Rep., 2019. [Online]. Available: <https://pjm.com/-/media/committees-groups/committees/mic/20190206/20190206-item-07c-faq-for-order-841-and-hybrids.ashx>
- [134] M. Goggin and R. Gramlich, “Consumer impacts of ferc interference with state policies,” Grid Strategies, LLC, Tech. Rep., 2019.
- [135] G. Thomas and T. Snitchler, “Pjm policy to add \$5.7b cost to capacity market? we don’t think so,” *Utility Dive*, September 2019.
- [136] M. Goggin, “Rebuttal to epsa’s response to grid strategies’ mopr analysis,” Grid Strategies, LLC, Tech. Rep., 2019.
- [137] G. Bade, “Pjm pushes ferc to act on capacity market rules, citing ‘uncertainty’ and ‘confusion’,” *Utility Dive*, March 2019. [Online]. Available: <https://www.utilitydive.com/news/pjm-pushes-ferc-to-act-on-capacity-market-rules-citing-uncertainty-and/550297/>
- [138] R. Fu, T. W. Remo, and R. M. Margolis, “2018 us utility-scale photovoltaics-plus-energy storage system costs benchmark,” National Renewable Energy Lab.(NREL), Golden, CO (United States), Tech. Rep., 2018.
- [139] W. J. Cole and A. Frazier, “Cost projections for utility-scale battery storage,” National Renewable Energy Lab.(NREL), Golden, CO (United States), Tech. Rep., 2019.
- [140] S. Reed, “Could beer brewed with wind power help save the planet?” *New York Times*, May 2019. [Online]. Available: <https://www.nytimes.com/2019/05/12/climate/renewable-wind-solar-energy.html>
- [141] R. U. Ayres, J. C. van den Bergh, and J. M. Gowdy, “Weak versus strong sustainability.”
- [142] J. Elkington, *Cannibals with Forks: The Triple Bottom Line of 21st Century Business*. New Society Publishers, 1998.
- [143] “Us installed and potential wind power capacity and generation,” 2020.

- [144] “Us offshore 90-meter wind resource potential,” 2020.
- [145] A. Lopez, B. Roberts, D. Heimiller, N. Blair, and G. Porro, “Us renewable energy technical potentials: A gis-based analysis,” National Renewable Energy Laboratory, Tech. Rep., 2012.
- [146] P. Kurup and C. Turchi, “Potential for solar industrial process heat in the united states: A look at california,” in *AIP Conference Proceedings*. AIP Publishing, 2016, p. 110001.
- [147] “Assessment of moderate- and high-temperature geothermal resources of the united states,” USGS, Tech. Rep., 2008. [Online]. Available: <https://pubs.usgs.gov/fs/2008/3082/>
- [148] B. Hadjerioua, Y. Wei, and S.-C. Kao, “An assessment of energy potential at non-powered dams in the united states,” US Department of Energy, Tech. Rep., 2012.
- [149] S.-C. Kao, R. A. McManamay, K. M. Stewart, N. M. Samu, B. Hadjerioua, S. T. DeNeale, D. Yeasmin, M. F. K. Pasha, A. A. Oubeidillah, and B. T. Smith, “New stream-reach development: A comprehensive assessment of hydropower energy potential in the united states,” US Department of Energy, Tech. Rep., 2014. [Online]. Available: <https://www.osti.gov/servlets/purl/1130425>
- [150] F. de Llano-Paz, A. Calvo-Silvosa, S. Iglesias Antelo, and I. Soares, “Energy planning and modern portfolio theory: A review,” *Renewable and Sustainable Energy Reviews*, vol. 77, pp. 636–651, 2017.
- [151] M. Arnesano, A. Carlucci, and D. Laforgia, “Extension of portfolio theory application to energy planning problem—the italian case,” *Energy*, vol. 39, pp. 112–124, 2012.
- [152] L. Vimmerstedt, S. Akar, C. Augustine, P. Beiter, W. Cole, D. Feldman, P. Kurup, E. Lantz, R. Margolis, T. Stehly, and C. Turchi, “2019 annual technology baseline,” 2019.
- [153] R. Perez Odeh, D. Watts, and Y. Flores, “Planning in a changing environment: Applications of portfolio optimisation to deal with risk in the electricity sector,” *Renewable and Sustainable Energy Reviews*, vol. 82, pp. 3808–3823, 2018.
- [154] E. Wachs and B. Engel, “Reliability versus renewables: Modeling decision making in caiso and pjm to identify market barriers and supports to renewable energy adoption in the us,” *Engrxiv.org*, 2019.
- [155] S. Awerbuch, “Portfolio-based electricity generation planning: policy implications for renewables and energy security,” *Mitigation and adaptation strategies for Global Change*, vol. 11, no. 3, pp. 693–710, 2006.
- [156] R. Wiser and M. Bolinger, “2017 wind technologies market report,” Lawrence Berkeley Lab, Electricity Markets & Policy Group, Tech. Rep., 2018.
- [157] R. C. Garcia, V. González, J. Contreras, and J. E. Custodio, “Applying modern portfolio theory for a dynamic energy portfolio allocation in electricity markets,” *Electric Power Systems Research*, vol. 150, pp. 11–23, 2017.

- [158] F. d.-L. Paz, S. I. Antelo, A. C. Silvosa, and I. Soares, “The technological and environmental efficiency of the eu-27 power mix: An evaluation based on mpt,” *Energy*, vol. 69, pp. 67–81, 2014.
- [159] “Design optimization of a welded beam,” 2020. [Online]. Available: <https://www.mathworks.com/help/gads/multiobjective-optimization-welded-beam.html>
- [160] B. Alarcon, A. Aguado, R. Manga, and A. Josa, “A value function for assessing sustainability: Application to industrial buildings,” *Sustainability*, vol. 3, pp. 35–50, 2011.
- [161] J. Farfan and C. Breyer, “Structural changes of global power generation capacity towards sustainability and the risk of stranded investments supported by a sustainability indicator,” *Journal of Cleaner Production*, vol. 141, pp. 370–384, 2017.
- [162] A. M. Trainor, R. I. McDonald, and J. Fargione, “Energy sprawl is the largest driver of land use change in united states,” *PloS one*, vol. 11, no. 9, 2016.
- [163] Colorado Division of Reclamation, Mining and Safety, “Colorado Coal Mines - Activity Status,” 2013, accessed 15 November 2019. [Online]. Available: <https://mining.state.co.us/SiteCollectionDocuments/ColoradoCoalMines.pdf>
- [164] M. Wackernagel and W. Rees, *Our ecological footprint: reducing human impact on the earth*. New Society Publishers, 1998.
- [165] V. Fthenakis and H. C. Kim, “Land use and electricity generation: A life-cycle analysis,” *Renewable and Sustainable Energy Reviews*, vol. 13, no. 6-7, pp. 1465–1474, 2009.
- [166] M. M. Hand, S. Baldwin, E. DeMeo, J. Reilly, T. Mai, D. Arent, G. Porro, M. Meshek, and D. Sandor, “Renewable electricity futures study. volume 1. exploration of high-penetration renewable electricity futures,” National Renewable Energy Lab.(NREL), Golden, CO (United States), Tech. Rep., 2012.
- [167] Solar Energy Industries Association (SEIA), “US Solar Market Insight,” 2019, accessed 6 January 2020. [Online]. Available: <https://www.seia.org/us-solar-market-insight>
- [168] S. Ong, C. Campbell, P. Denholm, R. Margolis, and G. Heath, “Land-use requirements for solar power plants in the united states,” National Renewable Energy Lab.(NREL), Golden, CO (United States), Tech. Rep., 2013.
- [169] P. Denholm, M. Hand, M. Jackson, and S. Ong, “Land use requirements of modern wind power plants in the united states,” National Renewable Energy Lab.(NREL), Golden, CO (United States), Tech. Rep., 2009.
- [170] Q. Vanhellemont and K. Ruddick, “Turbid wakes associated with offshore wind turbines observed with landsat 8,” *Remote Sensing of Environment*, vol. 145, pp. 105–115, 2014.
- [171] M. Welzel, A. Schendel, T. Schlurmann, and A. Hildebrandt, “Volume-based assessment of erosion patterns around a hydrodynamic transparent offshore structure,” *Energies*, vol. 12, no. 16, p. 3089, 2019.

- [172] A. B. Gill, “Offshore renewable energy: ecological implications of generating electricity in the coastal zone,” *Journal of Applied Ecology*, vol. 42, no. 4, pp. 605–615, 2005.
- [173] E. Topham and D. McMillan, “Sustainable decommissioning of an offshore wind farm,” *Renewable energy*, vol. 102, pp. 470–480, 2017.
- [174] US Department of Energy, *Energy Technology Characterizations Handbook: Environmental Pollution and Control Factors*, 1983.
- [175] Office of Surface Mining Reclamation and Enforcement (OSMRE), “OSMRE 2012 Annual Report,” 2013, accessed 15 November 2019. [Online]. Available: <https://www.osmre.gov/resources/reports/2012.pdf>
- [176] Peabody Energy, “North Antelope Rochelle Mine,” 2019, accessed 25 September 2019. [Online]. Available: <https://www.peabodyenergy.com/Operations/U-S-Mining/Powder-River-Basin-Mining/North-Antelope-Rochelle-Mine>
- [177] US Department of Energy, “Annual Energy Outlook 2016 Reference Case: US dry natural gas production by source in the Reference case, 1990-2040,” 2016.
- [178] M. D. Moran, N. T. Taylor, T. F. Mullins, S. S. Sardar, and M. R. McClung, “Land-use and ecosystem services costs of unconventional us oil and gas development,” *Frontiers in Ecology and the Environment*, vol. 15, no. 5, pp. 237–242, 2017.
- [179] US DOT Pipeline and Hazardous Materials Safety Administration, “Gas Transmission Miles By Decade Installed,” 2019, accessed 20 December 2019. [Online]. Available: <https://portal.phmsa.dot.gov/analytics/saw.dll?Dashboard>
- [180] US Energy Information Administration (EIA), “Today in Energy: Biomass and waste fuels made up 2% of total US electricity generation in 2016,” 2017, accessed 11 September 2019. [Online]. Available: <https://www.eia.gov/todayinenergy/detail.php?id=33872>
- [181] US Army Corps of Engineers, “National Inventory of Dams,” 2019, accessed 4 October 2019. [Online]. Available: <https://nid.sec.usace.army.mil/ords/f?p=105:1::::>
- [182] US Energy Information Administration (EIA), “Hydropower explained: Where hydropower is generated,” 2019, accessed 5 November 2019. [Online]. Available: <https://www.eia.gov/energyexplained/hydropower/where-hydropower-is-generated.php>
- [183] R. DiPippo, “Geothermal energy electricity generation and environmental impact,” *Energy Policy*, vol. 19, no. 8, pp. 798–807, 1991.
- [184] H. Copeland, A. Pocerwics, and J. Kiesecker, *Geography of Energy Development in Western North America: Potential Impacts on Terrestrial Ecosystems*. Island Press, 2011, ch. 1, pp. 7–22.
- [185] US Energy Information Administration (EIA), “Today in Energy: Geothermal resources used to produce renewable electricity in western states,” 2014, accessed 19 December 2019. [Online]. Available: <https://www.eia.gov/todayinenergy/detail.php?id=17871>

- [186] A. B. Lovins, “Renewable energy’s ‘footprint’ myth,” *The Electricity Journal*, vol. 24, no. 6, pp. 40–47, 2011.
- [187] S. Philippe and A. Glaser, “Nuclear archaeology for gaseous diffusion enrichment plants,” *Science & Global Security*, vol. 22, no. 1, pp. 27–49, 2014.
- [188] US Energy Information Administration (EIA), “Nuclear explained: Where our uranium comes from,” 2019, accessed 19 November 2019. [Online]. Available: <https://www.eia.gov/energyexplained/nuclear/where-our-uranium-comes-from.php>
- [189] Nuclear Energy Institute, “Land Needs for Wind, Solar Dwarf Nuclear Plant’s Footprint,” 2015, accessed 19 November 2019. [Online]. Available: <https://www.nei.org/news/2015/land-needs-for-wind-solar-dwarf-nuclear-plants>
- [190] F. Cebulla, J. Haas, J. Eichman, W. Nowak, and P. Mancarella, “How much electrical energy storage do we need? a synthesis for the us, europe, and germany,” *Journal of Cleaner Production*, vol. 181, pp. 449–459, 2018.
- [191] US Energy Information Administration (EIA), “Today in Energy: Record US electricity generation in 2018 driven by record residential, commercial sales,” 2019, accessed 19 December 2019. [Online]. Available: <https://www.eia.gov/todayinenergy/detail.php?id=38572>
- [192] A. Immendoerfer, I. Tietze, H. Hottenroth, and T. Viere, “Life-cycle impacts of pumped hydropower storage and battery storage,” *International Journal of Energy and Environmental Engineering*, vol. 8, no. 3, pp. 231–245, 2017.
- [193] Florida Power and Light, “FPL announces plan to build the world’s largest solar-powered battery and drive accelerated retirement of fossil fuel generation,” <http://newsroom.fpl.com/2019-03-28-FPL-announces-plan-to-build-the-worlds-largest-solar-powered-battery-and-drive-accelerated-retirement-of-fossil-fuel-generation>, 2019, accessed 3 January 2020.
- [194] C. K. Miskin, Y. Li, A. Perna, R. G. Ellis, E. K. Grubbs, P. Bermel, and R. Agrawal, “Sustainable co-production of food and solar power to relax land-use constraints,” *Nature Sustainability*, vol. 2, no. 10, pp. 972–980, 2019.
- [195] E. Wachs and B. Engel, “Do market barriers exist for renewables? a portfolio approach,” in *Energy Transitions in the 21st Century*. United States Association of Engineering Economics, November 2019.
- [196] N. F. Jones, L. Pejchar, and J. M. Kiesecker, “The energy footprint: how oil, natural gas, and wind energy affect land for biodiversity and the flow of ecosystem services,” *BioScience*, vol. 65, no. 3, pp. 290–301, 2015.
- [197] B. K. Sovacool, “Contextualizing avian mortality: A preliminary appraisal of bird and bat fatalities from wind, fossil-fuel, and nuclear electricity,” *Energy Policy*, vol. 37, no. 6, pp. 2241–2248, 2009.
- [198] N. F. Jones and L. Pejchar, “Comparing the ecological impacts of wind and oil & gas development: a landscape scale assessment,” *PLoS one*, vol. 8, no. 11, 2013.

- [199] S. R. Loss, M. A. Dorning, and J. E. Diffendorfer, "Biases in the literature on direct wildlife mortality from energy development," *BioScience*, vol. 69, no. 5, pp. 348–359, 2019.
- [200] W. S. Stripling, "Wind energy's dirty word: Decommissioning," *Tex. L. Rev.*, vol. 95, p. 123, 2016.
- [201] M. M., "If you want 'renewable energy,' get ready to dig," *Wall Street Journal*, August 2019.
- [202] H.-W. Sinn, "Public policies against global warming: a supply side approach," *International Tax and Public Finance*, vol. 15, no. 4, pp. 360–394, 2008.
- [203] E. W. Weisstein, "Logistic equation."
- [204] A. V. Da Rosa, *Fundamentals of renewable energy processes*. Academic Press, 2012.
- [205] J. Warner-Freeman, "Markets report," Tech. Rep., March 2018. [Online]. Available: <https://www.pjm.com/-/media/committees-groups/committees/mc/20180319-webinar/20180319-item-07a-markets-report.ashx>
- [206] K. P. Bhandari, J. M. Collier, R. J. Ellingson, and D. S. Apul, "Energy payback time (epbt) and energy return on energy invested (eroi) of solar photovoltaic systems: A systematic review and meta-analysis," *Renewable and Sustainable Energy Reviews*, vol. 47, pp. 133–141, 2015.
- [207] J. Lambert, C. Hall, S. Balogh, A. Poisson, and A. Gupta, "Eroi of global energy resources: preliminary status and trends. report 1 of 2," State University of New York, College of Environmental Science and Forestry, Tech. Rep., 2012.
- [208] S. Schlömer, T. Bruckner, L. Fulton, E. Hertwich, A. McKinnon, D. Perczyk, J. Roy, R. Schaeffer, R. Sims, P. Smith *et al.*, "Annex iii: Technology-specific cost and performance parameters," *Climate change*, pp. 1329–1356, 2014.
- [209] "Table 7.4 weighted average cost of fossil fuels for the electric power industry, 2007-2017," October 2018.
- [210] P. Baruya, "International finance for coal-fired power plants," IEA Clean Coal Centre, Tech. Rep., 2017.
- [211] L. Jenssen and T. Gjermundsen, "Financing of small-scale hydropower projects," International Energy Agency, Tech. Rep., 2000.
- [212] F. Lucet, "Conditions and possibilities for financing new nuclear power plants," *Journal of World Energy Law & Business*, vol. 12, pp. 21–35.
- [213] "Targeted report: financing large scale integrated ccs demonstration projects," Societe Generale Corporate & Investment Bank, Tech. Rep., May 2014.
- [214] E. W. E. Association *et al.*, "Where's the money coming from? financing off-shore wind farms," *Brussels, Belgium: European Wind Energy Association. Accessed September*, vol. 7, p. 2014, 2013.
- [215] "Q1 2018 report on market issues and performance," CAISO, Tech. Rep., 2018.

- [216] “Q2 2018 report on market issues and performance,” CAISO, Tech. Rep., 2018.
- [217] “Q3 2018 report on market issues and performance,” CAISO, Tech. Rep., 2018.
- [218] “Q4 2018 report on market issues and performance,” CAISO, Tech. Rep., 2018.
- [219] “Data miner 2,” accessed January 9, 2019.
- [220] “Daily renewables output data 1/15/2018, 2/15/2018, 3/15/2018, 4/14/2018, 5/15/2018, 6/15/2018, 7/15/2018, 8/15/2018, 9/15/2018, 10/15/2018, 11/15/2018, 12/15/2018,” May 2019.
- [221] “Data miner,” accessed January 9, 2019.
- [222] D. Blockstein, L. Wiegman *et al.*, *The climate solutions consensus: What we know and what to do about it*. Island Press, 2012.
- [223] A. R. Brandt, Y. Sun, S. Bharadwaj, D. Livingston, E. Tan, and D. Gordon, “Energy return on investment (eroi) for forty global oilfields using a detailed engineering-based model of oil production,” *PloS one*, vol. 10, no. 12, p. e0144141, 2015.
- [224] C. A. Hall, J. G. Lambert, and S. B. Balogh, “Eroi of different fuels and the implications for society,” *Energy policy*, vol. 64, pp. 141–152, 2014.
- [225] B. Commission *et al.*, “World commission on environment and development. our common future,” 1987.
- [226] J. Meldrum, S. Nettles-Anderson, G. Heath, and J. Macknick, “Life cycle water use for electricity generation: a review and harmonization of literature estimates,” *Environmental Research Letters*, vol. 8, no. 1, p. 015031, 2013.
- [227] “Some us electricity generating plants use dry cooling,” *Today in Energy*, August 2018. [Online]. Available: <https://www.eia.gov/todayinenergy/detail.php?id=36773>
- [228] V. Fthenakis and H. C. Kim, “Life-cycle uses of water in us electricity generation,” *Renewable and Sustainable Energy Reviews*, vol. 14, no. 7, pp. 2039–2048, 2010.
- [229] US Energy Information Administration (EIA), “Coal Data Browser,” 2019, accessed 25 September 2019. [Online]. Available: <https://www.eia.gov/coal/data/browser/>

APPENDICES

A. MARKET PENETRATION

The penetration of new technologies into the marketplace is not instantaneous, but instead relies on gradual replacement of existing solutions, particularly when these solutions involve expensive capital equipment. The logistic or Verhulst equation was initially developed to model population dynamics.

The continuous logistic equation [203] is shown:

$$\frac{dN}{dt} = \frac{rN(K - N)}{K} \quad (\text{A.1})$$

Where K is the carrying capacity, N is the actual population and r is the Malthusian parameter, which represents the maximum growth rate. Applying this to the energy marketplace, da Vieira [204] rearranges the logistic equation to:

$$\frac{1}{x} \frac{dx}{dt} = rx(1 - x) \quad (\text{A.2})$$

Where $x \equiv \frac{N}{K}$, or the proportion of the total possible population occupied by technology x . The fractional change in the population of x over time ($\frac{1}{x} \frac{dx}{dt}$) is therefore directly proportional to the percentage of the total population not using x , that is, $(1 - x)$. Da Rosa walks through the solution for x , which is given by:

$$x = \frac{\exp\{(rt + b)\}}{1 + \exp\{(rt + b)\}} \quad (\text{A.3})$$

In this case, b represents the integration constant. It is thus possible to graph x over t for any given r and b to see an S shaped diffusion curve.

B. SUPPLEMENTARY MATERIAL FOR CHAPTER TWO

The supplementary material contains the dataset used for the electricity regression model used in chapter 2, as well as all results by city for per capita heating, cooling and electricity energy demand. In addition, information pertaining to the statistical extrapolation test run, including the code, h values and results is provided.

B.1 New data set for electricity modeling

As described in section 3.1 in the main paper, the regression coefficients differed slightly from the published models. The data used for the electricity regression model is given here in table B.1.

Table B.1.: Data used for the electricity regression model referred to in the text as S-K

City	HDD	Inverse Density (Ha/cap)	Electricity Consumption (MWh/cap)
Tianjin	2693	4.446E-03	4.146
Mumbai	1	4.836E-03	1.038
Dar es Salaam	6	5.051E-03	0.164
Seoul	2870	1.102E-02	4.455
Delhi	396	8.094E-03	1.295
Moscow	4562	1.987E-02	4.516
Manila	0	9.425E-03	1.294
Shanghai	1566	9.569E-03	5.455
Beijing	2865	1.074E-02	3.915
Jakarta	0	1.112E-02	2.906
Rio de Janeiro	7	1.149E-02	2.303
Dhaka	50	5.836E-03	0.619
Sao Paulo	329	1.258E-02	2.903
Geneva	2902	1.305E-02	6.460
Kolkata	96	3.644E-03	0.877
Lagos	0	4.865E-03	0.078
Buenos Aires	863	1.443E-02	4.187
Paris-IDF	2605	1.520E-02	5.020
Barcelona	1295	1.555E-02	4.660
Mexico City	873	8.952E-03	1.544
London	2559	1.695E-02	5.330
Cape Town	1013	1.783E-02	3.860
Osaka	1728	2.265E-02	8.271
Shenzhen	377	1.903E-02	6.650
Amman	1257	1.969E-02	2.239
Bangkok	0	2.020E-02	5.040
Karachi	153	4.246E-03	1.335
Tokyo	1594	1.968E-02	6.759
Toronto	3722	2.825E-02	10.040
Prague	3550	2.874E-02	4.660
New York City	2372	3.058E-02	6.070
Los Angeles	691	3.322E-02	6.710
Istanbul	1996	1.166E-02	2.837
Chicago	3400	4.484E-02	10.350
Denver	3425	5.650E-02	11.490
Guangzhou	539	5.830E-02	4.950
Cairo	440	7.677E-03	1.508
Tehran	1977	1.141E-02	2.027
Indianapolis	2881.5	1.161E-01	8.062

Table B.2.: Data used for heating regression. Based on the published S-K model. Industrial heating shares were assumed for each city and the modified totals were used for the regression.

Country	City	Actual Heating GJ/c/yr	Adjusted Heating GJ/c/yr	HDD	Assumption	Industrial Htg Share
Thailand	Bangkok	28.40	22.72	0	middle industry	20%
Spain	Barcelona	15.00	13.50	1295	limited industry	10%
South Africa	Cape Town	3.90	3.12	1013	middle industry	20%
USA	Denver	73.52	66.17	3425	limited industry	10%
Switzerland	Geneva	51.30	46.17	2902	limited industry	10%
UK	London	44.90	40.41	2559	limited industry	10%
USA	Los Angeles	24.20	21.78	691	limited industry	10%
USA	New York City	50.80	45.72	2372	limited industry	10%
Czech Republic	Prague	46.80	42.12	3550	limited industry	10%
Canada	Toronto	58.90	53.01	3722	limited industry	10%
China	Tianjin	46.50	30.22	2693	high industry	35%
China	Shanghai	55.06	35.79	1566	high industry	35%
China	Beijing	49.19	31.97	2865	high industry	35%
USA	Chicago	62.40	56.16	3400	limited industry	10%
France	Paris-IDF	36.00	32.40	2605	limited industry	10%
Indonesia	Jakarta	5.10	4.08	0	middle industry	20%
Jordan	Amman	5.13	4.10	1257	middle industry	20%
Argentina	Buenos Aires	21.32	19.19	863	limited industry	10%
Brazil	Sao Paulo	3.49	3.14	329	limited industry	10%
Brazil	Rio de Janeiro	5.48	4.93	7	limited industry	10%

B.2 Detailed Results for Fig. 1 in Main Text

Table B.3.: Heating demand by city for each time period. Demand is measured in GJ/capita and the cumulative percent increase or decrease from the 2015 figure is included.

Timeframe	2015		2050				2080			
Scenario	RCP 4.5	RCP 8.5	RCP 4.5		RCP 8.5		RCP 4.5		RCP 8.5	
City/Units	GJ/c	GJ/c	GJ/c	% +/-	GJ/c	% +/-	GJ/c	% +/-	GJ/c	% +/-
Bloomington	33.52	33.35	30.67	-8.5%	28.62	-14.2%	28.92	-13.7%	23.90	-28.3%
Cincinnati	34.21	34.04	31.35	-8.3%	29.28	-14.0%	29.62	-13.4%	24.41	-28.3%
Columbus	35.12	35.00	32.26	-8.1%	30.26	-13.5%	30.53	-13.1%	25.26	-27.8%
Elkhart-Gosh.	42.80	42.59	39.58	-7.5%	37.08	-12.9%	37.46	-12.5%	31.07	-27.0%
Evansville	29.04	28.91	26.21	-9.7%	24.47	-15.3%	24.75	-14.8%	20.29	-29.8%
Fort Wayne	41.81	41.60	38.76	-7.3%	36.38	-12.5%	36.75	-12.1%	30.56	-26.5%
Gary	41.19	40.94	37.96	-7.8%	35.51	-13.3%	35.86	-12.9%	29.91	-26.9%
Indianapolis	36.94	36.77	34.11	-7.6%	31.98	-13.0%	32.26	-12.7%	26.85	-27.0%
Kokomo	38.88	38.68	36.19	-6.9%	33.77	-12.7%	34.13	-12.2%	28.29	-26.9%
Lafayette-WL	39.22	39.03	36.44	-7.1%	34.08	-12.7%	34.42	-12.3%	28.57	-26.8%
Louisville	31.92	31.78	29.04	-9.0%	27.04	-14.9%	27.32	-14.4%	22.40	-29.5%
Mich City-L.P.	42.32	42.10	39.05	-7.7%	36.56	-13.2%	36.94	-12.7%	30.74	-27.0%
Muncie	38.75	38.57	36.00	-7.1%	33.69	-12.6%	34.05	-12.1%	28.21	-26.9%
South Bend-M	43.02	42.81	39.79	-7.5%	37.26	-13.0%	37.64	-12.5%	31.29	-26.9%
Terre Haute	35.72	35.53	32.92	-7.9%	30.81	-13.3%	31.08	-13.0%	25.90	-27.1%
Average	37.87	37.69	34.86	-8.0%	32.65	-13.4%	32.94	-13.0%	27.36	-27.4%
St. Dev.	4.15	4.12	4.03		3.81		3.84		3.29	

B.3 Hidden extrapolation test results

In order to ensure that the results of our regression model were not subject to hidden extrapolation, a test for hidden extrapolation was run. In B.3.1 we include the MATLAB code for running the hidden extrapolation test. Tables B.7 and B.8 have the h values for heating and electricity. Table B.9 has the test values for heating in each scenario (no hidden extrapolation was present in any modeled scenario). Table B.10 has the test values for electricity, with the extrapolated values shaded in gray.

Table B.4.: Electricity demand by city for each time period. Demand is measured in MWh/capita and the cumulative percent increase or decrease from the 2015 figure is included.

Timeframe	2015		2050				2080			
RCP Scenario	4.5	8.5	4.5		8.5		4.5		8.5	
City/Units	MWh/c	MWh/c	MWh/c	% +	MWh/c	% +	MWh/c	% +	MWh/c	% +
Bloomington	7.98	7.97	10.20	27.8%	10.06	26.3%	14.73	84.6%	14.47	81.6%
Cincinnati	11.87	11.86	15.71	32.3%	15.57	31.3%	23.66	99.3%	23.39	97.2%
Columbus	16.48	16.47	22.23	34.9%	22.10	34.2%	34.22	107.6%	33.94	106.1%
Elkhart-Gosh.	10.80	10.79	13.92	28.9%	13.75	27.5%	20.25	87.5%	19.91	84.6%
Evansville	8.52	8.51	11.09	30.2%	10.97	29.0%	14.27	67.6%	13.97	64.2%
Fort Wayne	13.29	13.28	17.50	31.7%	17.34	30.6%	22.60	70.0%	22.18	67.1%
Gary	10.33	10.31	13.30	28.7%	13.13	27.3%	16.93	63.9%	16.53	60.3%
Indianapolis	11.89	11.88	15.66	31.7%	15.52	30.6%	20.23	70.2%	19.87	67.3%
Kokomo	11.43	11.42	14.96	30.9%	14.80	29.6%	19.23	68.2%	18.84	65.0%
Lafayette-WL	9.87	9.86	12.73	28.9%	12.57	27.5%	16.21	64.2%	15.81	60.4%
Louisville	10.50	10.49	13.82	31.7%	13.68	30.5%	17.88	70.3%	17.54	67.3%
Mich City-L.P.	13.91	13.89	18.34	31.9%	18.17	30.8%	23.73	70.6%	23.31	67.8%
Muncie	11.72	11.71	15.37	31.2%	15.22	30.0%	19.79	68.9%	19.40	65.7%
South Bend-M	11.53	11.52	14.95	29.6%	14.78	28.3%	19.12	65.8%	18.70	62.3%
Terre Haute	10.30	10.29	13.44	30.5%	13.30	29.2%	17.26	67.6%	16.92	64.4%
Average	11.36	11.35	14.88	31.0%	14.73	29.8%	20.01	76.1%	19.65	73.2%
St. Dev.	2.03	2.03	2.85		2.85		4.72		4.73	

B.3.1 MATLAB Code to check for hidden extrapolation in one result dataset

```

%%%%%%%%%%%%%%%%%%%%%%%%%%%%%%%%%%%%%%%%%%%%%%%%%%%%%%%%%%%%%%%%%%%%%%%%%%
OurXData = xlsread('OurHtgData.xlsx', 'B2:B21');
OurXmatrix = OurXData;
OurXprimematrix = transpose(OurXmatrix);
OurYData = xlsread('OurHtgData.xlsx', 'C2:C21');
OurXprimeXmatrix = OurXprimematrix * OurXmatrix;
OurXprimeYmatrix = OurXprimematrix * OurYData;
OurBetaVector = inv(OurXprimeXmatrix) * OurXprimeYmatrix;
OurYHat = OurXmatrix .* OurBetaVector;
Oure = OurYData - OurYHat;

```

Table B.5.: Cooling in kWh per capita. Efficiency gains are assumed for air conditioning systems. The cumulative percent increase or decrease from the 2015 figure is included.

Timeframe	2015		2050				2080			
Scenario	RCP 4.5	RCP 8.5	RCP 4.5		RCP 8.5		RCP 4.5		RCP 8.5	
City/Units	kWh/c	kWh/c	kWh/c	% +	kWh/c	% +	kWh/c	% +	kWh/c	% +
Bloomington	338.80	350.03	327.23	-3.4%	341.60	-2.4%	310.11	-8.5%	334.90	-4.3%
Cincinnati	360.65	374.05	339.31	-5.9%	356.72	-4.6%	322.75	-10.5%	352.70	-5.7%
Columbus	325.80	333.91	295.61	-9.3%	310.57	-7.0%	281.66	-13.6%	306.59	-8.2%
Elkhart-Gosh.	177.50	187.57	213.33	20.2%	259.76	38.5%	235.06	32.4%	269.71	43.8%
Evansville	398.36	400.71	345.21	-13.3%	356.25	-11.1%	324.11	-18.6%	341.70	-14.7%
Fort Wayne	200.44	210.71	241.08	20.3%	289.06	37.2%	261.34	30.4%	295.73	40.4%
Gary	234.07	245.22	266.36	13.8%	284.90	16.2%	258.79	10.6%	291.09	18.7%
Indianapolis	299.09	311.09	288.00	-3.7%	303.21	-2.5%	275.06	-8.0%	300.74	-3.3%
Kokomo	280.43	295.65	312.48	11.4%	331.45	12.1%	300.21	7.1%	330.56	11.8%
Lafayette-WL	257.95	271.40	304.22	17.9%	324.92	19.7%	294.84	14.3%	325.89	20.1%
Louisville	348.40	351.54	307.95	-11.6%	320.66	-8.8%	291.22	-16.4%	313.22	-10.9%
Mich City-L.P.	190.49	200.71	238.73	25.3%	309.83	54.4%	287.51	50.9%	327.96	63.4%
Muncie	214.81	225.48	274.96	28.0%	318.93	41.4%	288.58	34.3%	322.92	43.2%
South Bend-M	175.65	185.12	211.64	20.5%	277.36	49.8%	251.67	43.3%	289.08	56.2%
Terre Haute	309.54	320.34	311.97	0.8%	326.34	1.9%	296.52	-4.2%	321.51	0.4%
Average	274.82	285.28	280.91	2.2%	304.26	6.7%	275.89	0.4%	304.00	6.6%
St. Dev.	70.26	69.19	41.55		26.98		24.58		21.77	

Table B.6.: Cooling in kWh per capita. No efficiency gains are assumed for air conditioning systems. The cumulative percent increase or decrease from the 2015 figure is included.

Timeframe	2015		2050				2080			
Scenario	RCP 4.5	RCP 8.5	RCP 4.5		RCP 8.5		RCP 4.5		RCP 8.5	
City/Units	kWh/c	kWh/c	kWh/c	% +	kWh/c	% +	kWh/c	% +	kWh/c	% +
Bloomington	338.80	350.03	392.98	16.0%	410.24	17.2%	406.76	20.1%	439.28	25.5%
Cincinnati	360.65	374.05	407.49	13.0%	428.40	14.5%	423.34	17.4%	462.62	23.7%
Columbus	325.80	333.91	355.00	9.0%	372.97	11.7%	369.44	13.4%	402.14	20.4%
Elkhart-Gosh.	177.50	187.57	256.20	44.3%	311.95	66.3%	308.32	73.7%	353.76	88.6%
Evansville	398.36	400.71	414.57	4.1%	427.84	6.8%	425.13	6.7%	448.20	11.9%
Fort Wayne	200.44	210.71	289.52	44.4%	347.14	64.7%	342.79	71.0%	387.90	84.1%
Gary	234.07	245.22	319.88	36.7%	342.14	39.5%	339.44	45.0%	381.82	55.7%
Indianapolis	299.09	311.09	345.87	15.6%	364.13	17.1%	360.78	20.6%	394.47	26.8%
Kokomo	280.43	295.65	375.27	33.8%	398.04	34.6%	393.78	40.4%	433.58	46.7%
Lafayette-WL	257.95	271.40	365.34	41.6%	390.20	43.8%	386.73	49.9%	427.46	57.5%
Louisville	348.40	351.54	369.82	6.2%	385.09	9.5%	381.98	9.6%	410.84	16.9%
Mich City-L.P.	190.49	200.71	286.70	50.5%	372.08	85.4%	377.11	98.0%	430.17	114.3%
Muncie	214.81	225.48	330.21	53.7%	383.02	69.9%	378.52	76.2%	423.56	87.8%
South Bend-M	175.65	185.12	254.17	44.7%	333.09	79.9%	330.10	87.9%	379.18	104.8%
Terre Haute	309.54	320.34	374.65	21.0%	391.91	22.3%	388.94	25.6%	421.72	31.6%
Average	274.82	285.28	337.36	22.8%	365.39	28.1%	361.88	31.7%	398.74	39.8%
St. Dev.	70.26	69.19	49.90		32.40		32.25		28.55	

```
OurHatmatrix = OurXmatrix * inv(OurXprimeXmatrix) * OurXprimematrix;  
ModelHValues = diag(OurHatmatrix);  
HtgModelHTable = ModelHValues;  
csvwrite('HtgModelHValues.csv', ModelHValues)  
  
OurNewXData = xlsread('ModelHtgResults2015RCP26.xlsx', 'B2:B16');  
OurXoMatrix = OurNewXData;  
OurXoPrimeMatrix = transpose(OurXoMatrix);  
OurHooMatrix = OurXoMatrix * inv(OurXprimeXmatrix) * OurXoPrimeMatrix;  
OurHooVector = diag(OurHooMatrix);  
M = max(ModelHValues);  
HiddenExtrapolationH2015RCP26 = OurHooVector > M;
```

Table B.7.: H values for Heating Model

City	H value
Bangkok	0
Barcelona	0.0167
Cape Town	0.0102
Denver	0.1165
Geneva	0.0837
London	0.0651
Los Angeles	0.0047
New York City	0.0559
Prague	0.1252
Toronto	0.1376
Tianjin	0.0721
Shanghai	0.0244
Beijing	0.0815
Chicago	0.1149
Paris-IDF	0.0674
Jakarta	0
Amman	0.0157
Buenos Aires	0.0074
Sao Paulo	0.0011
Rio de Janeiro	0

Table B.8.: H values for Electricity Model

City	H Value
Tianjin	0.0797
Mumbai	0.0015
Dar es Salaam	0.0016
Seoul	0.0739
Delhi	0.0021
Moscow	0.1786
Manila	0.0056
Shanghai	0.0184
Beijing	0.0742
Jakarta	0.0079
Rio de Janeiro	0.0083
Dhaka	0.0018
Sao Paulo	0.0062
Geneva	0.0714
Kolkata	0.0005
Lagos	0.0015
Buenos Aires	0.007
Paris-IDF	0.0519
Barcelona	0.0114
Mexico City	0.005
London	0.0476
Cape Town	0.0104
Osaka	0.0213
Shenzhen	0.0157
Amman	0.0135
Bangkok	0.0259
Karachi	0.0006
Tokyo	0.0175
Toronto	0.0958
Prague	0.0854
New York City	0.0397
Los Angeles	0.0471
Istanbul	0.0305
Chicago	0.0829
Denver	0.1079
Guangzhou	0.1797
Cairo	0.0019
Tehran	0.03
Indianapolis	0.538

Table B.9.: Heating Test values for Hidden Extrapolation

City	RCP 2.6			RCP 4.5			RCP 8.5		
	2015	2050	2080	2015	2050	2080	2015	2050	2080
Bloomington	0.0479	0.0432	0.0424	0.0515	0.0431	0.0383	0.051	0.0375	0.0262
Cincinnati	0.0497	0.0451	0.0446	0.0536	0.045	0.0402	0.0531	0.0393	0.0273
Columbus	0.0526	0.0475	0.0467	0.0565	0.0477	0.0427	0.0561	0.0419	0.0292
Elkhart-Gosh.	0.0826	0.075	0.0736	0.0839	0.0718	0.0643	0.0831	0.063	0.0442
Evansville	0.0354	0.0315	0.031	0.0386	0.0315	0.0281	0.0383	0.0274	0.0189
Fort Wayne	0.0781	0.0718	0.0706	0.0801	0.0688	0.0619	0.0793	0.0607	0.0428
Gary	0.0751	0.0689	0.0676	0.0777	0.066	0.0589	0.0768	0.0578	0.041
Indianapolis	0.0593	0.0544	0.0534	0.0625	0.0533	0.0477	0.0619	0.0469	0.033
Kokomo	0.0672	0.063	0.0614	0.0693	0.06	0.0534	0.0686	0.0522	0.0367
Lafayette/WL	0.0681	0.0631	0.0618	0.0705	0.0608	0.0543	0.0698	0.0532	0.0374
Louisville	0.0431	0.0382	0.038	0.0467	0.0386	0.0342	0.0463	0.0335	0.023
Mich City/L P	0.0798	0.0725	0.0711	0.0821	0.0699	0.0625	0.0812	0.0612	0.0433
Muncie	0.0661	0.0613	0.06	0.0688	0.0594	0.0531	0.0682	0.052	0.0365
South Bend/M	0.0834	0.0757	0.0743	0.0848	0.0725	0.0649	0.084	0.0636	0.0449
Terre Haute	0.0552	0.0506	0.0496	0.0585	0.0497	0.0442	0.0578	0.0435	0.0307

Table B.10.: Electricity Test Values for Hidden Extrapolation. Shaded values indicate extrapolation.

City	RCP 2.6			RCP 4.5			RCP 8.5		
	2015	2050	2080	2015	2050	2080	2015	2050	2080
Bloomington	0.051	0.1076	0.2219	0.0516	0.1076	0.2265	0.0515	0.1103	0.2437
Cincinnati	0.154	0.3648	0.7409	0.1518	0.3649	0.7524	0.152	0.3742	0.7929
Columbus	0.3869	0.897	1.7752	0.3815	0.8964	1.7928	0.382	0.913	1.8608
Elkhart-Gosh.	0.0965	0.2094	0.4331	0.0967	0.2111	0.4448	0.0966	0.2165	0.4768
Evansville	0.0676	0.1586	0.3264	0.0669	0.1586	0.3321	0.067	0.163	0.3537
Fort Wayne	0.1759	0.4136	0.8488	0.1752	0.4171	0.8676	0.1755	0.4276	0.9173
Gary	0.088	0.1905	0.3941	0.0882	0.1921	0.4049	0.0881	0.1971	0.4333
Indianapolis	0.143	0.3372	0.6907	0.1418	0.3385	0.7037	0.142	0.3472	0.7431
Kokomo	0.1212	0.2802	0.5792	0.1208	0.283	0.5939	0.1209	0.2911	0.6313
Lafayette/WL	0.0804	0.1743	0.3606	0.0807	0.1755	0.37	0.0806	0.1801	0.3966
Louisville	0.1143	0.2719	0.5539	0.1128	0.2713	0.563	0.1129	0.2788	0.5956
Mich City/L P	0.1986	0.4697	0.9613	0.1977	0.4731	0.9813	0.1981	0.4853	1.035
Muncie	0.1308	0.3052	0.6287	0.1301	0.3071	0.6422	0.1303	0.3154	0.6817
South Bend/M	0.1144	0.2572	0.5324	0.1144	0.2594	0.5463	0.1144	0.2663	0.5832
Terre Haute	0.0971	0.225	0.4645	0.0965	0.2259	0.4742	0.0966	0.232	0.5035

Table B.11.: In the work published in [63] the efficiency figure of 3.81 was used for 2015. This table gives the city by city cooling results with no efficiency change (so 3.81 is used for all years), that correspond to that report.

Timeframe	2015		2050				2080			
Scenario	RCP 4.5	RCP 8.5	RCP 4.5		RCP 8.5		RCP 4.5		RCP 8.5	
City/Units	kWh/c	kWh/c	kWh/c	% +	kWh/c	% +	kWh/c	% +	kWh/c	% +
Bloomington	297.90	307.77	345.53	16.0%	360.71	17.2%	357.65	20.1%	386.24	25.5%
Cincinnati	317.11	328.89	358.29	13.0%	376.68	14.5%	372.23	17.4%	406.76	23.7%
Columbus	286.47	293.59	312.14	9.0%	327.94	11.7%	324.83	13.4%	353.59	20.4%
Elkhart-Gosh.	156.07	164.93	225.26	44.3%	274.29	66.3%	271.10	73.7%	311.05	88.6%
Evansville	350.27	352.33	364.52	4.1%	376.18	6.8%	373.80	6.7%	394.09	11.9%
Fort Wayne	176.24	185.27	254.56	44.4%	305.23	64.7%	301.40	71.0%	341.07	84.1%
Gary	205.81	215.61	281.26	36.7%	300.83	39.5%	298.46	45.0%	335.72	55.7%
Indianapolis	262.98	273.53	304.11	15.6%	320.17	17.1%	317.22	20.6%	346.84	26.8%
Kokomo	246.57	259.96	329.96	33.8%	349.99	34.6%	346.24	40.4%	381.23	46.7%
Lafayette-WL	226.81	238.63	321.23	41.6%	343.09	43.8%	340.04	49.9%	375.85	57.5%
Louisville	306.33	309.09	325.17	6.2%	338.60	9.5%	335.86	9.6%	361.24	16.9%
Mich City-L.P.	167.49	176.48	252.08	50.5%	327.16	85.4%	331.58	98.0%	378.23	114.3%
Muncie	188.88	198.26	290.34	53.7%	336.77	69.9%	332.82	76.2%	372.42	87.8%
South Bend-M	154.44	162.77	223.48	44.7%	292.88	79.9%	290.25	87.9%	333.40	104.8%
Terre Haute	272.17	281.66	329.42	21.0%	344.59	22.3%	341.98	25.6%	370.80	31.6%
Average	241.64	250.84	296.62	22.8%	321.28	28.1%	318.19	31.7%	350.60	39.8%
St. Dev.	61.78	60.83	43.87		28.49		28.35		25.10	

Table B.12.: In the work published in [63] the efficiency figure of 3.81 was used for 2015. This table gives the city by city cooling results with efficiency changes that correspond to that report.

Timeframe	2015				2050				2080			
Scenario	RCP 4.5	RCP 8.5	RCP 4.5	RCP 8.5	RCP 4.5	RCP 8.5	RCP 4.5	RCP 8.5	RCP 4.5	RCP 8.5	RCP 4.5	RCP 8.5
City/Units	kWh/c	kWh/c	kWh/c	% +	kWh/c	% +	kWh/c	% +	kWh/c	% +	kWh/c	% +
Bloomington	297.90	307.77	327.23	9.8%	341.60	11.0%	310.11	4.1%	334.90	8.8%		
Cincinnati	317.11	328.89	339.31	7.0%	356.72	8.5%	322.75	1.8%	352.70	7.2%		
Columbus	286.47	293.59	295.61	3.2%	310.57	5.8%	281.66	-1.7%	306.59	4.4%		
Elkhart-Gosh.	156.07	164.93	213.33	36.7%	259.76	57.5%	235.06	50.6%	269.71	63.5%		
Evansville	350.27	352.33	345.21	-1.4%	356.25	1.1%	324.11	-7.5%	341.70	-3.0%		
Fort Wayne	176.24	185.27	241.08	36.8%	289.06	56.0%	261.34	48.3%	295.73	59.6%		
Gary	205.81	215.61	266.36	29.4%	284.90	32.1%	258.79	25.7%	291.09	35.0%		
Indianapolis	262.98	273.53	288.00	9.5%	303.21	10.8%	275.06	4.6%	300.74	9.9%		
Kokomo	246.57	259.96	312.48	26.7%	331.45	27.5%	300.21	21.8%	330.56	27.2%		
Lafayette-WL	226.81	238.63	304.22	34.1%	324.92	36.2%	294.84	30.0%	325.89	36.6%		
Louisville	306.33	309.09	307.95	0.5%	320.66	3.7%	291.22	-4.9%	313.22	1.3%		
Mich City-L.P.	167.49	176.48	238.73	42.5%	309.83	75.6%	287.51	71.7%	327.96	85.8%		
Muncie	188.88	198.26	274.96	45.6%	318.93	60.9%	288.58	52.8%	322.92	62.9%		
South Bend-M	154.44	162.77	211.64	37.0%	277.36	70.4%	251.67	63.0%	289.08	77.6%		
Terre Haute	272.17	281.66	311.97	14.6%	326.34	15.9%	296.52	8.9%	321.51	14.1%		
Average	241.64	250.84	280.91	16.3%	304.26	21.3%	275.89	14.2%	304.00	21.2%		
St. Dev.	61.78	60.83	41.55		26.98		24.58		21.77			

C. SUPPLEMENT TO CHAPTER THREE ON RELIABILITY AND RENEWABLES

C.1 Repository for models and data files

The models used for this work are stored in the following github repositories:
<https://github.com/LizWachs/ga-power-gen-knapsack>

KnapsackmultiobjGA.mlx and KnapsackmultiobjGA_overnightLCOE.mlx are the main optimization files. The others must be present in the working directory.

<https://github.com/LizWachs/NPV-power-generation>

NPV_Calc_CAISO.mlx is the NPV calculation for CAISO. NPV_Calc_PJM.mlx is the NPV calculation for PJM. Both are set with a 30 year generation lifetime by default, but the user can change this. EnergySources_NPV.xlsx that accompanies the files must be stored in the same active directory for the NPV programs to run.

C.2 Annual Cost of Energy in PJM and CAISO

Tables C.1 and Table C.2 show the cost of energy in the two markets from their reporting [104, 122, 205], for the sake of comparison and understanding of what is discussed in the main text.

C.3 Data used with sources

Data sources for the work are shown in table C.3. The data used for the least cost optimization is shown in table C.4. Additional data used for the NPV calculation is shown in table C.5, with data used for both regions, and table C.6, with data used specifically for PJM or CAISO. Other parameters used for all technologies in the NPV calculations are shown in table C.7.

Table C.1.: Cost of energy in PJM from 2014-2018 with breakdown according to cost type (2018 data from table 1-8 in [104], prior years' data from [205])

	\$/MWh							
PJM	2014	2015	2016	2017	2018	5 yr	Share	STD
						avg	%	
Energy	53.13	36.25	29.27	31.06	38.24	37.59	66%	8.43
Reliability Capacity	8.91	11.14	9.39	8.73	13.01	10.24	18%	1.63
Transmission	5.75	6.93	7.63	8.58	9.47	7.67	13%	1.29
Other	2.58	1.56	1.2	1.27	1.57	1.64	3%	0.50
Total	70.37	55.88	47.49	49.64	62.29	57.13		8.40

Table C.2.: Cost of energy in CAISO from 2013-2017 broken down by cost type [122].

	\$/MWh							
CAISO	2013	2014	2015	2016	2017	5 yr	Share	STD
						avg	%	
Day ahead	44.14	48.57	34.54	30.7	37.59	39.11	93%	6.46
Real time	0.57	1.98	0.69	1.03	2.01	1.26	3%	0.62
Grid management	0.8	0.8	0.8	0.81	0.81	0.8	2%	0.01
Bid cost recovery	0.47	0.4	0.39	0.33	0.47	0.41	1%	0.05
Reliability	0.1	0.14	0.12	0.11	0.1	0.11	0%	0.02
Reserve costs	0.26	0.3	0.27	0.54	0.77	0.43	1%	0.20
Total	46.34	52.19	36.81	33.52	41.75	42.12		6.66

Parameter	Data Source
Overnight Capital Cost	2018 Projections [109]
Capacity Factor	[112]
EROI Coefficient for Solar PV	[206]
EROI Coefficients	[207]
GHG Emissions	[208]
Human Health Score	characterization factors from [111]; emissions from [110]
Degradation Factors	[99]
Fuel Price	Coal and NG from [209]; projections for biomass; nuclear from [109]
Heat Rate	2018 Projections [109]
Insurance Percent	[99]
Debt Term	Coal from [210]; hydropower from [211]; nuclear from [212]—shorter end, 15 years from the 15-18 year term mentioned; CCS from [213]; offshore wind from [214]; others from [99]
O&M Costs	2018 Projections [109]
Electricity Prices	CAISO weighted average price 2017 from [122]; hourly/quarterly prices from day ahead estimates from [215–218], PJM weighted average price 2018 from [104]; hourly/monthly prices from [219]
LCOE	Midrange and overnight 2018 projections from [109]
Generation by Type	CAISO from Daily Renewables Watch [220]; PJM from generation on 15th of every month from [221]

Table C.3.: Data sources for the NPV calculations

Table C.4.: Energy sources with parameters used for modeling. Abbreviations used in headings are average capacity (AC), capacity factor (CF), LCOE Midpoint (L-M), LCOE overnight (L-O), and useful capacity (UC). All units are per MWh. Greenhouse gases are in carbon dioxide equivalents.

Energy Source	AC	CF	EROI	GHG	Health	L-M	L-O	UC
				kg	DALY			
Solar (PV) utility scale	100	20%	17.78	48	0	37	8	20
Solar thermal (CSP)	100	21%	20	27	0	123	130	20
Advanced Nuclear	1000	92%	14	12	0	63	53	900
Wind–Onshore	100	35%	20	11	0	63	54	40
NGCC	250	56%	23.5	490	4.14E-05	39	16	150
NGCC with CCS	250	56%	23.5	170	4.14E-05	65	38	150
NG CT	250	8%	23.5	490	4.39E-05	126	90	20
Coal 30% with CCS	500	53%	28	220	2.73E-04	138	110	250
Coal 90% with CCS	500	53%	28	220	2.73E-04	157	124	250
Biomass	50	56%	4	230	1.36E-05	109	108	30
Solar PV Residential	1	16%	17.78	41	0	109	154	1
Solar PV Commercial	1	15%	17.78	41	0	80	113	1
Offshore Wind–s	600	42%	20	12	0	121	116	250
Offshore wind–m	600	48%	20	12	0	129	121	300
Offshore wind–d	600	36%	20	12	0	207	186	200
Hydro–new stream	1	63%	84	24	0	53	52	1
Geothermal–flash	50	90%	9	38	1.75E-05	82	69	50
Geothermal–binary	50	80%	9	38	0	110	101	40
Coal–supercritical	500	53%	28	820	2.73E-04	99	75	250
Coal–IGCC	500	53%	28	820	2.73E-04	111	88	250

Table C.5.: Parameters used for NPV calculations in both regions

Generation Type	OCC	Degrad Fac- tor	Fuel Price	Heat Rate	Insurance Pct	Debt Term	O_M Base
Solar (PV)	\$1,050	0.75	\$ -	0	0.3	20	9
Solar thermal	\$7,099	0.5	\$ -	0	0.3	20	67
Nuclear	\$5,656	0.18	\$0.64	10.459	0	15	99
Onshore Wind	\$1,581	0.3	\$ -	0	0.6	20	51
NGCC	\$1,029	0.178	\$3.37	6.44	0.6	10	10
NGCC with CCS	\$2,137	0.178	\$3.37	7.52	0.6	11	33
NG CT	\$876	0.016	\$3.37	9.78	0.6	10	12
Coal 30% with CCS	\$5,015	0.18	\$2.06	9.71	0.45	11	69
Coal 90% with CCS	\$5,546	0.178	\$2.06	11.47	0.45	11	80
Biomass	\$3,795	0.1	\$2.92	13.5	0.6	20	110
Offshore Wind (s)	\$3,549	0.3	\$ -	0	0.45	13	146
Offshore wind (m)	\$5,239	0.3	\$ -	0	0.45	13	115
Offshore wind (d)	\$5,811	0.3	\$ -	0	0.45	13	134
Hydro-new stream	\$6,393	0.3	\$ -	0	0.45	10	79
Geothermal-flash	\$4,720	0.5	\$ -	0	0.6	20	145
Geothermal-binary	\$5,648	0.5	\$ -	0	0.6	20	169
Coal-supercritical	\$3,611	0.18	\$2.06	8.8	0.45	10	33
Coal-IGCC	\$3,872	0.18	\$2.06	8.6	0.45	10	54

Table C.6.: Region specific parameters used in the NPV calculations

Generation Type	PJM			CAISO		
	CF	ICAP	EFORd	Price	Price	Ad Valorem
		Factor		Factor	Factor	Factor
Solar (PV)	0.177	0.38	0.000	1.025	0.82	0.1
Solar thermal	0.56	0.38	0.000	1.025	0.83	0.1
Nuclear	0.942	0.913	0.014	0.953	0.96	1
Onshore wind	0.284	0.13	0.000	0.963	0.996	1
NGCC	0.6	0.836	0.044	0.985	1.087	1
NGCC with CCS	0.6	0.836	0.044	0.985	1.087	1
NG CT	0.069	0.836	0.095	1.58	1.087	1
Coal 30% with CCS	0.444	0.836	0.119	1.056	1.087	1
Coal 90% with CCS	0.444	0.836	0.119	1.056	1.087	1
Biomass	0.686	0.836	0.119	0.953	0.959	1
Offshore Wind (s)	0.42	0.13	0.000	0.963	0.996	1
Offshore wind (m)	0.48	0.13	0.000	0.963	0.996	1
Offshore wind (d)	0.36	0.13	0.000	0.963	0.996	1
Hydro–new stream	0.468	0.836	0.000	1.141	1.007	1
geothermal–flash	0.9	0.836	0.000	0.953	0.945	1
geothermal–binary	0.8	0.836	0.000	0.953	0.945	1
Coal–supercritical	0.444	0.836	0.119	1.056	1.087	1
Coal–IGCC	0.444	0.836	0.119	1.056	1.087	1

Table C.7.: Parameters used for NPV calculations independent of technology.

Parameter Name	Value
Discount Rate	0.079
Inflation Factor	2.00%
Federal Tax Rate	21.00%
Debt Equity Pct	45%
Interest Rate	6.50%
State Depreciation Lifetime	20 years
Federal Depreciation Lifetime	5 years
PJM	
State Tax Rate	8.00%
Price	\$38.24
Property Tax Rate	2.00%
GHG Permit Price (Initial)	0
Capacity Price	\$36.64
CAISO	
State Tax Rate	8.84%
Price	\$37.61
Property Tax Rate	1.00%
GHG Permit Price (Initial)	\$17.00

C.4 Verification

To put results in context, we used 2017 data from the survey Form EIA-860 [124]. The form records the physical address of the planned unit, but does not include the relevant regional transmission organization (RTO) or independent system operator (ISO). To compare the data, we used all California plants to represent CAISO. To represent PJM, we included all generation from relevant states, except for the following states where plants from the counties listed were assumed to be from PJM, and any others, including those with no county given, were excluded. Note that in KY, only two plants were planned, so other counties were not relevant.

C.5 Energy Return on Investment (EROI)

Due to the complex regulatory framework including subsidies and taxes at multiple levels, the “true” cost of given technologies is difficult to estimate and compare. If a certain energy technology or resource is subsidized, its cost appears low, but later the cost rises if the subsidy is removed. To skirt this opacity, a set of metrics called “net energy analysis” was developed to evaluate energy sources based on more fundamental criteria. One of the easiest to understand and apply is energy return on investment (EROI). Energy return on investment can be defined simply as in equation C.1 [222]:

$$EROI = \frac{EnergyOutput}{EnergyInput} \quad (C.1)$$

The *EnergyOutput* (numerator) refers to the energy value finally produced. For coal, natural gas, biomass, petroleum or any substance converted into a liquid fuel, it is typically the higher heating value (HHV). Further efficiency losses result when this fuel is used to create electricity or other kinds of work instead of heat. Solar or wind power provide “higher quality” energy directly suitable for work. The *EnergyInput* (denominator) includes all energy used along the production route, from the manufacture of drilling equipment to the gas needed for the freighter that carries the fuel. EROI estimates tend to be characterized by high variability because of differ-

Table C.8.: Counties whose planned generation was included for PJM Verification calculations.

State	County	State	County
MI	St. Joseph	IL	Henry
MI	Cass	IL	Lake
MI	Kalamazoo	IL	LaSalle
MI	Van Buren	IL	Lee
MI	Berrien	IL	McLean
IN	La Porte	NC	Perquimans
IN	St. Joseph	NC	Chown
IN	Elkhart	NC	Hyde
IN	Miami	NC	Dare
IN	Howard	NC	Tyrell
IN	Tipton	NC	Washington
IN	Hamilton	NC	Martin
IN	Steuben	NC	Bertie
IN	De Kalb	NC	Nash
IN	Allen	NC	Edgecombe
IN	Adams	NC	Pitt
IN	Jay	NC	Beaufort
IN	Randolph	NC	Currituck
IN	Wells	NC	Camden
IN	Blackford	NC	Pasquotank
IN	Delaware	NC	Gates
IN	Noble	NC	Hertford
IN	Whitley	NC	Northhampton
IN	Huntington	NC	Halifax
IN	Grant	KY	Greenup
IN	Madison	KY	Scott
IN	Wabash		

ing production systems (see [223] for an example for oilfields). EROI values are not stagnant, since technological improvements/scarcity affect values. EROI is an important metric nonetheless, since it removes distortions from subsidies and taxation and thus may provide a better picture for long-term planning than monetary cost at any particular point in time. Estimates have been made as to the minimum EROI necessary to support human needs, from basic to the most decadent. Basic needs can be met with a relatively low EROI, but a much higher EROI is needed to support secondary and tertiary needs, such as the arts. The minimum EROI necessary for the amenities common to American life is hypothesized as 14 [224]. This means that a EROI below 14 may violate the principle of sustainable development, defined by the Brundtland Commission as “development that meets the needs of the present without compromising the ability of future generations to meet their own needs [225].”

When oil’s use as a cheap source of energy first became widespread, the return on investment for oil production was extremely high. Its EROI has been declining along with the reserves of the easiest resources to extract, although there is high variability over global oil fields. Offshore drilling currently shows ratios as high as 1000 MJ/MJ, while some fields (particularly those using thermal recovery) showed ratios <3 . The mean EROI for offshore drilling in a recent study by Brandt et al. was 32.5 MJ/MJ [223]. The revolutions in quality of life in the past century and a half can be attributed in part to the ability to capitalize on fuels that gave such a high return [224]. Renewables (except for hydro), on the other hand, typically utilize more dispersed energy reserves, so do not necessarily offer the benefits of high EROI given by fossil fuels, whose high energy density accumulated over millennia. For both renewables and fossil fuels, technological advances can offer improvements to EROI. EROI is shown in table C.4.

The highest energy return on investment is hydro by far, with coal the runner up, and natural gas as the only other technology with an EROI higher than 20. Solar and wind are between 15-20. As mentioned, fossil fuel EROI tends to be decreasing, while solar and wind have seen large increases due to technological advances. Nuclear

EROI is 14, just the level needed for comfort. Geothermal and biomass both have EROI below 10. This characteristic of geothermal and biomass indicates that they will not be a major part of a power generation mixture unless significant technological breakthroughs are achieved. Still, both geothermal and biomass also have high leveled costs. Neither is the lowest option in terms of GHG emissions or human health scores as well. This keeps them as only minor contributors in the cost minimization exercise, even without taking EROI into account. For this reason the EROI, while considered, was not included in the optimization performed.

D. APPENDIX FOR CHAPTER FIVE ON QUANTIFYING MARKET BARRIERS TO RENEWABLES

D.1 Supporting Data for Correlation and Risk Calculations

Table D.1.: The relative weighting of each cost category by technology and region. CO₂ costs for PJM are based on Regional Greenhouse Gas Initiative (RGGI) prices. CO₂ costs are higher in CAISO, so the proportion of CO₂ costs tends to be higher in CAISO. Insurance and Ad Valorem costs also differ between the two regions, leading to different proportions of OCC and O&M costs. Fuel costs between the two regions are similar, so their proportion is also similar in the two regions.

	PJM				CAISO			
	O&M	CO ₂	Fuel	OCC	O&M	CO ₂	Fuel	OCC
Solar_PV	41.10%	0.70%	0.00%	58.20%	22.60%	3.80%	0.00%	73.70%
Solar_Thermal	42.20%	0.20%	0.00%	57.70%	24.70%	0.60%	0.00%	74.70%
Nuclear	40.20%	0.10%	12.40%	47.30%	34.60%	0.40%	13.30%	51.70%
Wind_Onshore	57.70%	0.10%	0.00%	42.20%	54.00%	0.40%	0.00%	45.60%
NGCC	14.10%	8.10%	57.90%	19.90%	10.00%	19.70%	51.40%	18.90%
NGCC_CCS	24.20%	1.90%	46.00%	27.90%	20.20%	5.20%	45.20%	29.40%
NG_CT	32.80%	2.30%	24.50%	40.40%	25.30%	7.10%	28.00%	39.70%
Coal_30_CCS	36.30%	1.20%	18.20%	44.30%	28.10%	4.20%	22.20%	45.50%
Coal_90_CCS	36.40%	1.10%	19.00%	43.50%	28.40%	3.70%	23.30%	44.60%
Biomass	31.40%	1.50%	42.50%	24.60%	30.00%	3.80%	38.70%	27.50%
Wind_Offshore_Shallow	61.10%	0.10%	0.00%	38.90%	57.60%	0.20%	0.00%	42.10%
Wind_Offshore_Med	51.20%	0.10%	0.00%	48.70%	45.70%	0.20%	0.00%	54.00%
Wind_Offshore_Deep	51.90%	0.10%	0.00%	48.00%	46.60%	0.20%	0.00%	53.20%
Hydro	43.70%	0.10%	0.00%	56.20%	36.40%	0.60%	0.00%	63.00%
Geothermal_Flash	56.80%	0.40%	0.00%	42.80%	52.60%	1.30%	0.00%	46.10%
Geothermal_Binary	56.40%	0.30%	0.00%	43.30%	52.30%	1.00%	0.00%	46.70%
Coal_Supercritical	29.50%	6.10%	21.90%	42.60%	19.10%	18.30%	23.80%	38.80%
Coal_IGCC	33.90%	5.50%	19.30%	41.30%	23.70%	16.80%	21.30%	38.20%

Table D.2.: Volatility (sigma) values for each technology and cost category. CAISO and PJM have different values for CO₂ pricing. Biomass doesn't have a long enough time series to estimate its volatility, so the value for coal is used.

	O&M	PJM CO2	CAISO CO2	Fuel	OCC
Solar_PV	4.10%	39.00%	7.00%	0.00%	8.80%
Solar_Thermal	4.10%	39.00%	7.00%	0.00%	7.60%
Nuclear	4.10%	39.00%	7.00%	7.00%	13.50%
Wind_Onshore	4.10%	39.00%	7.00%	0.00%	11.70%
NGCC	4.10%	39.00%	7.00%	27.00%	10.20%
NGCC_CCS	4.10%	39.00%	7.00%	27.00%	2.30%
NG_CT	4.10%	39.00%	7.00%	27.00%	1.50%
Coal_30_CCS	4.10%	39.00%	7.00%	7.00%	18.40%
Coal_90_CCS	4.10%	39.00%	7.00%	7.00%	18.40%
Biomass	4.10%	39.00%	7.00%	7.00%	3.40%
Wind_Offshore_Shallow	4.10%	39.00%	7.00%	0.00%	18.20%
Wind_Offshore_Med	4.10%	39.00%	7.00%	0.00%	18.20%
Wind_Offshore_Deep	4.10%	39.00%	7.00%	0.00%	18.20%
Hydro	4.10%	39.00%	7.00%	0.00%	7.60%
Geothermal_Flash	4.10%	39.00%	7.00%	0.00%	14.40%
Geothermal_Binary	4.10%	39.00%	7.00%	0.00%	14.40%
Coal_Supercritical	4.10%	39.00%	7.00%	7.00%	12.20%
Coal_IGCC	4.10%	39.00%	7.00%	7.00%	11.40%

Table D.3.: The correlation coefficients between cost categories shown as a heat map. Note that natural gas and PJM energy prices are almost perfectly correlated since natural gas is the marginal energy supplier. Cap here refers to capacity.

Coal	Gas	Uranium	CO ₂ PJM	CO ₂ CAISO	Biomass	Energy PJM	Energy CAISO	Cap PJM
1	-0.4	0.9	-0.33	-0.79	0	-0.04	0.32	0.17
-0.4	1	-0.21	-0.22	-0.17	0	0.96	0.59	-0.11
0.9	-0.2	1	-0.66	-0.78	0	0.13	-0.06	0.11
-0.3	-0.2	-0.66	1	0.31	0	-0.14	0.24	0.49
-0.8	-0.2	-0.78	0.31	1	0	-0.17	0.27	-0.26
0	0	0	0	0	1	0	0	0
-0	0.96	0.13	-0.14	-0.17	0	1	0.53	-0.01
0.32	0.59	-0.06	0.24	0.27	0	0.53	1	-0.08
0.17	-0.1	0.11	0.49	-0.26	0	-0.01	-0.08	1

Table D.4.: Risk factors for each technology type in PJM and CAISO. The largest are for combined cycle technologies, which have a high relative proportion of fuel costs from natural gas, whose prices experience high variability. Offshore wind's construction costs are relatively high and variable. Coal also has high fuel costs, but coal prices have been less variable than natural gas prices in US markets. Since lack of data prevented calculating a variability for biomass costs, coal's value was used.

Technology	PJM	CAISO
NGCC	0.154	0.1384
NGCC_CCS	0.1233	0.122
Wind_Offshore_Med	0.0912	0.1002
Wind_Offshore_Deep	0.0901	0.0988
Coal_30_CCS	0.0837	0.0855
Coal_90_CCS	0.0823	0.0841
Wind_Offshore_Shallow	0.0751	0.0803
Geothermal_Binary	0.0666	0.0708
NG_CT	0.0665	0.0758
Nuclear	0.0664	0.0718
Geothermal_Flash	0.0661	0.07
Coal_Supercritical	0.0585	0.0493
Wind_Onshore	0.0548	0.0579
Solar_PV	0.0537	0.0652
Coal_IGCC	0.0536	0.0456
Solar_Thermal	0.0469	0.0574
Hydro	0.0464	0.0503
Biomass	0.034	0.0313

Table D.5.: Correlation coefficients used for O&M costs between technologies. Assumptions are detailed in the text. Shading is used to make the scale of correlation clear; dark blue is very close correlation (~ 1) and dark red is a strong negative correlation (~ -1). Abbreviations for technologies are used including natural gas combined cycle (NGCC), natural gas combustion turbine (NG CT), coal integrated gasification combined cycle (IGCC).

	Solar PV	Solar Thermal	Nuclear	Wind Onshore	NGCC	NGCC CCS	NG CT	Coal 30 CCS	Coal 90 CCS	Biomass	Offshore Wind	Hydro	Geothermal	Coal Supercritical	Coal IGCC
Solar PV	1	0.6	0.6	0.6	0.6	0.6	0.6	0.6	0.6	0.6	0.6	0.6	0.6	0.6	0.6
Solar Thermal	0.6	1	0.6	0.6	0.6	0.6	0.6	0.6	0.6	0.6	0.6	0.6	0.6	0.6	0.6
Nuclear	0.6	0.6	1	0.5	0.55	0.55	-0.56	0.55	0.55	0.6	0.6	0.64	0.6	0.55	0.55
Wind Onshore	0.6	0.6	0.6	1	0.6	0.6	0.6	0.6	0.6	0.6	0.6	0.6	0.6	0.6	0.6
NGCC	0.6	0.6	0.55	0.6	1	0.9	-0.76	0.9	0.9	0.6	0.6	0.75	0.6	1	1
NGCC CCS	0.6	0.6	0.55	0.6	0.9	1	-0.76	1	1	0.6	0.6	0.75	0.6	0.9	0.9
NG CT	0.6	0.6	-0.56	0.6	-0.76	-0.76	1	-0.76	-0.76	0.6	0.6	-0.59	0.6	-0.76	-0.76
Coal 30 CCS	0.6	0.6	0.55	0.6	0.9	1	-0.76	1	1	0.6	0.6	0.75	0.6	0.9	0.9
Coal 90 CCS	0.6	0.6	0.55	0.6	0.9	1	-0.76	1	1	0.6	0.6	0.75	0.6	0.9	0.9
Biomass	0.6	0.6	0.6	0.6	0.6	0.6	0.6	0.6	0.6	1	0.6	0.6	0.6	0.6	0.6
Offshore Wind	0.6	0.6	0.6	0.6	0.6	0.6	0.6	0.6	0.6	0.6	1	0.6	0.6	0.6	0.6
Hydro	0.6	0.6	0.64	0.6	0.75	0.75	-0.59	0.75	0.75	0.6	0.6	1	0.6	0.75	0.75
Geothermal	0.6	0.6	0.6	0.6	0.6	0.6	0.6	0.6	0.6	0.6	0.6	0.6	1	0.6	0.6
Coal Supercritical	0.6	0.6	0.55	0.6	1	0.9	-0.76	0.9	0.9	0.6	0.6	0.75	0.6	1	1
Coal IGCC	0.6	0.6	0.55	0.6	1	0.9	-0.76	0.9	0.9	0.6	0.6	0.75	0.6	1	1

Table D.6.: Correlation matrix obtained for CAISO using the determinant method. Row names are omitted for fit, but are identical to column names.

Solar PV	Solar Thermal	Nuclear	Wind Onshore	NGCC	NGCC CCS	NG CT	Coal 30 CCS	Coal 90 CCS	Biomass	Offshore Wind	Hydro	Geothermal	Coal Supercritical	Coal IGCC
1	0.6	0	0.6	0	0	0	0	0	0	0.6	0.6	0.6	0	0
0.6	1	0	0.6	0	0	0	0	0	0	0.6	0.6	0.6	0	0
0	0	1	0	-0.19	-0.19	0.192	0.158	0.158	0	0	0	0	0.158	0.158
0.6	0.6	0	1	0	0	0	0	0	0	0.6	0.6	0.6	0	0
0	0	-0.19	0	1	0.873	-0.74	-0.51	-0.51	0	0	0	0	-0.56	-0.56
0	0	-0.19	0	0.873	1	-0.74	-0.56	-0.56	0	0	0	0	-0.51	-0.51
0	0	0.192	0	-0.74	-0.74	1	0.429	0.429	0	0	0	0	0.429	0.429
0	0	0.158	0	-0.51	-0.56	0.429	1	0.379	0	0	0	0	0.341	0.341
0	0	0.158	0	-0.51	-0.56	0.429	0.379	1	0	0	0	0	0.341	0.341
0	0	0	0	0	0	0	0	0	1	0	0	0	0	0
0.6	0.6	0	0.6	0	0	0	0	0	0	1	0.6	0.6	0	0
0.6	0.6	0	0.6	0	0	0	0	0	0	0.6	1	0.6	0	0
0.6	0.6	0	0.6	0	0	0	0	0	0	0.6	0.6	1	0	0
0	0	0.158	0	-0.56	-0.51	0.429	0.341	0.341	0	0	0	0	1	0.379
0	0	0.158	0	-0.56	-0.51	0.429	0.341	0.341	0	0	0	0	0.379	1

Table D.7.: Correlation table for PJM obtained using the determinant method. Column and row names are identical but row names are omitted for fit.

Solar PV	Solar Thermal	Nuclear	Wind Onshore	NGCC	NGCC CCS	NG CT	Coal 30 CCS	Coal 90 CCS	Biomass	Offshore Wind	Hydro	Geothermal	Coal Supercritical	Coal IGCC
1	0.6	0	0.6	0	0	0	0	0	0	0.6	0.6	0.6	0	0
0.6	1	0	0.6	0	0	0	0	0	0	0.6	0.6	0.6	0	0
0	0	1	0	-0.2	-0.2	0.2	0.38	0.38	0	0	0	0	0.38	0.38
0.6	0.6	0	1	0	0	0	0	0	0	0.6	0.6	0.6	0	0
0	0	-0.2	0	1	0.85	-0.72	-0.45	-0.45	0	0	0	0	-0.5	-0.5
0	0	-0.2	0	0.85	1	-0.72	-0.5	-0.5	0	0	0	0	-0.45	-0.45
0	0	0.2	0	-0.72	-0.72	1	0.38	0.38	0	0	0	0	0.38	0.38
0	0	0.38	0	-0.45	-0.5	0.38	1	0.89	0	0	0	0	0.8	0.8
0	0	0.38	0	-0.45	-0.5	0.38	0.89	1	0	0	0	0	0.8	0.8
0	0	0	0	0	0	0	0	0	1	0	0	0	0	0
0.6	0.6	0	0.6	0	0	0	0	0	0	1	0.6	0.6	0	0
0.6	0.6	0	0.6	0	0	0	0	0	0	0.6	1	0.6	0	0
0.6	0.6	0	0.6	0	0	0	0	0	0	0.6	0.6	1	0	0
0.6	0.6	0	0.6	0	0	0	0	0	0	0.6	0.6	1	0	0
0	0	0.38	0	-0.5	-0.45	0.38	0.8	0.8	0	0	0	0	1	0.89
0	0	0.38	0	-0.5	-0.45	0.38	0.8	0.8	0	0	0	0	0.89	1

Table D.8.: CAISO correlation matrix obtained using scaled matrix method. Row names are omitted for fit but are identical to column names.

Solar PV	Solar Thermal	Nuclear	Wind Onshore	NGCC	NGCC CCS	NG CT	Coal 30 CCS	Coal 90 CCS	Biomass	Offshore Wind (S)	Offshore Wind (M)	Offshore Wind (D)	Hydro	Geothermal	Coal Supercritical	Coal IGCC
1	0.58	0.42	0.41	0.16	0.24	0.33	0.37	0.36	0.24	0.39	0.46	0.46	0.51	0.41	0.31	0.31
0.58	1	0.44	0.42	0.16	0.25	0.33	0.38	0.37	0.25	0.4	0.47	0.47	0.52	0.42	0.32	0.32
0.42	0.44	1	0.33	0.08	0.17	0.14	0.31	0.31	0.2	0.34	0.37	0.37	0.41	0.35	0.25	0.25
0.41	0.42	0.35	1	0.12	0.2	0.26	0.3	0.29	0.22	0.38	0.39	0.39	0.41	0.38	0.24	0.25
0.16	0.16	0.08	0.12	1	0.3	0.2	0.03	0.03	0.07	0.11	0.13	0.13	0.15	0.12	0.02	0.03
0.24	0.25	0.17	0.2	0.3	1	0.2	0.14	0.13	0.12	0.19	0.21	0.21	0.24	0.2	0.09	0.1
0.33	0.33	0.14	0.26	0.2	0.2	1	0.09	0.08	0.16	0.25	0.28	0.28	0.2	0.26	0.08	0.07
0.37	0.38	0.31	0.3	0.03	0.14	0.09	1	0.32	0.17	0.29	0.32	0.32	0.36	0.3	0.25	0.25
0.36	0.37	0.31	0.29	0.03	0.13	0.08	0.32	1	0.17	0.29	0.32	0.32	0.36	0.29	0.24	0.25
0.24	0.25	0.2	0.22	0.07	0.12	0.16	0.17	0.17	1	0.22	0.23	0.23	0.24	0.22	0.14	0.15
0.39	0.4	0.34	0.38	0.11	0.19	0.25	0.29	0.29	0.22	1	0.49	0.49	0.39	0.38	0.23	0.24
0.46	0.47	0.37	0.39	0.13	0.21	0.28	0.32	0.32	0.23	0.49	1	0.5	0.44	0.39	0.26	0.27
0.46	0.47	0.37	0.39	0.13	0.21	0.28	0.32	0.32	0.23	0.49	0.5	1	0.44	0.39	0.26	0.27
0.51	0.52	0.41	0.41	0.15	0.24	0.2	0.36	0.36	0.24	0.39	0.44	0.44	1	0.41	0.3	0.31
0.41	0.42	0.35	0.38	0.12	0.2	0.26	0.3	0.29	0.22	0.38	0.39	0.39	0.41	1	0.24	0.25
0.31	0.32	0.25	0.24	0.02	0.09	0.08	0.25	0.24	0.14	0.23	0.26	0.26	0.3	0.24	1	0.21
0.31	0.32	0.25	0.25	0.03	0.1	0.07	0.25	0.25	0.15	0.24	0.27	0.27	0.31	0.25	0.21	1

Table D.9.: Correlation table for PJM using the scaled matrix method. The row names are the same as the column names but are omitted for fit.

Solar PV	Solar Thermal	Nuclear	Wind Onshore	NGCC	NGCC CCS	NG CT	Coal 30 CCS	Coal 90 CCS	Biomass	Offshore Wind (S)	Offshore Wind (M)	Offshore Wind (D)	Hydro	Geothermal	Coal Supercritical	Coal IGCC
1	0.44	0.37	0.39	0.15	0.22	0.32	0.35	0.34	0.22	0.38	0.41	0.41	0.43	0.39	0.32	0.32
0.44	1	0.37	0.39	0.15	0.22	0.32	0.35	0.34	0.22	0.38	0.41	0.41	0.43	0.39	0.32	0.32
0.37	0.37	1	0.32	0.1	0.17	0.11	0.31	0.31	0.19	0.33	0.35	0.35	0.38	0.34	0.29	0.29
0.39	0.39	0.34	1	0.13	0.2	0.28	0.31	0.31	0.21	0.38	0.38	0.38	0.39	0.38	0.28	0.29
0.15	0.15	0.1	0.13	1	0.34	0.18	0.08	0.08	0.07	0.13	0.14	0.14	0.16	0.13	0.06	0.07
0.22	0.22	0.17	0.2	0.34	1	0.16	0.17	0.17	0.11	0.2	0.21	0.21	0.24	0.2	0.13	0.14
0.32	0.32	0.11	0.28	0.18	0.16	1	0.07	0.06	0.16	0.28	0.3	0.3	0.14	0.28	0.07	0.06
0.35	0.35	0.31	0.31	0.08	0.17	0.07	1	0.36	0.18	0.31	0.33	0.33	0.37	0.31	0.32	0.33
0.34	0.34	0.31	0.31	0.08	0.17	0.06	0.36	1	0.17	0.3	0.32	0.32	0.36	0.31	0.32	0.32
0.22	0.22	0.19	0.21	0.07	0.11	0.16	0.18	0.17	1	0.21	0.22	0.22	0.22	0.21	0.16	0.17
0.38	0.38	0.33	0.38	0.13	0.2	0.28	0.31	0.3	0.21	1	0.5	0.5	0.38	0.37	0.27	0.28
0.41	0.41	0.35	0.38	0.14	0.21	0.3	0.33	0.32	0.22	0.5	1	0.5	0.41	0.38	0.3	0.31
0.41	0.41	0.35	0.38	0.14	0.21	0.3	0.33	0.32	0.22	0.5	0.5	1	0.41	0.38	0.3	0.3
0.43	0.43	0.38	0.39	0.16	0.24	0.14	0.37	0.36	0.22	0.38	0.41	0.41	1	0.39	0.34	0.34
0.39	0.39	0.34	0.38	0.13	0.2	0.28	0.31	0.31	0.21	0.37	0.38	0.38	0.39	1	0.28	0.29
0.32	0.32	0.29	0.28	0.06	0.13	0.07	0.32	0.32	0.16	0.27	0.3	0.3	0.34	0.28	1	0.31
0.32	0.32	0.29	0.29	0.07	0.14	0.06	0.33	0.32	0.17	0.28	0.31	0.3	0.34	0.29	0.31	1

D.2 Sustainability Indicators

Table D.10.: Sustainability indicators used in this analysis. The future category (F) represents risks with current (C) as a separate category. Quantitative factors (Q) have defined functions. Categorical indicators (C) are step functions.

	Indicator	Type	Timing
Economic	Investment Costs, levelized	Q	C
	Fuel & CO2 Costs, levelized	Q	C
	Operations Costs, levelized	Q	C
	Price factor	Q	F
Social	Employment	Q	C
	Population Displacement	C	C
	Development of New Areas	C	C
	Accident Risk	C	C
	Visual Impact	C	C
	Water Consumption	C	F
	Water Withdrawal	C	F
	Land Use	Q	F
Environmental	Global Warming Potential	Q	F
	Human Health	Q	C
	Resources	Q	F
	Noise	C	C
	Odor	C	C
	Local/Regional/Global Impact	C	F

D.3 Life Cycle Water Use

Literature search revealed no current studies with original data on water footprints or use for all electricity generating technologies. The best source found was Meldrum et al. [226], who performed an extensive review of literature and harmonized estimates. They noted the dearth of original data in this area as well, as well as vast ranges in some of the literature around particular technologies or processes. Their study is important, however, in providing benchmarks for most of the technologies included here, and for showing how water use is distributed between different phases (i.e. power plant construction, fuel cycle, and operations) as well as how it varies by cooling system employed and between consumption and withdrawal in some cases. One important takeaway from Meldrum et al. is that without cooling water use, all technologies except geothermal binary (for which water is used as a working fluid), would have less than 200 gallons/MWh. Also, only solar PV and CSP show a significant water use (≥ 100 gal/MWh) for power plant construction. For all fossil generation as well as nuclear, the water use before operations comes from the fuel cycle, and in all cases it is ≤ 50 gal/MWh. A sea change in cooling methods or more efficient cooling technology in fossils would eliminate the difference between water footprints of fossil versus renewable sources. Also, for renewables except geothermal, all the water use is virtual, that is, it can come from other places, whereas for fossil sources, the water use is almost all for the operations.

Due to the very high uncertainty and age of data available, a categorical indicator was chosen for water use. The indicator has two parts, which are equally weighted. They are tied to figures for water consumption for the first and water withdrawal in the second. An important takeaway from Meldrum et al. [226] is that for most power generation systems, water use is incurred primarily in the cooling process. There are very large gaps between water use by different cooling systems. Traditionally cooling towers have been built, which evaporated cooling water after recirculation. With attention placed on water use, in recent years this type of system still predominates.

Still, many plants are beginning to rely on dry cooling or hybrid systems [115, 227]. Meldrum et al. [226] did not include biomass in their analysis. A prior review by Fthenakis and Kim [228] does include biomass but note the very wide estimates for water use. The variation is largely due to uncertainty around feedstocks, and they show that agriculture requiring irrigation in particular has a very high water footprint. Biomass used for electricity in the US, however, comes largely from paper byproducts, as well as wood and other wastes (see [180]). For this reason, assumptions are made that water is not used in the fuel cycle and thus the biomass plant is given the same rating as NGCC.

E. APPENDIX TO CHAPTER FIVE ON LAND USE FOR POWER GENERATION

E.1 Literature Estimates for Land Use

In Figs. E.1 and E.2, we show the wide range of estimates in the literature for land use/power density of different technologies. A logarithmic scale is used, showing that the estimates for electricity generation from each technology tend to vary by orders of magnitude. The narrowest ranges are for solar, although the land use in all cases is based on retrospective use when only a small fraction of current installations were in place. The triangle markers in our estimates show that for wind, part of the range of the estimates is due to the difference between direct and landscape footprints. For a similar power density to conventionals, Hand et al.'s estimates place geothermal and hydropower close [166]. Hydro is based on their estimates on run of the river type plants. Wind direct footprint by our estimate is similar as well. Gagnon's high estimate for biomass power density is based on the use of wood waste [34], which has not been modeled in other literature reviewed.

E.2 Coal Production Today

In 2017, the most recent year from which data is available, a total of 774 billion short tons of coal were produced from 680 mines [229]. Roughly 2/3 of annual production came from surface mines with 1/3 coming from underground mines. Coal came primarily from 4 basins: the Powder River basin in Wyoming and Montana (43.2% of production, all surface mines), Appalachia (25.6% of production, primarily surface mines), the Illinois Basin (13.3% of production), and the Uinta Basin (3.6% of production). Additional interior states provide 5.4% of production and western

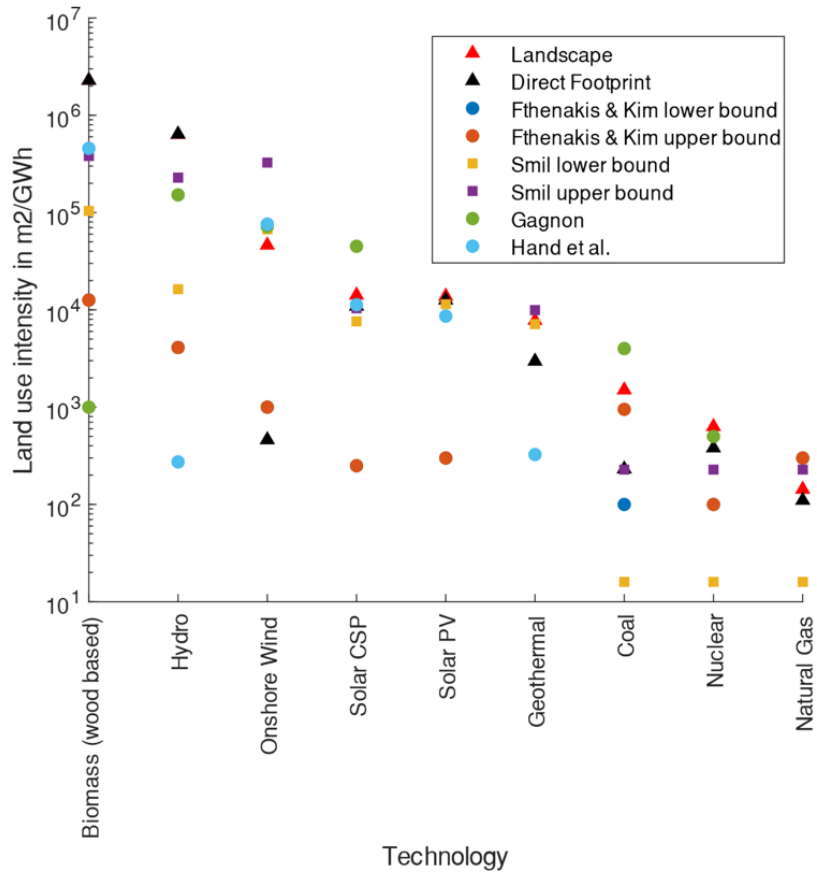


Fig. E.1.: Land use intensity estimates from literature review. Fthenakis and Kim estimates taken from visual inspection of results figure 3 [165]. Smil estimates taken from visual inspection of Fig. 7.3 [35]. Hand et al. [166] estimates available only for renewables. Capacity factors from our work were used on their values from table A-10 [166]. Gagnon's biomass estimate for wood wastes was used [34].

states contribute the final 8.8% of production. Only 6 mines, all in Wyoming, accounted for over 2% of total US coal production in 2017. Thus, coal mining in the US is quite distributed. While the largest mine, the North Antelope Rochelle Mine (NARM), accounted for over 13% of production, and the second largest, the Black Thunder Mine, accounted for over 9% of production, the mines quickly scale down, with the third largest, Antelope Coal Mine, accounting for only 3.7% of production.

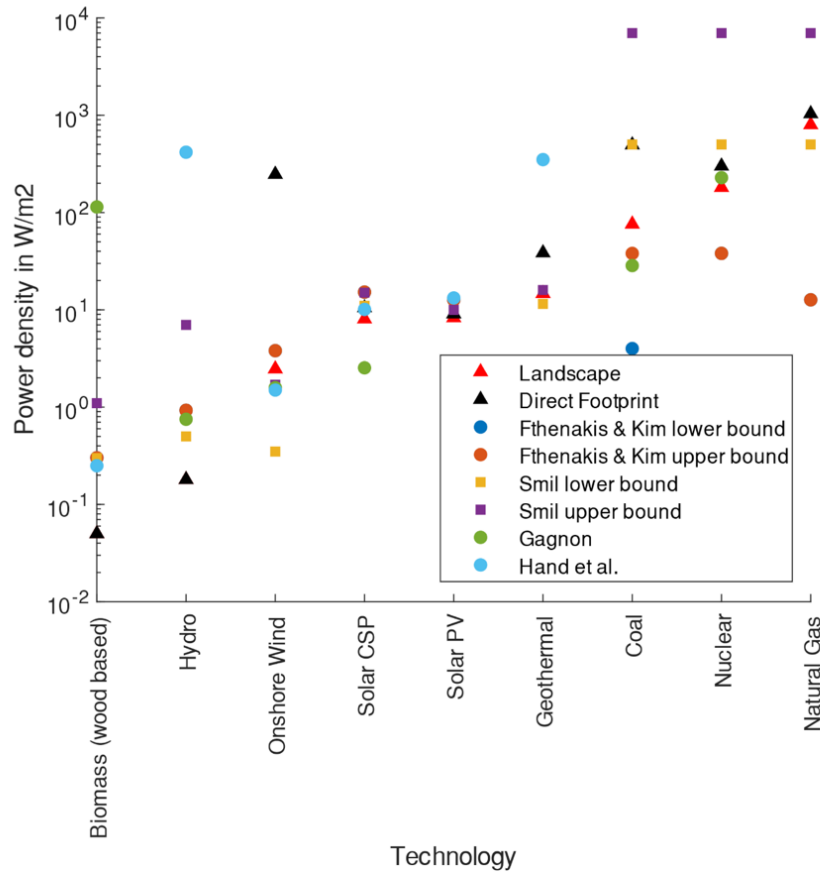


Fig. E.2.: Power density estimates from literature. Fthenakis and Kim estimates taken from visual inspection of results figure 3 [165]. Smil estimates taken from visual inspection of Fig. 7.3 [35]. Hand et al. [166] estimates available only for renewables. Capacity factors from our work were used on their values from table A-10 [166]. Gagnon’s biomass estimate for wood wastes was used [34].

Appalachia represents the majority of mines but only around a quarter of production. In the US Energy Information Administration statistics Appalachia represented 559 of the 680 mines with nonzero production or 799 of 959 mines included in the statistics (80%) [229].

Due to the distributed nature of mining, its spatial and technical variation, and differing coal composition and heating value, researchers have attempted to segment

the market in their analyses. This also means that the reader or analyst must read these statistics and employ them with caution—what do they represent? Are historical trends indicative of future trends? How can single values be extrapolated from systems that are quite different from each other? As in the case of wind, disturbed land versus total landscape effects for coal are quite different, but have not been adequately characterized. Three papers with significant analysis include [35, 162, 165]. Here, calculations are based on the largest surface mine in the US, and a calculation method is suggested that gives single values for the major mining technologies in the US.

Focusing on the question of system boundaries, available data on Colorado coal mines lists 3 categories of land use: total lease area, disturbed area, and affected area. For underground mines, the disturbed area ranged from 1-20% of the total area, with most values below 5%. Affected areas ranged from 25-100% of the mine lease, however. Only three surface mines were included, with identical areas listed as disturbed and affected. The mine listed as nearing complete extraction was at roughly 95% affected area with the other two at around 25-35% of the area. Therefore, for the underground mines, 1/3 of the total, the direct footprint could be calculated at 5% of the total lease, but this would exclude much of the affected area. For surface mines, the land will ultimately be almost totally affected or disturbed, although several years may pass before this occurs.

E.2.1 Measurements and Bounds from the Literature

Table B1 gives estimates for the land use intensity of the entire cradle to gate life cycle of coal from three sources. Immediately it is clear that the estimates vary by orders of magnitude. This is the case for example between Trainor et al.'s values and those of Fthenakis and Kim, even though they seem to rely largely on the same data set.

Source	Description	Total, Direct m ² /GWh	Total, Landscape m ² /GWh
[162]	Underground - low	240	
[162]	Underground - single value	640	640
[162]	Underground - high	1510	
[162]	Surface - low	4690	
[162]	Surface - single value	8190	8190
[162]	Surface - high	16420	
[35]	Surface - low	71	71
[35]	Surface - high	120	120
[165]	Underground - single value	250	250
[165]	Surface - low	100	100
[165]	Surface - high	950	950

Table E.1.: Values for land use intensity from three sources with any necessary unit conversions made by the author. Note that while Trainor et al. pioneer the idea of landscape level versus direct footprint, they do not differentiate here in the case of coal. Values from Fthenakis and Kim come from visual inspection of Fig. 6. Values for Smil come from pages 135-136.

One of the largest issues with the coal calculations in [165] is that the data sets are very old. The reader is not presented with enough information to replicate the calculations that lead to the results in Fig. 6. Inconsistencies found were that mining land is not discounted over lifetime of the project unlike other stages, the data source drawn on for mining land use is from 1983, and there is a typo on table 3, which lists tonnes of coal mined from the surface which were thousand short tons in the original sources.

Fthenakis and Kim [165] as well as Trainor et al. [162] use the divisions West and East to classify coal production without specifying which production is included in

each area. For example, the representative case for Trainor et al. includes mines in Texas, North Dakota and Colorado, but not from other states. Together, however, the production from those three states represents only 10% of US production. Wyoming alone contributes more than 40% of US production, however, so a representative Western case needs to include Wyoming numbers. In fact, the NARM alone produced more than all the mines included in the representative case for Trainor et al [162]. Using the figures from either source may be problematic, therefore, since niche cases are taken as representative.

VITA

VITA

Liz Wachs holds a BA in Ancient History and Classical Civilization from the University of Texas at Austin and a BS in Chemical Engineering from Purdue University. She holds an MA in Desert Studies from Ben-Gurion University of the Negev focused on environmental policy and livestock husbandry systems in Israel. Wachs began her PhD studies in Agricultural and Biological Engineering in August 2015. She is a member of the American Institute of Chemical Engineers (AIChE), the International Society of Industrial Ecology (ISIE), the International Input-Output Association (IIOA) and the United States Association for Energy Economics (USAEE).